The behaviour of bismuth oxide in the oxidative dehydrodimerization and aromatization of propylene

THE BEHAVIOUR OF BISMUTH OXIDE IN THE OXIDATIVE DEHYDRODIMERIZATION AND AROMATIZATION OF PROPYLENE

M. A. M. BOERSMA

THE BEHAVIOUR OF BISMUTH OXIDE IN THE OXIDATIVE DEHYDRODIMERIZATION AND AROMATIZATION OF PROPYLENE

THE BEHAVIOUR OF BISMUTH OXIDE IN THE OXIDATIVE DEHYDRODIMERIZATION AND AROMATIZATION OF PROPYLENE

PROEFSCHRIFT

TER VERKRIJGING VAN DE GRAAD VAN DOCTOR IN DE TECHNISCHE WETENSCHAPPEN AAN DE TECHNISCHE HOGESCHOOL TE EINDHOVEN, OP GEZAG VAN DE RECTOR MAGNIFICUS, PROF. DR. P. VAN DER LEEDEN, VOOR EEN COMMISSIE AANGEWEZEN DOOR HET COLLEGE VAN DEKANEN IN HET OPENBAAR TE VERDEDIGEN OP VRIJDAG 6 MEI 1977 TE 16.00 UUR

DOOR

MICHAEL ADRIAAN MARIA BOERSMA

GEBOREN TE 'S-HERTOGENBOSCH

DIT PROEFSCHRIFT IS GOEDGEKEURD DOOR DE PROMOTOREN:

Prof. Drs. H.S. van der Baan

Prof. Dr. W.M.H. Sachtler

Aan mijn ouders

Aan Rita.

Contents

CHAPTER 1

Introduction

1.1 CATALYTIC OXIDATION IN GENERAL

Since organic products containing heteroatoms may be very important as intermediates in the petrochemical industry, intensive research programmes have been developed and carried out during the past fifty years to discover processes to prepare those with high selectivity.

As far as the introduction of oxygen atoms in the hydrocarbon is concerned, research has been directed to heterogeneous gas phase oxidation processes. These can relatively easily be carried out in a tubular reactor while oxygen is freely available from the air. Two drawbacks, however, have to be considered in this connection. Firstly, thermodynamic calculations show that, although a large number of intermediate oxidation products are thermodynamically accessible, complete oxidation to carbon dioxide and water is preferred at the temperatures of interest, even when the oxygen/hydrocarbon ratio is lower than that required for complete combustion. Secondly, homogeneous oxidations may take place. Since these reactions are free radical chain processes a complex mixture of products may result. This would not only require an extensive separation of the product mixture but also, even when only two products are obtained with high selectivity from the same process, a less favourable market for one of the products could make the process unattractive.

The discovery of V_2O_5 as an oxidation catalyst (1) for the conversion of naphthalene to phthalic acid anhydride may be visualized as a major breakthrough in chemical technology, since this finding initiated research in many countries to

discover similar catalytic oxidation processes. One has to realize in this connection that the demands that have to be made upon suitable catalysts are not only related to the route and the depth of the oxidation, but also to the increase of the rate of the desired reaction in such a way that the unwanted homogeneous reactions occur only to a negligible extent.

Catalysts that have proven their usefulness in selective oxidation reactions are mostly oxides and mixed oxides of the transition metals. Some of these catalysts are very versatile, being effective in various processes. Examples are vanadium pentoxide and bismuth molybdate. The former is not only an effective catalyst for the conversion of naphthalene to phthalic anhydride and of benzene to maleic anhydride, but e.g. also for the oxidation of sulphur dioxide to sulphur trioxide. The latter is a good catalyst for the oxidation of propylene to acrolein and to acrylonitrile and also active for the oxidative dehydrogenation of n-butenes to 1,3-butadiene.

Although nowadays many hydrocarbon oxidations are carried out on a commercial scale, the selective properties of the applied catalysts have in most cases been discovered accidentally. Moreover, basic understanding of the way in which the catalysts act lags far behind the technological knowledge of the processes. In recent years, however, a number of fundamental research studies have been carried out to unravel the surface characteristics of the active oxide surface together with the role the oxygen plays, since these factors determine primarily the activity and selectivity of the catalyst for a specific oxidation reaction.

Although some of these studies have revealed fairly good relationships between the catalytic activity and selectivity and certain oxide properties, like metal-oxygen bond energy (2,3), Fermi level (4), heat of formation of the metal oxides (5-8), exchange with gas phase oxygen (9-11), reducibility (12) and semiconductor properties (13,14), the controlling parameters are not yet understood to such an extent that they

enable us to predict the behaviour of a catalyst for a specific reaction.

Two fundamental principles, however, have become clear. Firstly, the oxygen atom that reacts with either the hydrogen atom being split off after adsorption of the hydrocarbon or the organic fragment or both comes from the catalyst surface (15). Complete combustion generally results from loosely bonded or gas phase oxygen. Moreover, the overall picture may be complicated by the occurrence of surface-initiated, homogeneous reactions (16-18). Secondly, most heterogeneous oxidation reactions take place according to a sequential scheme (19,20), in which the catalyst surface is alternately oxidized and reduced. In this process anion vacancies play an important role.

1.2 THE OXIDATION OF PROPYLENE OVER OXIDE CATALYSTS

Following Haber's (21) classification of heterogeneous oxidation reactions of hydrocarbons three types of oxidation processes can be discerned in the case of propylene.

a. Processes in which the structure of the molecule undergoes only slight changes. These oxidations, which are characterized by the fact that an oxygen atom is incorporated in the carbon skeleton, include conversion of propylene to propylene oxide, acrolein, acrylic acid, acrylonitrile and acetone. Catalysts are mainly binary oxide systems containing at least either molybdenum or antimony oxide.
b. Processes in which the carbon chain of the propylene molecule is enlarged or ruptured. Examples are the conversion of propylene to acetic acid (22), the dimerization of propylene to 1,5-hexadiene and the dehydroaromatization to benzene. In recent years the latter two oxidations have been reported to take place by various single and binary oxides, including Bi_2O_3 (23), Tl_2O_3 (24), In_2O_3 (25), Sb_2O_4, Fe_2O_3, SnO_2 (26), Bi_2O_3-SnO_2 (27,28), Bi_2O_3-P_2O_5,

Bi_2O_3-As_2O_3 and Bi_2O_3-TiO_2 (29,30). As compared to type a. oxidations reaction conditions normally are more severe (500-600°C), while introduction of gaseous oxygen in the feed mixture usually results in low selectivities. Practical operation will, therefore, require a reducing atmosphere, which will put limits to the usefulness of many oxides in view of the volatility of the metals formed by reduction of the oxides.

c. Oxidations in which the hydrocarbon molecule is completely converted to CO_2 and water. Active catalysts for this reaction are the group VIII metals as well as oxide systems containing cobalt, manganese or chromium.

Table 1.1 gives a survey of the most relevant reaction conditions, catalyst systems, conversions and product selectivities for the above mentioned reactions of propylene.

Table 1.1 Catalytic vapour phase oxidation reactions of propylene.

Product	Catalyst	Conditions	Conv. %	Sel. %	Ref.
propylene oxide	thallium Fe-tungstates	185°C, 22.5 bar	35	40	31
acrolein	$Bi_9PMo_{12}O_{52}$	450°C	92.5	60.5	32
acrylonitrile	$Bi_9PMo_{12}O_{52}$	470°C	95.6	68.2	33
acrylic acid	Co-molybdate +WTe_2	435°C	54.9	51.7	34
acetone	SnO_2-MoO_3	348°C	5	43	22
	Co_3O_4-MoO_3	185°C	18	76	35
acetic acid	SnO_2-MoO_3	348°C	5	37	22
1,5-hexadiene	Bi_2O_3	560°C	7	61.4	23
benzene	$(Bi_2O_3)_2$-P_2O_5	500°C	85	45	29

In this thesis we shall confine ourselves to the type b. oxidation of propylene, viz. the dehydrodimerization and dehydroaromatization reaction.

1.3 BENZENE MANUFACTURE

Benzene, which is at present the largest volume aromatic, is derived either from coal or petroleum. In 1970 production amounted to 12 million tons world wide (36). It is primarily produced as a building block for fibers, plastics and elastomers. Over 40% is used for ethylbenzene-styrene production.

Coal based benzene, which in Western Europe contributes for only a quarter to the total benzene production, is obtained from coal tar, which results as byproduct from coking and town gas manufacture. To obtain the benzene, the coal tar light oil, which contains 50-70% by vol benzene, is washed with sulphuric acid, neutralized with caustic soda and subsequently distilled.

Petroleum benzene can be obtained directly from reformate and pyrolysis gasoline. Reforming is necessary since the amount of benzene present in most crude oils is small and its separation in a relatively pure state is ordinarily uneconomic. After reforming two routes are open for isolation. Firstly, fractional distillation of the reformate yields a narrow boiling benzene concentrate cut, from which the benzene is isolated by solvent extraction followed by fractional distillation of the aromatic mixture thus obtained.

Secondly since most reformates contain more xylenes and toluene than benzene and in a proportion which does not correspond to normal market demand large quantities of benzene are also produced by demethylation of toluene and xylene fractions. Commercial operation usually is carried out in the presence of hydrogen over Cr_2O_3-Al_2O_3 or Pt/Al_2O_3 catalysts according to

$$C_6H_5CH_3 + H_2 \rightarrow C_6H_6 + CH_4 \qquad (1)$$

Oxidative demethylation, however, is also a possible route, as has been demonstrated by Steenhof de Jong in 1972 (37). He described a process in which toluene is passed over bismuth uranate at 400-500^{o}C, giving benzene with 80% selectivity.

Yet another method to produce benzene is by dehydro-aromatization of propylene. Whereas the direct aromatization reaction,

$$2C_3H_6 \rightarrow C_6H_6 + 3H_2 \qquad \Delta G^{o}_{700} = 60.71 \text{ kJ/mol} \qquad (2)$$

is thermodynamically not favoured in the temperature range of interest (up to 700°C), the oxidative way offers better perspectives.

$$2C_3H_6 + \tfrac{3}{2} O_2 \rightarrow C_6H_6 + 3H_2O \qquad \Delta G^{o}_{800} = -63.74 \text{kJ/mol} \qquad (3)$$

The first report of this reaction has been published by Seiyama et.al. (29) with bismuth phosphate catalysts. Later investigations (27,28,38) have revealed that the formation of benzene takes place by a two step mechanism:

$$2C_3H_6 + \tfrac{1}{2}O_2 \rightarrow C_6H_{10} + H_2O \qquad (4)$$

$$C_6H_{10} + O_2 \rightarrow C_6H_6 + 2H_2O. \qquad (5)$$

In Western Europe, where almost every country uses propylene as a fuel - in Italy for instance propylene is simply flared (39) - selective production of benzene by this route could offer a good alternative both from an economical and energy conservation point of view. However, also in the U.S., where propylene demand is rather strong, this production method can still be competitive with other routes.

1.4 AIM AND OUTLINE OF THIS THESIS

Although in the literature various studies have been published in recent years concerning the oxidative dehydro-dimerization and dehydroaromatization over oxide catalysts (23-30,38), no detailed description of the kinetics as well

as of the mechanism of the main and side reactions has appeared so far. Therefore, as the possibility exists that the oxidative dehydroaromatization might be a competitive route for benzene manufacture, this investigation was started with the aim to fill some of the gaps in our knowledge on this reaction.

On account of the observation that combinations of oxides are often more active and selective than the pure constituents the bismuth oxide-zinc oxide system, of which the pure oxides were quoted to be selective for the reaction under study (40), was initially chosen as catalyst. It appeared, however, that the product selectivities for all compositions were roughly the same as those for pure bismuth oxide. We decided,therefore, to focus our attention mainly on this oxide.

In chapter 2 the apparatus that has been used for studying the kinetics is described.

Chapter 3 is devoted to the preparation and properties of the various bismuth oxide containing catalyst systems. Also a qualitative reaction model is proposed for the conversion of propylene to benzene. From these preliminary experiments it will emerge that in the aromatization reaction bismuth oxide can be used either as an oxidant or as a catalyst.

The reaction kinetics when bismuth oxide is used as oxidant, i.e. in the absence of gaseous oxygen, are described in chapter 4. Since in this case one is interested in the mechanism that controls the reduction of the oxide, studies are carried out in a thermobalance as well as in a fixed bed tubular reactor. Agreement between the results obtained with both techniques appears to be very satisfactory. A model in which the reduction of bismuth oxide is controlled by the catalytic reaction taking place at the oxide surface and being first order in oxygen from the catalyst is offered. Since the use of bismuth oxide as oxidant actually means that the solid deactivates continuously during the reduction cycle, experiments are performed to study the restoration of the activity after reoxidation with air.

Chapter 5 deals with the kinetics of the dimerization and

aromatization reaction in the presence of oxygen. It turns out that in describing the kinetics of the heterogeneous reaction accurately, one has to account for the homogeneous conversion of propylene to carbon dioxide and water.

The kinetic experiments which have been performed with the bismuth oxide - zinc oxide system are described in chapter 6.

Finally, in chapter 7 a general discussion is given where the results reported in the three preceding chapters are compared with the studies which have already been published on the title reactions.

CHAPTER 2

Apparatus and Analysis

2.1 INTRODUCTION

In the dimerization and aromatization of propylene, Bi_2O_3 and the binary oxide system Bi_2O_3-ZnO can act as oxidant or as catalyst. It is obvious that in studying the kinetic parameters different methods will be needed for both cases.

When the oxide is used as oxidant a gas-solid reaction is involved, the oxygen being supplied continuously by the oxide. In addition to gaseous products also solid reaction products are formed. Moreover, studying the kinetics of a gas-solid reaction is complicated by the fact that usually no constant reaction rate is obtained. Whether this will be the case depends on the mechanism that controls the reduction as well as on the type of reactor that is used.

Preliminary experiments* in a small plug flow fixed bed tubular reactor with Bi_2O_3-ZnO samples in various compositions acting as oxidant showed that, indeed, the reaction rate of both reaction steps, viz. the dimerization of propylene and the cyclization of 1,5-hexadiene, decreased continuously with time. Analysis by GLC and IR spectroscopy of the reaction products enabled us in the case of propylene dimerization to study the parameters that determine the kinetics of catalyst reduction as well as of the chemical reaction that takes place at the catalyst surface.

Reduction of the oxides with 1,5-hexadiene, on the other hand, was so fast that in first instance the results were thought not to be reliable enough to determine the kinetic parameters of this reduction reaction. These studies were,

* These investigations will be dealt with in chapter 3.

therefore, repeated in a thermobalance, where the oxygen depletion can be measured directly and accurately.

As both the rate and the mechanism by which the oxide looses its oxygen are important factors in describing the overall kinetics of the separate reactions, the thermobalance was also used for studying the dimerization of propylene. Moreover, carrying out the experiments in the fixed-bed reactor implies that there exists a gradient in the propylene concentration over the bed. In the thermobalance, on the contrary, the conversion levels are very low, which may make this technique suitable for evaluating kinetic data. One must keep in mind, however, that in the thermobalance the exact surface concentration is not very well known.

Assuming no adsorption of reagents or products taking place the thermobalance provides information about the total degree of reduction as well as the total rate of oxygen depletion. As from chapter 3 and 4 it will emerge that in the reduction of the oxides with propylene and 1,5-hexadiene partial oxidized products and carbon dioxide are formed in parallel reactions, which not necessarily need to take place by the same mechanism, analysis of all gaseous products, formed during the reduction, is required. To account for this the thermobalance was coupled with a gas chromatograph for analyzing hydrocarbons and an infrared monitor for carbon dioxide.

Besides being suitable for determining the reduction kinetics the thermobalance is also a useful device for studying the parameters that determine the reoxidation of the oxide sample after reduction to various degrees. Since knowledge about restoration of the oxidant activity becomes necessary when the reaction is carried out on a commercial scale, we also used the balance system to obtain information on this point.

For the investigation of the kinetics with bismuth oxide acting as a catalyst, experiments were also carried out in a plug flow fixed bed reactor, operating under differential conditions. Analysis of all products was performed by gas

chromatography.

Adsorption of reactants and products often plays an important role in catalysis (41). Therefore, since studying the adsorption behaviour can contribute to the interpretation of the kinetic data and may deliver information about the reaction mechanism, we investigated the adsorption behaviour of propylene on bismuth oxide.

2.2 *ADSORPTION APPARATUS*

The measurements are carried out in a pyrex glass volumetric adsorption apparatus shown in figure 2.1. It consists of a high vacuum system, gas bulbs to introduce the hydrocarbons to be adsorbed on the oxide samples, and a system to measure the adsorption characteristics. The vacuum appara-

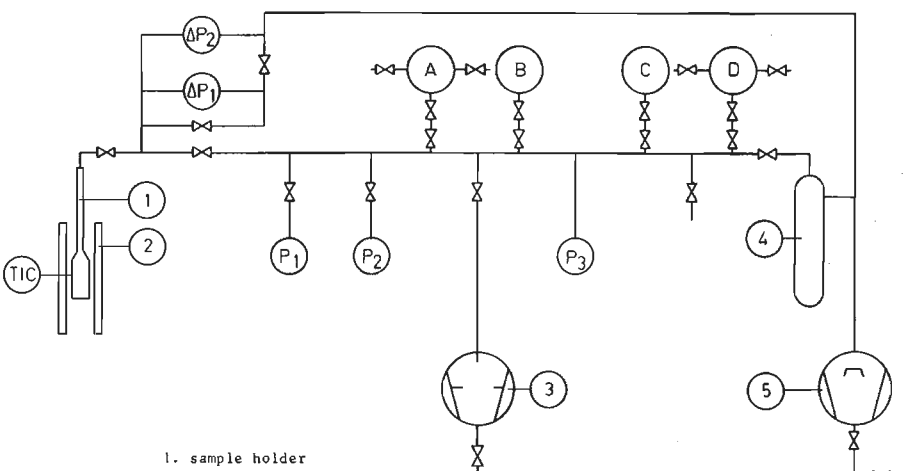

1. sample holder
2. furnace
3. Leybold-Heraeus S2 one stage rotary vacuum pump
4. cold trap
5. Leybold-Heraeus Diff 170 oil diffusion pump
6. Leybold-Heraeus D6 two stage rotary vacuum pump

A,B,C,D	gas storage bulbs
P1	Mc Leod manometer, $4.0\ 10^{-8}$ - $3.6\ 10^{-3}$ bar
P2	Mc Leod manometer, $1.6\ 10^{-7}$ - $26.2\ 10^{-3}$ bar
P3	manometer for rough pressure indication, 0-1 bar
ΔP1, ΔP2	Hottinger Baldwin PDI differential pressure indicators ΔP1: 0-0.01 bar, ΔP2: 0-0.1 bar.

Figure 2.1 Adsorption apparatus.

ratus consists of a twostage rotary pump and a water cooled oil diffusion pump with cold trap, immersed in liquid nitrogen. With both pumps operating in series pressures in the order of 10^{-9} bar can be reached. After adsorption equilibrium has been established, pressure readings are made by one of the two Mc Leod manometers. From the results adsorption isotherms are derived.

Although for adsorption of permanent gases the Mc Leod manometer gives excellent results, the device is less suitable for studying the adsorption of compounds which have rather low vapour pressures at room temperature, as condensation may take place in the top of the Mc Leod gauge during the pressure determination. For such measurements the system is, therefore, equipped with a differential pressure indicator, which does not suffer from this drawback.

In all measurements the adsorption vessel, which can be heated by an electric furnace is filled with about 5 g of sample. Temperature is measured with a thermocouple placed in a cilindrical thermowell. Compounds which are liquid at room temperature are purified by low temperature sublimation from the solid state before they are introduced in the storage bulbs.

2.3 REACTION SYSTEM FOR EXPERIMENTS WITHOUT OXYGEN IN THE FEED

The flow system which is used for both catalyst testing and kinetic measurements is depicted in figure 2.2. In the gas mixing part mixtures of helium, propylene and nitrogen can be prepared in all desired compositions and subsequently fed to the oxide in the reactor. For the experiments involving liquid reactants (1,5-hexadiene and benzene) the inert gas is passed through a double-walled thermostated vaporizer filled with the component in question. The desired reactant concentration is established by adjusting the temperature of the vaporizer. By varying the height of the liquid and analyzing

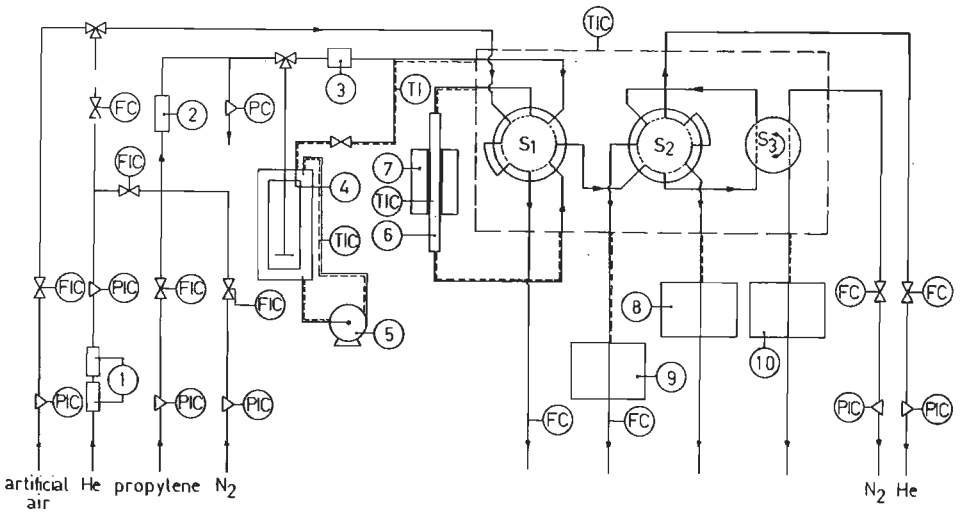

1. tubes filled with BTS catalyst and mol sieve
2. van Dyke mixer
3. flame extinguisher
4. vaporizer
5. circulation pump
6. reactor tube
7. furnace
8. GLC 2
9. IR CO_2-analyzer
10. GLC 1

S1,S2 8-way Becker gas sampling valves

S3 4-way disc gas sampling valve

Figure 2.2 Flow reactor system for experiments without oxygen in the feed.

the gas leaving the vaporizer it has been ascertained that the gaseous feed mixture is completely saturated. As no re-oxidation of the catalyst sample should take place the diluent is made oxygen free by passing it over a reduced BTS* catalyst.

The reactor, which is made from stainless steel or quartz glass, has an internal diameter of 6 mm and is electrically heated. Temperature is controlled within 1°C with a Eurotherm thyristor controller. In the stainless steel reactor the temperature is measured with two thermocouples, one placed in and the other placed just above the oxidant, while in the quartz glass reactor the temperature is measured with one thermocouple placed in the middle of the bed.

In both reactors normally 0.5-1 gram oxidant is used

*BTS stands for reduced BASF R3-11 catalyst.

with a particle size of 0.3-0.5 mm. To assure plug flow conditions silicon carbide particles with the same diameter are added on top of the oxide, yielding a totale zone of solid material of 30-40 mm. Pressure build up over this bed is negligible. All experiments are carried out at atmospheric pressure.

Since the kinetic runs with the bismuth oxide - zinc oxide samples are for the most part carried out with the same reactor filling, for each run only a slight reduction of the sample (∿10%) is allowed to occur in order to prevent activity loss of the oxidant. To restore the activity after partial reduction the sample can be reoxidized with air by switching valve S1, an 8-way Becker gas sampling valve. At the same time the feed gases are introduced in the sampling system and subsequently analysed. After such a reoxidation period the reactor system is flushed with inert gas for 30 minutes. Before an experiment with a fresh oxidant is started, it is heated in a flow of helium till the desired reaction temperature is reached and held at this temperature for 30 minutes. Thereafter the experiment is started by turning valve S1.

The product gas from the reactor passes two sample valves and is analysed gas chromatographically. To prevent condensation of high boiling compounds the sample valves are placed in thermostats kept at 150°C, while all lines are heated electrically.

2.3.1 ANALYSIS

Due to the absence of oxygen in the feed, oxygen is consumed continuously from the oxidant sample. As from analysis of the reaction products the amount of oxygen removed from the oxidant can be calculated, analysis of products has to be fast in order to obtain accurate information on the rate of reduction of the oxidant. Therefore, we developed a sampling and analysis system, which made it possible to inject and analyse gas mixtures simultaneously on two gas

chromatographs. The injection system consists of two sample valves, of which valve S3, a 4-way disc valve (42), is placed in the sample loop of an 8-way Becker gas sampling valve, S2. The injection volume for valve S2 and S3 are 1.5 cm^3 and 50µl, respectively.

Samples injected with S3 are analysed on GLC1, a Pye series 104 gas chromatograph with flame ionization detector, for propylene, 1,5-hexadiene, 1,3-cyclohexadiene, benzene and 3-allylcyclohexene. The separation is carried out on a 6 m stainless steel column, ID 2 mm, filled with 10% by wt carbowax 20M on chromosorb WAW and kept at 70°C. As carrier gas we use nitrogen. Total analysis time is 11 minutes. However, when only propylene and 1,5-hexadiene need to be analysed, as is the case in the differential kinetic measurements, elution time is only 2 minutes. Figure 2.3 shows a chromatogram of a typical sample of the reactor oulet stream.

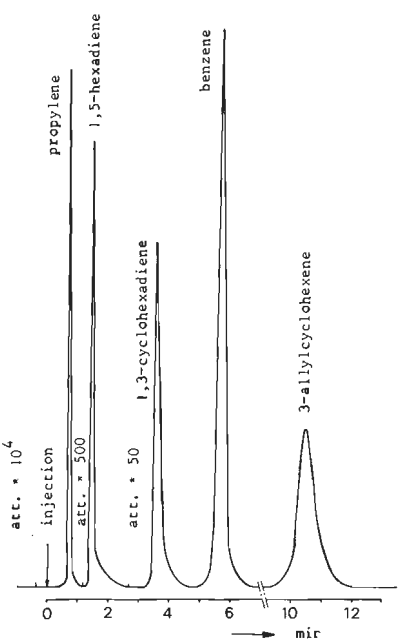

Figure 2.3 Chromatogram of hydrocarbon analysis on GLC 1.

Assuming the peak area of a component to be proportional to its mole fraction, quantitative analysis of the product mixture can take place by using the relation

$$x_A = f_A \frac{A_A}{A_{prop}} x_{prop} \qquad (1)$$

where

x_A : mole fraction of component A

x_{prop} : mole fraction of propylene

A_A : peak area of component A

A_{prop} : peak area of propylene

f_A : response factor of component A.

The response factors for propylene, 1,5-hexadiene and benzene

are determined by injecting mixtures of nitrogen with these compounds. For propylene mixtures of different compositions are obtained with two Wösthoff plunger pumps. Mixtures of nitrogen and 1,5-hexadiene or benzene are prepared in the vaporizer. Finally, the calibration factors for 1,3-cyclohexadiene and 3-allylcyclohexene are calculated with the formula:

$$f_A = \frac{M_{prop}}{M_A} \qquad (2)$$

where

M_{prop} : molecular weight propylene
M_A : molecular weight of component A.

This relation is applicable to compounds analysed with a flame ionization detector, for which the detector response calculated for unit weight of hydrocarbon is practically constant.

For 1,5-hexadiene-nitrogen mixtures it appears that when the mole fractions are calculated by vapour pressures, obtained by extrapolating literature data (43,44), no linear relationship exists between the peak area and the mole fraction. Moreover, the response factors for 1,5-hexadiene and benzene calculated on this basis turn out not to be equal, although this should be the case according to formula (2). We, therefore, decided to determine the vapour pressure data in the temperature traject of interest.

Thus, at a certain temperature a stream of inert gas is saturated with 1,5-hexadiene and subsequently led through a cold trap, cooled with liquid nitrogen. By GLC analysis of the gas leaving the cold trap it is established that all the 1,5-hexadiene is condensed. From the weight of 1,5-hexadiene and the gas flow the vapour pressure can now be calculated. We found the following relation to be valid in the temperature range $253 < T < 278$:

$$\log P = 6.31639 - \frac{2020.7}{T} \quad (P \text{ in bar; } T \text{ in K}). \qquad (3)$$

This expression agrees at high temperature quite well with

that of Cummings and Mc Laughlin (44). Extrapolation of Cummings' results to lower temperature, however, is not allowed. With equation (3) a linear relationship is obtained between peak area and mole fraction of 1,5-hexadiene.

Quantitative determination of carbon dioxide, water and propylene is carried out on GLC2, a Pye Series 104 gas chromatograph with a katharometer detector. Samples for this analysis are injected with valve S2. The separation column (glass, 2.5 m,ID=1.5 mm) is filled with porapak T (150 cm) and porapak Q (100 cm) and kept at 100°C. Carrier gas is helium. Since 1,5-hexadiene, benzene and higher boiling compounds are retained on the column frequent regeneration at 150°C is required. However, by temperature programming it is possible to elute these compounds. A chromatogram of such an analysis where temperature programming is applied, is depicted in figure 2.4. Total analysis time is 18 minutes. Peak areas are determined with an Infotronics model CRS 208 electronic integrator. The response factors for the various compounds are obtained in the same way as described for the hydrocarbon analysis.

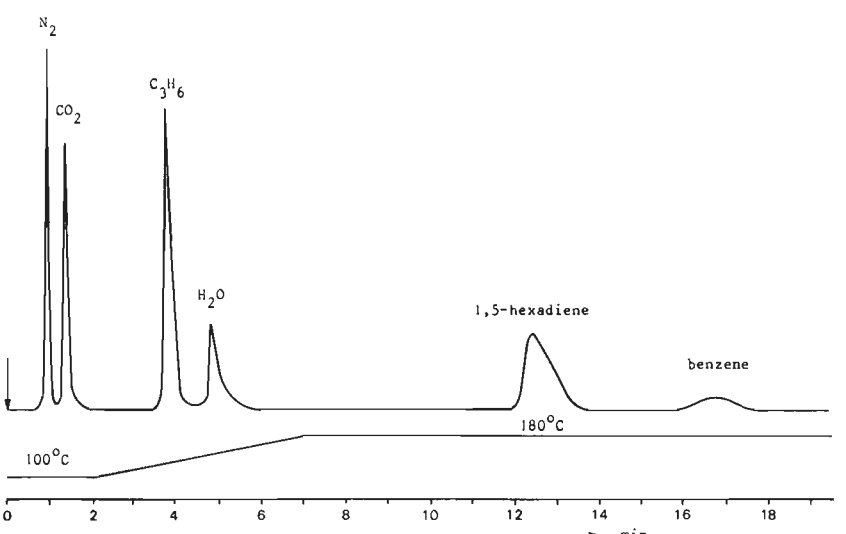

Figure 2.4 Chromatogram of product mixture analysed on GLC 2.

Since in the reaction of propylene and 1,5-hexadiene with bismuth oxide the number of moles increases considerably the mole fractions have to be corrected to actual conditions in the reactor. Therefore, when the conversion is appreciable, nitrogen, which does not take part in the reaction, is added as an internal standard.

The analysis system described so far has been used for catalyst testing as well as for the kinetic experiments with the bismuth oxide- zinc oxide system, the results of which will be described in chapter 6. For studying the kinetics of the reactions with bismuth oxide, however, the gas chromatographic analysis of CO_2 proved to be less suitable. We therefore determined the carbon dioxide concentrations in this case with a Maihak infrared CO_2 monitor, which enabled us to analyse the process stream very accurately and continuously.

2.4 REACTION SYSTEM FOR EXPERIMENTS WITH OXYGEN IN THE FEED

A flow diagram of the reaction system is shown in figure 2.5. Mixtures of helium and oxygen with propylene or 1,5-hexadiene are prepared in a way similar to that described in par.2.3. Since the number of moles increases only slightly in this reaction no nitrogen is added as internal standard. Ignoring this correction is further justified because propylene mole fractions are always less than 30%, while propylene conversions never exceed 25%.

Like in the experiments without oxygen in the feed we used a quartz glass reactor surrounded by an electrically heated oven. Reactor set up, temperature control, as well as the amount and sieve fraction of the catalyst are also identical to that described for the experiments carried out in a reducing atmosphere. When reaction conditions have been established, steady state is usually reached within one hour.

The feed mixture passes either through the reactor to the sample valves S1, S2 and S3 or directly via by pass B to these valves. The latter operation mode enables us to determine the

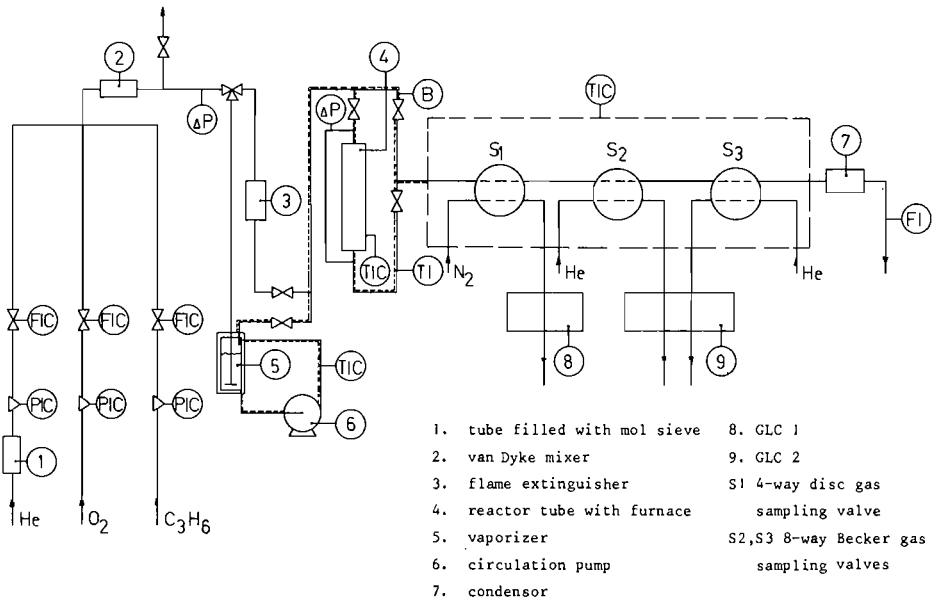

Figure 2.5 Reactor system for experiments with oxygen in the feed.

feed composition. The valves S1, S2 and S3 are sample valves for the analysis sytem consisting of two gas chromatographs, GLC1 and GLC2. Valve S1, which applies to GLC1, is a four way disc valve. Valves S2 and S3, which are both 8-way Becker sample valves with sample volumes of 2 cm^3, are used to inject samples on GLC 2.

2.4.1 ANALYSIS

The hydrocarbons are analysed on GLC1, a Pye series 104 gas chromatograph with flame ionization detector. Both the separation column and the gas chromatographic conditions are identical to those described in par.2.3.1.

GLC2, a 5700A Hewlett Packard gas chromatograph with two thermal conductivity detectors, is used for analysing CO, CO_2, oxygen, propylene and water. For separation of these compounds

three columns are applied, two of which are connected in series, and two sample valves, S2 and S3. Figure 2.6 shows the sampling system as well as the way in which the columns are arranged.

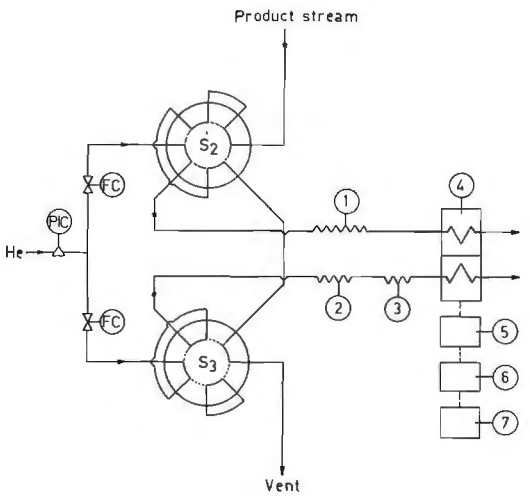

1. column Porapak Q+T, 100°C
2. column Porapak Q, 0°C
3. column mol sieve 13X, 25°C
4. dual thermal conductivity detector
5. amplifier
6. Infotronics CRS 208 integrator
7. recorder

Figure 2.6 Analysis system for experiments with oxygen in the feed.

On the first column (glass, 2.5 m, ID=1.5 mm), which is filled with porapak Q (1 m) and porapak T (1.5 m) and operates as described in paragraph 2.3.1, the sample is separated in water, propylene, CO_2 and a mixture of oxygen and CO. Samples are injected on this column with sample valve S2. When this valve is in the injection mode, the sample loop of valve S3 is flushed with product or feed gas. By switching both valves simultaneously the loop of valve S2 is flushed with gas, while the sample is now injected on the second column system. This consists of two GLC columns in series. On the first of these (40 cm, stainless steel, porapak Q, 0°C) the hydrocarbons and water are retained, while on the second column (2 m, stainless steel, 20°C), filled with molecular sieve 13X, the gases carbon monoxide and oxygen are separated. Carbon dioxide remains on this column which therefore has to be regenerated frequently. When it should be necessary to add nitrogen as an internal standard, this column also allows separation of this

gas. Both column systems operate with helium as carrier gas. Total analysis time is 20 minutes. A chromatogram of components separated on the mol sieve 13X column is shown in figure 2.7.

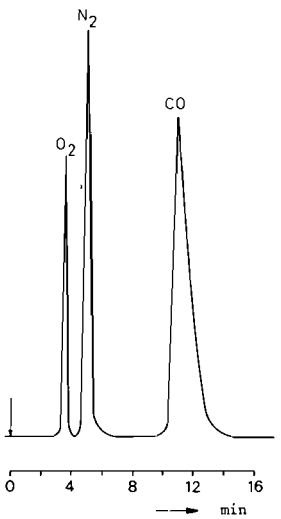

Figure 2.7 Chromatogram for separation of permanent gases on mol sieve 13X.

2.5 THERMOGRAVIMETRIC ANALYSIS

Figure 2.8 shows a diagram of the set-up for the experiments, which are carried out in a Dupont series 900/950 thermobalance. Mixtures of nitrogen and the reducing agent are prepared either by mixing a constant flow of nitrogen, carefully freed from oxygen by a reduced BTS catalyst, with a constant flow of hydrogen or propylene, or by passing the nitrogen flow through a thermostated vaporizer filled with 1,5-hexadiene or benzene. The mixtures so obtained are subsequently introduced into the sample chamber of the thermoanalyzer by means of valve S. The sample chamber, consisting of a quartz glass tube with inner diameter 2.1 cm, is heated by an electric furnace.

The reduction experiments are carried out under isobaric (1 bar) and isothermal (within 2^{o}C) conditions. The reaction

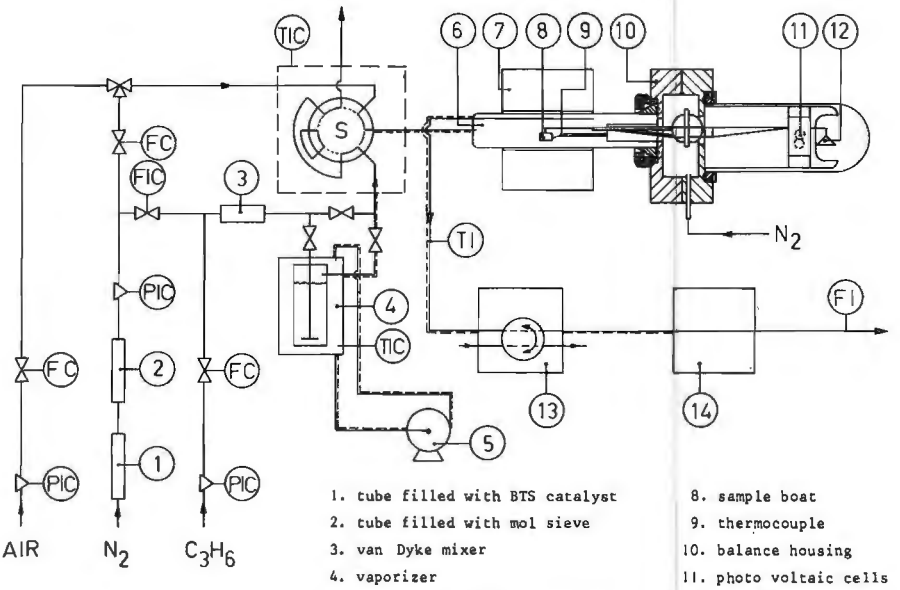

1. tube filled with BTS catalyst
2. tube filled with mol sieve
3. van Dyke mixer
4. vaporizer
5. circulation pump
6. quartz glass furnace tube
7. furnace
8. sample boat
9. thermocouple
10. balance housing
11. photo voltaic cells
12. counter-weight pan
13. GLC with 4-way disc gas sampling valve
14. IR CO_2 monitor

Figure 2.8 Thermobalance apparatus.

temperature is measured with a chromel-alumel thermocouple placed just above the 5*10 mm quartz glass sample bucket usually containing 50 mg of sample. Since the part of the balance where the weight changes are measured may be contaminated by the reducing agent, this side of the system is continuously purged with nitrogen.

From the introductionary experiments* it appears that during the reduction of bismuth oxide and mixed oxides of bismuth and zinc with propylene carbon dioxide and 1,5-hexadiene are formed by parallel reactions. Therefore, analysis of the effluent from the microbalance reactor is necessary in order to determine the amount of oxygen removed from the oxidant in the separate reactions. For analysis of combustible gases we used the gas chromatographic method described in paragraph 2.3.1. Quantitative analysis of carbon dioxide is carried out with the Maihak IR CO_2 monitor.

*These investigations will be dealt with in chapter 3.

CHAPTER 3

Preparation and Properties of Bismuth Oxide Containing Catalysts

3.1 INTRODUCTION

The chemical and physical properties of the binary oxide system Bi_2O_3-ZnO are not very well documented in the literature. From the phase diagram, which has been published recently (45), it appears that over a wide range of compositions the bcc phase of bismuth oxide (γ-Bi_2O_3) and the hexagonal zinc oxide are present. There exists, however, no agreement about the composition of a compound with high bismuth content. According to Levin and Roth (46) there is a cubic phase with a composition close to that of $(Bi_2O_3)_6ZnO$, but Safronov et.al. (45) have attributed a composition $(Bi_2O_3)_{24}ZnO$ to this compound. The disagreement about the accurate ratio of the two components is probably due to the incongruent fusion of the compound.

Bismuth oxide can exist in four crystallographic modifications (47,48). The monoclinic form (α-Bi_2O_3) stable at low temperature transforms upon heating at 730 $\pm$ 5°C to the stable cubic form (δ-Bi_2O_3), which then melts at 825 $\pm$ 5°C. Controlled cooling of the melt results in the appearance at about 625°C of the metastable tetragonal phase (β-Bi_2O_3) and/or the metastable bcc modification (γ-Bi_2O_3). Tetragonal Bi_2O_3, which can be easily prepared by decomposing bismutite ($Bi_2O_3.CO_2$) at 400°C, transforms to the monoclinic phase between 550°C-500°C. The bcc modification can be preserved at room temperature, provided stabilizing ions like Zn^{2+}, B^{3+}, Ga^{3+}, Fe^{3+}, Si^{4+}, Ge^{4+}, Ti^{4+} or P^{5+} are present. The resulting solids form a series of isomorphous compounds of individual composition called sillenites (49,50).

The addition of zinc oxide to bismuth oxide means that a

structural parameter is introduced, since zinc oxide stabilizes the γ-modification of Bi_2O_3, which may be a better catalyst for the dimerization reaction than α-Bi_2O_3.

3.2 CATALYST PREPARATION

The mixed oxides of bismuth and zinc are prepared as described by Batist et.al. (51) for the preparation of bismuth molybdate. To a 1M solution of zinc acetate in warm water is added under stirring 2M ammonia until the pH reaches a value of 6-7. The white precipitate is filtered off, washed with water and transferred to a round bottom flask filled with water. After heating to 90°C a suspension of basic bismuth nitrate in water is added to the zinc hydroxide suspension. The resulting mixture is then heated for 16 h under vigorous stirring at 90°C, after which the solid material is filtered off, washed with water and dried at 150°C overnight. Finally the samples are calcined at 600-625°C until X-ray analysis with a Philips diffractometer, using Ni-filtered Cu-radiation, shows no difference between samples calcined for different times. In all cases the γ-phase of Bi_2O_3 together with ZnO is obtained. The final composition of the catalyst is determined by spectrophotometric determination of the amount of zinc.

Bismuth oxide is prepared by dissolving bismuth nitrate in hot diluted nitric acid and adding this solution to an excess (50%) of warm concentrated (7M) ammonia. The white precipitate is filtered off and washed with water until no more nitrate can be detected in the filtrate. The solid mass is then dried at 140°C for 20 h and finally calcined at 600°C for 16 h. The resulting bismuth oxide is subsequently broken and sieved to the required mesh size. X-ray diffraction shows that the compound consists of α-Bi_2O_3.

Zinc oxide is prepared in an analogous way as bismuth oxide. After precipitation of zinc hydroxide from an aqueous zinc acetate solution by 2M ammonia the white mass is

filtered off, dried and calcined for 5 h at 625°C. X-ray diffraction indicated pure zinc oxide to be present.

3.3 PHYSICAL PROPERTIES

Table 3.1 summarizes some characteristic physical properties of the prepared oxides. The specific surface areas were determined with an areameter according to the BET method, using nitrogen as the adsorbate.

Table 3.1 Properties of bismuth oxide-zinc oxide catalysts.

Composition	Colour	Calcination conditions	Surface area ($m^2\ g^{-1}$)
α-Bi_2O_3	yellow	16 h, 600°C	0.25
$Bi_2O_3(ZnO)_{0.06}$	light-yellow	1 h, 625°C	0.17
$Bi_2O_3(ZnO)_{0.31}$	light-yellow	2 h, 625°C	0.29
$Bi_2O_3(ZnO)_{1.36}$	light-yellow	3 h, 600°C	0.66
$Bi_2O_3(ZnO)_{3.31}$	light-yellow	3 h, 625°C	0.56
ZnO	white	7 h, 625°C	2.85

Since the kinetic measurements described in the following chapters were carried out with α-Bi_2O_3 and $Bi_2O_3(ZnO)_{1.36}$ we studied these oxide systems in more detail. From the theoretical density which has a value of 8.9 and 8.2 g cm^{-3} for α-Bi_2O_3 and $Bi_2O_3(ZnO)_{1.36}$, respectively, and the assumption that the particles have a uniform spherical shape an average crystallite size of 1.3 µm and 0.6 µm for α-Bi_2O_3 and $Bi_2O_3(ZnO)_{1.36}$, respectively can be calculated. Additional information about this parameter was obtained by examining the oxides with a scanning electron microscope. Figures 3.1 and 3.2 are typical photographs of α-Bi_2O_3 and $Bi_2O_3(ZnO)_{1.36}$, respectively, obtained by this technique. The pictures clearly show that the grains are in fact agglomerates of small crystallites of various shapes. The crystallite size which follows from the

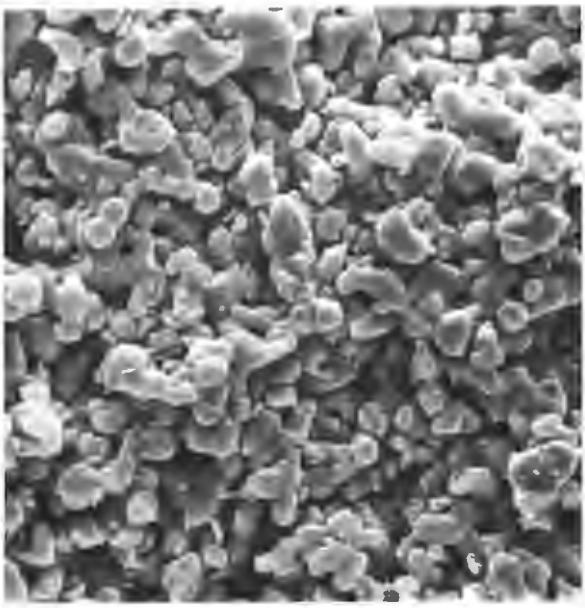

Figure 3.1 Electron micrograph of α-Bi_2O_3.

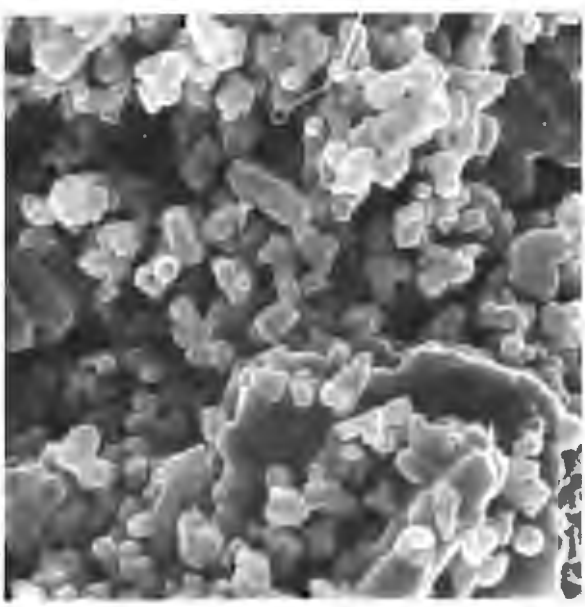

Figure 3.2 Electron micrograph of $Bi_2O_3(ZnO)_{1.36}$.

micrographs corresponds quite well with those calculated from the surface area measurements.

We also measured the pore size distribution for both oxide samples using a Carlo Erba mercury porosimeter. The results are depicted in figure 3.3. It can be concluded that in the case of α-Bi_2O_3 90% of the pore volume is made up by pores having a radius smaller than 2μm. For $Bi_2O_3(ZnO)_{1.36}$ this value amounts to 1.4 μm. Total pore volume is 0.12 and 0.20 $cm^3\ g^{-1}$ for α-Bi_2O_3 and $Bi_2O_3(ZnO)_{1.36}$, respectively. From these values an average pore radius can be calculated, using the relation

$$\text{pore radius } (r_p) = \frac{2 \times \text{pore volume}}{\text{surface area}} \quad . \qquad (1)$$

This results in a value of 0.96 μm for α-Bi_2O_3 and 0.61μm for $Bi_2O_3(ZnO)_{1.36}$. These pore diameters agree quite well with the electron micrograph pictures, i.e. the pores are between the small crystallites of which the grain is composed.

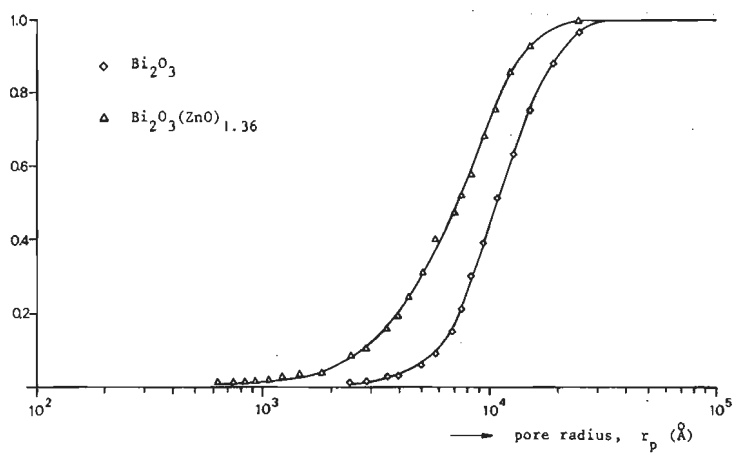

Figure 3.3 Fraction of pores with a radius smaller than r_p as a function of r_p.

3.4 CRYSTAL STRUCTURE OF α- AND γ-Bi_2O_3

A detailed investigation of the crystal structure of bismuth oxides have been carried out by Sillen (47). The X-ray results of the monoclinic form α-Bi_2O_3 can be interpreted

either by a base centered pseudo orthorhombic cell, containing 8 Bi_2O_3 molecules with the dimensions a=5.83 Å, b=8.14 Å and c=13.78 Å or by a monoclinic unit cell containing 4 Bi_2O_3 molecules with a=5.83 Å, b=8.14 Å and c=7.48 Å, β now being 67.07°. Each Bi atom is surrounded by 6 oxygen atoms, while each O-atom is surrounded by 4 Bi atoms. The distance between an oxygen and bismuth atom can have 3 values, i.e. 2.38, 2.49 or 2.53 Å.

For the body centered cubic phase Sillen (47) reports a value of 10.08 Å for the edge of the cell, permitting 24 Bi atoms per cell. Every Bi atom is surrounded by 4 oxygen atoms, three of which are identical. Interatomic Bi-O distances are 2.20 Å and 2.24 Å, respectively.

In case the bcc γ-phase is stabilized by other metal ions a structure corresponding to $Me_2\ Bi_{24}O_{40}$ is present. Now three kinds of oxygen have to be considered. The Me-atoms are surrounded by tetrahedra of type 1 oxygen, which in turn are envelopped by two spherical shells containing 12 Bi and 12 type 2 oxygen atoms. Type 3 oxygen, finally, connects the blocks thus formed. Every Bi atom is surrounded by 4 type 2 oxygen atoms, 1 type 1 and 1 type 3 oxygen atom.

3.5 PROPYLENE OXIDATION ON THE Bi_2O_3-ZnO SYSTEM. ACTIVITY AND PRODUCT DISTRIBUTION

Earlier investigations on the dimerization and aromatization of propylene and isobutene have established that for many catalysts the selectivity for dienes and aromatics depends highly on the oxygen/propylene ratio of the feed (24,26). Therefore, introductory experiments were carried out without oxygen in the feed or with a varying oxygen concentration and a fixed propylene mole fraction at a fixed contact time. Reaction conditions are given in table 3.2. From figure 3.4, which shows the relation between selectivity for hexadiene and benzene and the oxygen/propylene ratio for different catalysts, we see that at the reaction conditions employed bismuth oxide has the highest overall

Table 3.2 Reaction conditions during preliminary experiments under oxidizing and reducing conditions.

	oxidizing	reducing
contact time (W/F)	0.5 g s ml^{-1}	0.1-2 g s ml^{-1}
reaction temperature	500-550°C	550°C
reaction pressure	1 bar	1 bar
amount of catalyst	0.7 g	0.5 g
particle size	0.5 - 0.8 mm	0.5 - 0.8 mm
propylene mole fraction	0.08	0.073

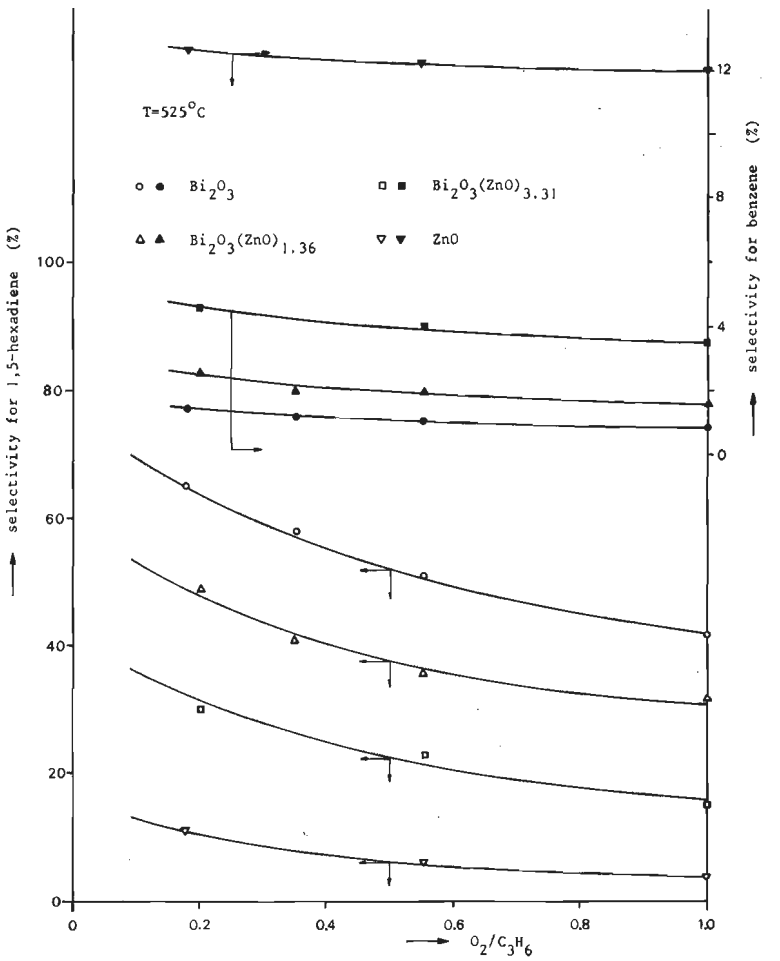

Figure 3.4 Selectivity for 1,5-hexadiene and benzene as a function of the O_2/C_3H_6 ratio. For conditions see table 3.2.

selectivity for hydrocarbon formation, while the addition of zinc oxide has the effect of improving the selectivity for benzene. The overall picture further agrees quite well with that reported earlier for other oxide systems (24,26). The corresponding propylene conversions range from about 5-15% to 22-35% at oxygen/propylene ratios of 0.2 and 1.5, respectively. When the catalysts are tested with oxygen/propylene ratios less than 0.1, stationary conditions cannot be established any more, due to oxygen deficiency in the feed mixture. During these runs appreciable reduction of the catalyst takes place. Regeneration of such a reduced sample is rarely possible.

The effect of temperature variations on the selectivity is shown in figure 3.5 for bismuth oxide. An almost independent behaviour is found in the case of 1,5-hexadiene, indicating in the first instance nearly equal activation energies

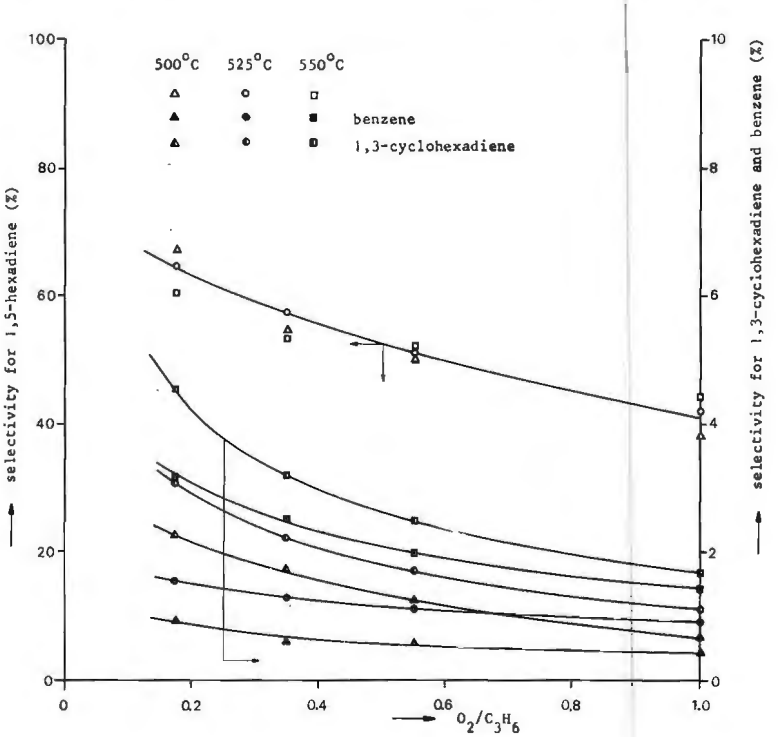

Figure 3.5 Selectivity for 1,5-hexadiene, 1,3-cyclohexadiene and benzene as a function of the O_2/C_3H_6 ratio at different temperatures. Catalyst α-Bi_2O_3. For conditions see table 3.2.

for the selective and non-selective reaction. However, two additional factors have to be considered in this connection. Firstly, from a test with a reactor only filled with silicon carbide it emerges that also a contribution from combustion of propylene by this material has to be expected. Secondly, at the reaction conditions used 1,5-hexadiene will certainly be converted to CO_2 and water by a consecutive reaction. An accurate description of these results, therefore, is only possible when the detailed kinetics of the reactions are known.

After having established that the addition of ZnO to Bi_2O_3 under overall oxidizing conditions does not result in a great improvement in selectivity for hydrocarbon formation we also tested the oxides without oxygen in the gas phase. The catalyst then provides the oxygen required for the reaction and acts as an oxidant. The reaction conditions are summarized in table 3.2. For each experiment a fresh oxidant is used. Major products in the exit stream of the reactor are carbon dioxide, 1,5-hexadiene and benzene. However, under certain conditions also small amounts of 1,3-cyclohexadiene and 3-allylcyclohexene are detected. Identification of the various hydrocarbons is carried out partly by comparing their retention times with those of the pure components partly by NMR and mass spectroscopy. For isolation the products are condensed in a cold trap cooled with liquid nitrogen and subsequently separated by preparative gas chromatography. In some cases, however, the product mixture has been injected directly on a GLC coupled with a mass spectrometer, allowing the detection of traces of unknown products. In this way also the formation of methyl(cyclo)pentanes, 3-methylcyclopentene and methylcyclohexene can be shown. The amounts, however, are so small that we decided to neglect these compounds in the kinetic study. From a test with a reactor only filled with silicon carbide it appears that all products orginate from the reaction of propylene with the oxide sample.

The results of the experiments, which are summarized in figure 3.6, show that the sum of the selectivities for

1,5-hexadiene and benzene is of the same order of magnitude for both the binary oxide system and pure bismuth oxide. Small differences in activities and partial selectivities for benzene and 1,5-hexadiene, however, are present. Zinc oxide possesses almost no selective properties under these conditions. It further appears that the selectivities for the bismuth oxide-zinc oxide system are independent of the degree of reduction up to a degree of reduction of α=25-30%. In the experiments with the bismuth oxide-zinc oxide system α always refers to the total amount of oxygen present in the oxide sample.

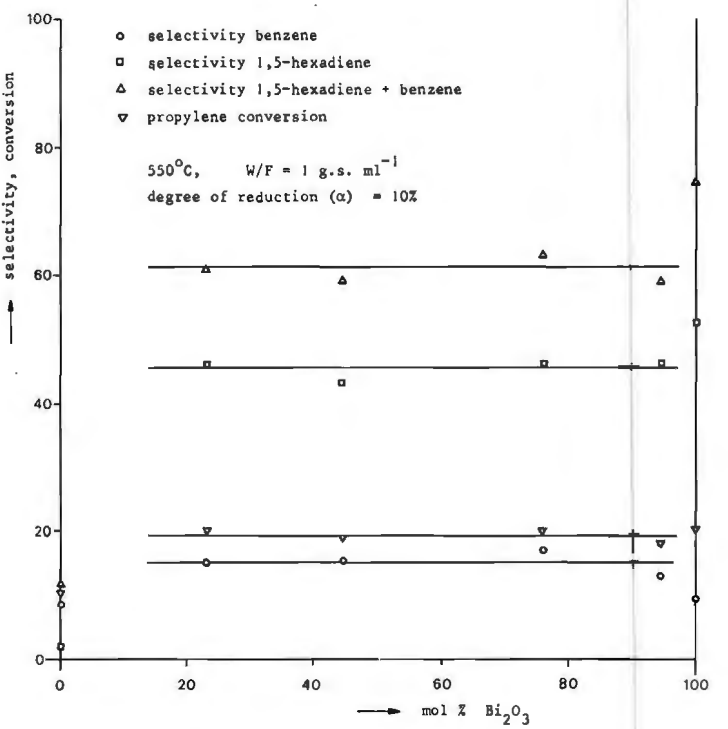

Figure 3.6 Selectivities for 1,5-hexadiene and benzene, and conversions as a function of the composition of the Bi_2O_3-ZnO system. Reducing conditions.

The data of figure 3.6 apply to a degree of reduction of the oxide of 10%. This value is calculated from the analysis results assuming only the following reactions to occur:

$$C_3H_6 + 9[O] \rightarrow 3CO_2 + 3\ H_2O$$
$$2C_3H_6 + [O] \rightarrow C_6H_{10} + H_2O$$
$$2C_3H_6 + 3[O] \rightarrow C_6H_6 + 3H_2O.$$

In case also 1,3-cyclohexadiene and 3-allylcyclohexene are formed, the reactions

$$2C_3H_6 + [O] \rightarrow C_6H_8 + 2H_2O$$
$$3C_3H_6 + 2[O] \rightarrow C_9H_{14} + 2H_2O$$

are also taken into account.

The selectivities for 1,5-hexadiene and benzene are influenced by the contact time, i.e. the selectivity for 1,5-hexadiene is largest at short contact times, while the selectivity for benzene, on the other hand, increases with contact time, indicating that this product is formed in a consecutive reaction from 1,5-hexadiene. This is illustrated by figure 3.7 which shows the course of the product concentrations with contact time for $Bi_2O_3(ZnO)_{1.36}$ at 550°C. Similar pictures are obtained for the other oxides. From the figure it can also be concluded that 1,5-hexadiene and

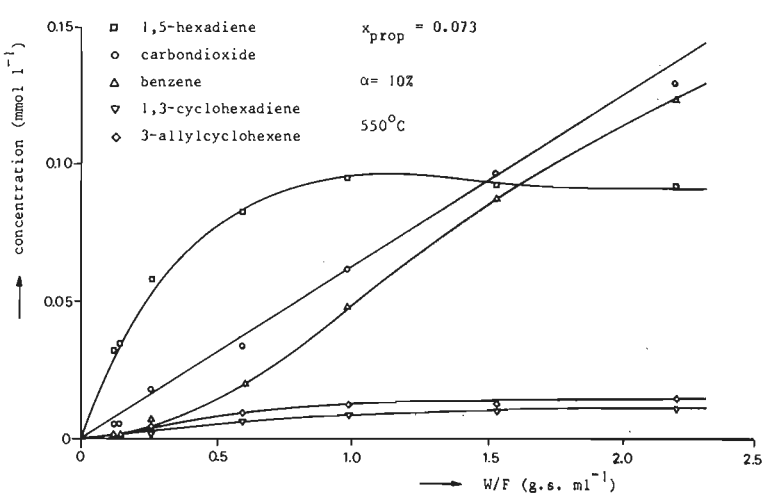

Figure 3.7 Concentrations as a function of contact time for $Bi_2O_3(ZnO)_{1.36}$. Reducing conditions. Concentrations based on conversion of 1 mole propylene.

carbon dioxide are formed in parallel reactions. The formation of 3-allylcyclohexene and 1,3-cyclohexadiene, on the other hand, is less clear. We shall return to this subject, however, in more detail in chapter 4 and 5.

In contrast with the earlier experiments the runs which are described in figure 3.7 are all made with the same oxide sample, which therefore is only reduced to a maximum value of α=15%. Experimentally it is confirmed that after reduction to this limit the activity can be restored to its original value by reoxidation with artificial air at 500°C. Even a sample that is used in 40 oxidation- reduction cycles shows no deactivation, while in the X-ray diagram no lines are present that can be attributed to metallic bismuth or zinc.

Summarizing, the results obtained so far indicate that the following reaction model is valid

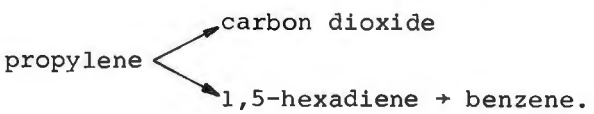

The question how far 1,5-hexadiene and benzene are oxidized in a consecutive reaction to carbon dioxide and water as well the way in which 1,3-cyclohexadiene and 3-allylcyclohexene enter the picture, will be discussed in the next chapter.

3.6 ADSORPTION OF PROPYLENE ON BISMUTH OXIDE

The adsorption experiments are carried out to gain additional information on the mechanism by which propylene is adsorbed on the oxide surface.

The adsorption of propylene is measured on both a fully oxidized and on a catalyst reduced to various degrees of reduction. This distinction is made since α-Bi_2O_3 in its reduced state may have other adsorption properties than a fully oxidized α-Bi_2O_3 sample.

3.6.1 ADSORPTION ON A FULLY OXIDIZED CATALYST

To make sure that the adsorption is studied on a fully oxidized catalyst all oxide samples are subjected to the following treatment prior to each measurement. The adsorption vessel, filled with α-Bi_2O_3 is heated to 500°C and evacuated till a pressure of $1.33\ 10^{-8}$ bar is reached. Oxygen is now admitted to the system to a pressure of 0.153 bar. The oxidation of the catalyst takes about 20 minutes. When no pressure decrease is observed any more the adsorption vessel is cooled to the temperature of the measurement and the excess oxygen is pumped off. After this treatment the oxide sample is in a fully oxidized state and the propylene adsorption can take place.

When the adsorption experiments are used to support the interpretation of kinetic data they have preferably to be carried out in the temperature range where the chemical reaction takes place (500-600°C). Determination of propylene adsorption on α-Bi_2O_3 in this temperature traject, however, is not possible as reduction of the oxide sample will take place. Therefore, we tried to adsorb propylene at 370°C, a temperature at which no reaction is observable. We found, however, that at this temperature no appreciable adsorption occurs. Two reasons may be put forward for this behaviour. Firstly, it may indicate that this temperature is situated in the transition region from physical adsorption to chemisorption. Secondly, the possibility exists that at 370°C the surface is so sparsely covered with propylene that the amount adsorbed is not measurable with our pressure gauges. To discriminate between these two possibilities we studied the propylene adsorption at low temperature since this may give an impression of the type of adsorption sites on which propylene is adsorbed by preference, provided no physical adsorption is involved at low temperature. Physical adsorption, however, ultimately will yield a full coverage of the surface with propylene.

Adsorption isotherms are measured at three temperatures, i.e. 22°C, 0°C and -10°C. The results are depicted in figure

3.8. It appears that a weak propylene adsorption is involved.

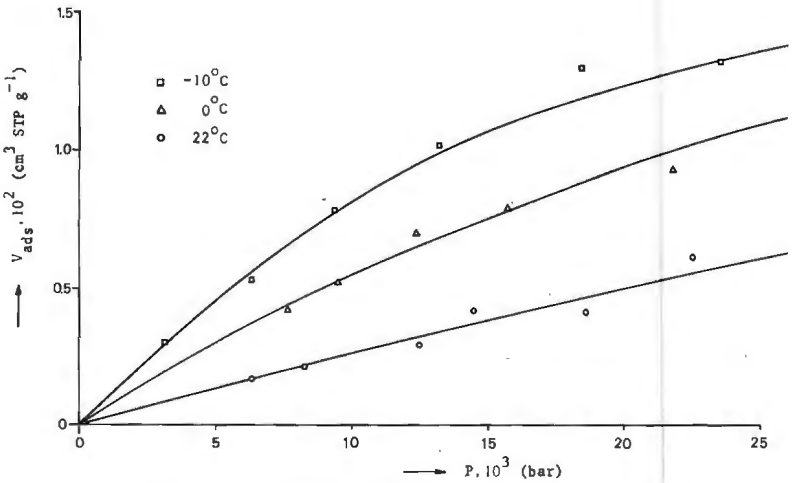

Figure 3.8 Adsorption isotherms for propylene on oxidized α-Bi_2O_3.

From figure 3.9 we see that the adsorption of propylene on α-Bi_2O_3 occurs by a single site adsorption mechanism, as the 1/V versus 1/P plot shows straight lines, corresponding to the Langmuir single site isotherm:

$$\frac{1}{V} = \frac{1}{V_m} + \frac{1}{V_m K}\,\frac{1}{P} \qquad (2)$$

where:

V : volume actually adsorbed ($cm^3\ g^{-1}$ at STP)

V_m : maximum adsorbable volume at full coverage ($cm^3\ g^{-1}$ at STP)

K : adsorption constant (bar^{-1})

P : pressure after adsorption of V $cm^3\ g^{-1}$ (bar).

The value for V_m amounts to 0.027 ± 0.004 $cm^3\ g^{-1}$ at STP. Assuming the surface area covered by one propylene molecule to be 20 $Å^2$ an estimation can be made of the total surface area occupied by propylene. This results in a 50% coverage of the oxide surface by propylene for $V=V_m$, which indicates that something else than physical adsorption is involved, since one might expect in that case the surface to be fully covered. We, therefore, conclude that the surface contains sites on which propylene is adsorbed preferably.

For the adsorption constant the following relation holds:

$$K = K_o e^{Q_{ads}/RT} \qquad (3)$$

in which K_o and Q_{ads} are in the first approximation thought to be temperature independent. From figure 3.10 a value of 26 kJ mol^{-1} for Q_{ads} and 2.4 10^{-4} bar^{-1} for K_o is found. With the aid of these parameters the entropy loss during adsorption can be calculated by the expression:

$$\Delta S_{ads} = - \frac{Q_{ads}}{T} + R \ln K. \qquad (4)$$

This results in a value of -69.2 J $(mol\ K)^{-1}$ at 25°C. Since in these experiments the heat of adsorption is derived from non-isosteric measurements we have assumed in the calculation of the entropy loss that K is independent of the degree of surface coverage.

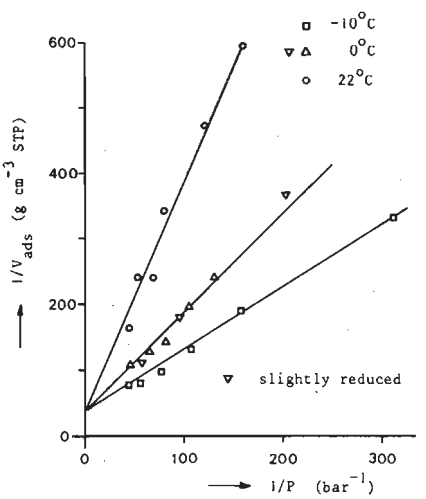

Figure 3.9 Single site adsorption of propylene on oxidized and slightly reduced α-Bi_2O_3.

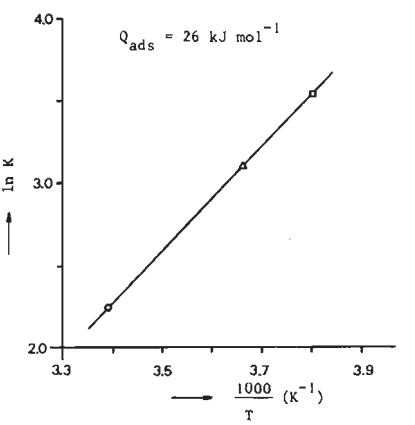

Figure 3.10 Plot for calculation of the heat of adsorption of propylene on oxidized bismuth oxide.

The total entropy of a gaseous molecule is built up from contributions of rotation, vibration and translation, each of which can be calculated theoretically. According to the procedure outlined by Wolfs (52), the following values are calculated for a gaseous propylene molecule at 25°C and P=0.12

bar, being the pressure for half coverage of the oxide surface at 25°C:

$$S_{trans} = 173.1 \text{ J (mol K)}^{-1}$$
$$S_{rot} = 92.5 \text{ J (mol K)}^{-1}$$
$$S_{vib} = 8.6 \text{ J (mol K)}^{-1}$$
$$S_{tot} = 274.2 \text{ J (mol K)}^{-1}.$$

If the adsorption was very strong one would expect that all translationary degrees of freedom would be lost. The resulting entropy loss could be compensated for a small part by new vibrational modes, i.e. perpendicular on the surface, but with strong adsorption an entropy loss of say 150 J (mol K)$^{-1}$ at 25°C and 0.12 bar stands to reason. The much lower entropy loss from the adsorption data indicates a mobile adsorption. When propylene would be adsorbed as a two dimensional gas an estimation can be made of the entropy loss by using Kemball's (53,54) equation for the translational entropy of a perfect two dimensional gas:

$$_2S_{trans} = R \ln(MTA) + 275.7 \qquad (5)$$

In this formula $_2S_{trans}$ is expressed in J (mol K)$^{-1}$, M is the molecular weight, T the temperature in K and A is the area available per molecule in cm^2, obtained from the volume of 1 mol.At 25°C and 0.12 bar we calculate with this formula an entropy loss of 59.1 J (mol K)$^{-1}$, which is of the same order of magnitude as the value obtained with equation (4).

3.6.2 ADSORPTION OF PROPYLENE ON REDUCED α-Bi_2O_3

The adsorption of propylene is in the first instance studied on a slightly reduced α-Bi_2O_3 sample. This state of reduction is obtained as follows. To an oxidized α-Bi_2O_3 sample propylene (0.13 bar) is admitted at room temperature. After the adsorption equilibrium is established the excess propylene is pumped off, the system is closed and the temperature is raised to 500°C. At this temperature reduction of the catalyst by the adsorbed propylene takes place. When no

pressure change is observed any more the oxidation products are pumped off and the catalyst is cooled to the temperature at which the adsorption measurement is carried out. After each measurement the oxide sample is again brought in the fully oxidized state according to the procedure described in the preceding paragraph.

Figure 3.9 shows that the adsorption isotherm at $0^{o}C$ measured in this way is identical to the $0^{o}C$ curve found with the fully oxidized catalyst. The reason for this behaviour is probably the fact that the surface reduction brought about by the adsorbed propylene will cause a transport of oxygen ions to the surface finally resulting in an equal oxygen concentration through the lattice and an almost fully oxidized surface. To investigate the dependence of propylene adsorption on the oxidation state of the surface, the adsorption behaviour is therefore studied after reduction of the oxide sample to a certain well defined degree of reduction.

The reduction is carried out with a 10% propylene-nitrogen mixture at $520^{o}C$ in a special adsorption vessel in which the same conditions can be maintained as in the flow reactor used for the kinetic measurements. After the desired degree of reduction is reached the catalyst is evacuated at $520^{o}C$ and subsequently cooled to the temperature for the adsorption measurement. Propylene adsorption is determined after reduction of α-Bi_2O_3 to 3.5, 7.5 and 15%. High degrees of reduction are not allowed since then clustering of bismuth atoms may take place, resulting in a decrease of the surface area and thus of the adsorption behaviour.

Table 3.3 Dependence of propylene adsorption at $0^{o}C$ on degree of reduction of α-Bi_2O_3.

Degree of reduction (%)	0	3.5	7.5	15
Pressure (bar)	$13.6\ 10^{-2}$	$13.7\ 10^{-2}$	$13.6\ 10^{-2}$	$13.3\ 10^{-2}$
Amount of propylene adsorbed (cm^3 STP g^{-1})	$0.7\ 10^{-2}$	$1.0\ 10^{-2}$	$1.4\ 10^{-2}$	$0.68\ 10^{-2}$

From table 3.3 we see that with increasing degree of reduction first an increase of the propylene adsorption followed by a decrease occurs. This indicates that the number of propylene adsorption sites increases upon reduction. We, therefore, assume that the adsorption of propylene takes place on oxygen vacancies on the surface. The decrease at α=15% may already be due to agglomeration of Bi-atoms.

CHAPTER 4

Reaction Kinetics Part one - Bismuth Oxide as Oxidant

4.1 INTRODUCTION

In this chapter we shall focus our attention on the oxidation of propylene to 1,5-hexadiene and of 1,5-hexadiene to other C_6-hydrocarbons using bismuth oxide as oxidant. The kinetics of these reactions have been studied both in a fixed bed reactor and in a thermobalance, each having its own merits. Experiments that are carried out in the fixed bed reactor resemble most practical applications, but yield no direct information about the activity decrease of the oxide. To investigate this activity loss during the reduction process the thermobalance is an eminently suited device, especially when it is coupled to a gas chromatographic system to analyse the product gas. In both cases the kinetic measurements can be complicated, however, by mass and heat transfer to and inside the oxide particle. These effects particularly have to be taken into account for the experiments in the thermobalance, since in this case the gases are not passed through but over the oxide particles.

In the next paragraph we shall deal in more detail with the mass transfer effects as well as with the theories which can be applied to gas-solid reactions like the reduction of oxides. Thereafter we shall discuss the results of the reduction of α-Bi_2O_3 with propylene and 1,5-hexadiene in the flow reactor. This will be followed by a discussion of the reduction with hydrogen, propylene, 1,5-hexadiene and benzene in the thermobalance apparatus. Finally, we shall consider the influence of various oxidation-reduction cycles on the activity pattern of α-Bi_2O_3 as well as some parameters that are important for the reoxidation process.

4.2 *THEORY OF REDUCTION OF OXIDES*

The reduction of oxides with gaseous substrates is usually described as a gas-solid reaction of the type

$$aA(gas) + B(solid) \rightarrow C(gas) + D(solid).$$

As far as the solid B is concerned the diffusion of oxygen ions through the lattice may play an important role in the reduction process. Models that take this aspect into account have been developed by Batist et.al. (55) for the butene reduction of bismuth molybdate and by Steenhof de Jong et.al. (56) for the reduction of bismuth uranate with toluene. Since it will turn out in this chapter that in the case of α-Bi_2O_3 reduction diffusion in the solid phase is not a limiting factor, we shall not deal further with these kind of models.

In addition to diffusion in the solid phase a number of other processes may have a limiting effect on the reaction rate, i.e.

- heat and mass transfer between gas and oxide particle
- heat and mass transfer inside the oxide particle
- change of activity during the reduction process.

The latter phenomenon is an important factor to account for. Reasons that may be responsible are decrease of active surface area, clustering of bismuth atoms, decreasing oxygen concentration of the solid and increase of resistance for diffusion through the product layer of bismuth metal.

When we consider a solid particle in a stream of gas the reactants have to be transported across the boundary layer around the particle. This process, which can be described in terms of a mass transport coefficient, k_m, will be strongly dependent on the fluid dynamics of the system. Above a certain Reynolds number, however, the mass transport and therefore the rate of reactions will be hardly influenced by changes of the flow conditions around the particle. Provided that then the mass transport coefficient is large as compared to the surface

reaction rate constant the concentration drop over the gas film is small and we may consider the concentration at the outside of the particle to be equal to that of the bulk gas phase.

When the particle is composed of highly porous material the gas may easily diffuse into the interior of the solid and the reaction will take place homogeneously throughout the solid. In this case a *homogeneous* model is involved. Depending on the ratio of the rate of diffusion in the particle and the chemical reaction in the particle various possibilities exist. Thus, when the rate of diffusion in the particle is high in comparison with the chemical reaction rate the concentration of gas A in the bulk gas phase will be equal to that in the particle. The reaction zone then comprises the whole particle and the oxygen concentration of the solid is independent of the radius, R, of the particle. In case both rates are of the same order of magnitude a concentration gradient exists in the particle. As a consequence the particle will be firstly exhausted at the outside, resulting in the formation of a product layer at the exterior of the particle. The gaseous reactants and products now have to diffuse through this layer before reaction can take place. When the diffusion through this product layer occurs in a way different from that through the porous oxide particle, the reduction process will from the beginning of product layer formation occur in two stages. We are then dealing with a *two stage model*. In case both diffusion coefficients are equal still the homogeneous model is involved.

A more general treatment of the zone reaction model starts from the existence of *three zones*, i.e. a product layer, a reaction zone and an unreacted core (57). The reduction process will then also take place in three stages (See figure 4.1). The width of the reaction zone, however, determines whether a homogeneous, a two stage or a three stage model is involved. A special case of the three stage model arises when the chemical reaction is very fast compared to the diffusion of gas A into the particle. The reaction zone will then be confined to the

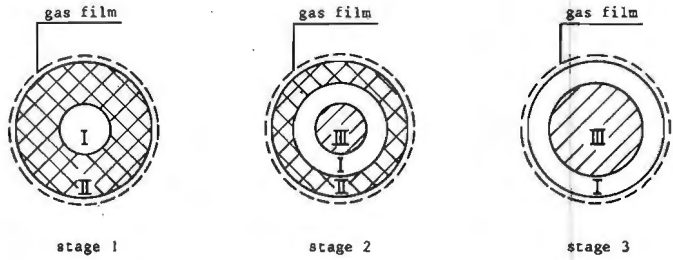

Figure 4.1 Three zone reaction model for gas-solid reactions. I: reaction zone; II: product layer; III: unreacted core.

interface between the product layer and the non-reacted solid and one deals with the socalled *unreacted shrinking core model*. This model is also applicable when the particle is hardly permeable to gas A.

A mass balance for gaseous reactant A and solid reactant B in a spherical shell yields the following differential equations for diffusion of gas A into the porous solid and consumption of oxygen from the solid:

$$\varepsilon \frac{\partial C_A}{\partial t} = ID_{eff}\left(\frac{\partial^2 C_A}{\partial r^2} + \frac{2}{r}\frac{\partial C_A}{\partial r}\right) - r_A \qquad (1)$$

$$-r_B = \frac{\partial C_B}{\partial t}, \text{ while } r_A = a r_B, \text{ and} \qquad (2)$$

where:

ε is the porosity of the solid particle; ID_{eff} is the effective diffusion coefficient of gas A; C_A is the substrate concentration at radial distance r; t is the time; r_A and r_B are rates of reaction. The equations are valid for the case that no product layer has yet been formed. Moreover, it is assumed that during the reduction the physical properties of the particle remain constant. For the initial and boundary conditions we can write:

$$ID_{eff}\left(\frac{\partial C_A}{\partial r}\right) = k_m (C_{A,o} - C_A) \quad \text{at } r=R \text{ (outside of particle)} \qquad (3)$$

$$\frac{\partial C_A}{\partial r} = 0 \quad \text{at } r=0 \text{ (centre of particle)} \qquad (4)$$

$$C_B = C_{B,o} \qquad \text{at } t=0 \text{ and } 0 < r < R \qquad (5)$$

When mass transfer across the boundary layer may be neglected equation (3) reduces to

$$C_A = C_{A,o} \qquad \text{at } r=R. \qquad (6)$$

For solution of the equations (1) - (5) usually the pseudo steady state approximation is assumed, which states that the rate of conversion of the solid material is much lower than the rate of diffusion of the reactant gas (58,59). The left hand side (=accumulation term) of equation (1) may then be neglected.

The rate at which oxygen is consumed from the oxide will be dependent on C_A, C_B and the area available for reaction. Two kind of models appear to be relevant in this connection, i.e. the volumetric reaction model and the grain model. Both are schematically shown in figure 4.2.

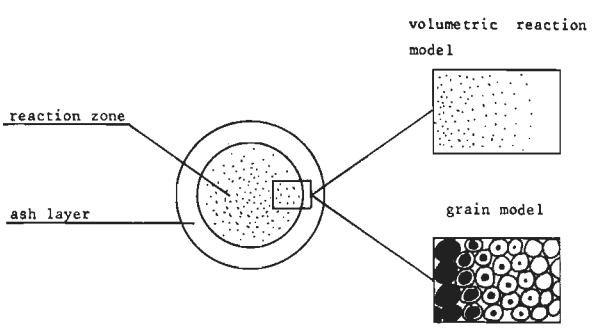

Figure 4.2 The volumetric reaction and grain model.

The volumetric reaction model is often invoked when the solid is highly porous. This will be the case when the particle is composed of very small grains of various sizes, which form together the porous structure or if the solid is embedded in a porous inert material. If we assume that for the reduction process the diffusion of oxygen ions through the solid is fast compared to the chemical reaction we may consider the concentration of oxygen in a surface layer equal to that in the bulk and write:

$$[O]_{bulk} = [O]_{surface} = [O]. \tag{7}$$

For the general rate equation we then get

$$-a \frac{\partial C_B}{\partial t} = -b \frac{\partial [O]}{\partial t} = k' [O]^n C_A, \tag{8}$$

assuming the reaction to be first order with respect to the gaseous reactant A and nth order with respect to the bulk oxygen concentration.

If we suppose that no limitation exists due to diffusion of gas into the particle equation (8) can be integrated directly, provided C_A is assumed to be independent of time. Two special cases have to be considered. When n is zero the rate is independent of the degree of reduction and there exists a linear relationship between the degree of reduction and the time:

$$\alpha = kO_o C_A t \text{ with } \alpha = \frac{O_o - O_t}{O_o} \tag{9}$$

where: O_o: number of oxygen atoms present at t=0.
O_t: number of oxygen atoms present at t=t.

When, on the other hand, the reaction is first order with respect to the oxygen concentration the time necessary for complete reduction becomes infinite. Equation (8) now changes to

$$- \frac{d[O]}{dt} = k[O]C_A = kO_o C_A (1-\alpha), \tag{10}$$

which after integration yields

$$- \ln(1-\alpha) = kC_A t. \tag{11}$$

Experiments that can be described by equation (9) or (11) are said to comply with the volumetric reaction model with zero or first order oxygen dependence, respectively.

In addition to the volumetric reaction model also the grain model has been found to apply under certain circumstances; especially when the solid material is composed of small highly dense grains which all react separately according

to the unreacted shrinking core model. Again two special cases can be discerned, viz. either the chemical reaction at the surface of the small grains or the diffusion of gases through the product layer is rate controlling. When the rate of diffusion of gas in the oxide particle is high compared with the chemical reaction rate the final equations describing the reduction process for these two special conditions are simple rate expressions (60). When, on the other hand, diffusion into the particle also becomes important equation (2) has to be solved in combination with equation (1) in the pseudo steady state. For the case that the chemical reaction can be described by the grain model this has been done by Papanastassiou (61) and Szekely (62), while the combination of gas diffusion into porous particles with a zero order volumetric reaction model has been worked out by Ishida (63) and Mantri (57).

No general solutions are available in the literature concerning the solution of equation (1) (without the accumulation term) together with a first order volumetric reaction model. Estimation of the influence of diffusion of gas in the porous particle, however, is possible in the very first stage of the reaction, since then the solutions for the zero order volumetric rate model can be applied. As in the course of the reaction the rate declines due to a decrease of the oxygen concentration of the solid, the absence of diffusion effects at the beginning of the reduction process implies that also in a further stage of the reaction diffusion will not be significant. For the solution of differential equation (1) in combination with a zero order volumetric reaction model and boundary conditions (3), (4) and (6) the following expression is obtained:

$$\frac{C_A}{C_{A,o}} = \frac{\sinh(\phi\rho)}{\rho \sinh \phi} \qquad (12)$$

where: $\rho = r/R, \quad \phi = R \left(\frac{akO_o}{ID_{eff}}\right)^{\frac{1}{2}}$.

When, however, we are interested in the overall conversion in a further stage of the reaction the equations (1) and (10)

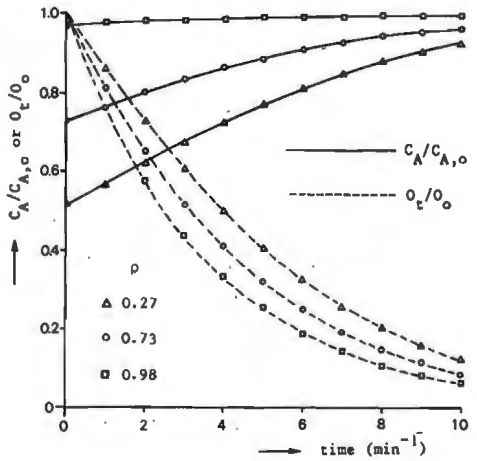

Figure 4.3 Substrate and bulk oxygen concentration as a function of time at various radial distances. ϕ=2.23; ψ=4.66 10^{-3}.

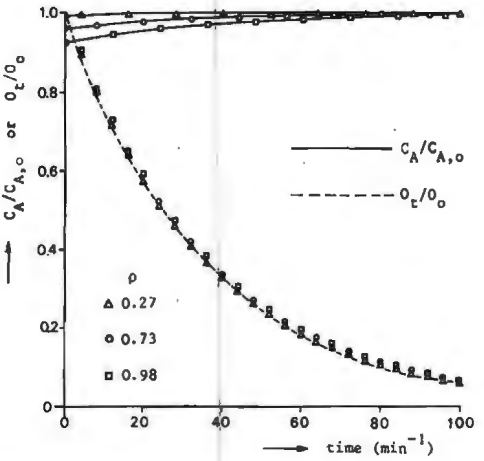

Figure 4.4 Substrate and bulk oxygen concentration as a function of time at various radial distances. ϕ=0.71 ; ψ=4.66 10^{-4}.

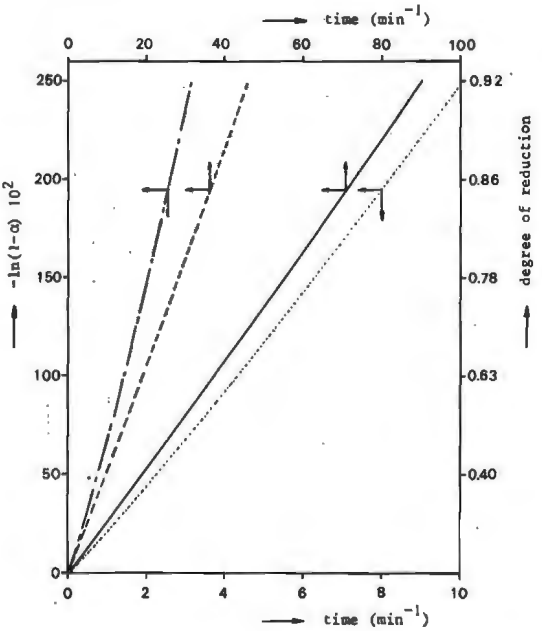

Figure 4.5 The volumetric reaction model with first order bulk oxygen dependence with and without influence of gas diffusion in the oxide pellet.

have to be solved numerically. For certain general conditions this has been done by the orthogonal collocation method (64) using five collocation points. Details of the numerical solution method are given in appendix I. The results of the calculations for various values of the parameters ϕ and $\psi(=kC_{A,o})$ are given in figure 4.3 - 4.5. Figure 4.3 shows the course of the solid and gas concentration as a function of time for various radial distances when diffusion of gas into the partical is important. We see that as the reaction proceeds the concentration gradient decreases. From figure 4.4 we may conclude that when $\phi < 1$ the influence of diffusion of the gaseous reactant may be neglected. When for the various cases the overall degree of reduction of the particle is calculated it follows that even when the reduction process is highly diffusion limited (ϕ=5) a plot of $-\ln(1-\alpha)$ versus time yields a straight line up to α=50%, as is shown by figure 4.5. One therefore, has to realize that when experimentally a linear relationship is found between $-\ln(1-\alpha)$ and the time this not necessarily means that the reaction is not diffusion limited. Whether diffusion of the gaseous substrate plays a role in the reduction process may, however, be verified by considering the temperature behaviour of the rate constant calculated from equation 11.

4.3 REDUCTION OF α-Bi_2O_3 IN THE FLOW SYSTEM

4.3.1 MASS AND HEAT TRANSFER EFFECTS IN THE FLOW REACTOR

When the kinetics of a gas-solid reaction are studied in a fixed bed reactor it is advantageous for the interpretation of the kinetic results that the fluid flow in the reactor can be considered to be an ideal plug flow. Then the equations resulting from the mechanical energy, heat and mass balance are most easily to be solved. Conditions that have to be fulfilled are that no mixing between the volume elements occurs in the flow direction, i.e. the diffusional transport can be neglected with respect to that of convection, while also the

axial flow rate as well as the properties of the fluid are constant over the cross section. Both requirements, however, are not always satisfied. Reasons that may be responsbile are:

- wall effects,
- temperature gradients in transversal direction,
- mass transport due to dispersion both in axial and radial direction.

The flatness of the velocity profile mostly can be guaranteed by a proper choice of the number of mixing cells in radial direction. The presence of radial temperature gradients, on the other hand, will be strongly dependent on the exothermicity of the reaction. When the experiments are carried out in a differential reactor the heat effect generally will be small, so that also this inconveniency can be circumvented. The influence of axial dispersion on the concentration profile in a plug flow reactor appears to be negligible when the Péclet number for mass transport ($Pé_L = \bar{u}L/\varepsilon ID_{ax}$) > 60 (65). Since in laboratory reactors the Reynolds number ($\rho\bar{u}d_p/\mu$) usually is in the order of 0.5, which implies that $Pé_{dp}$ ($=ud_p/\varepsilon\ ID_{ax}$) $\tilde{>}$ 0.5 (66), axial mixing may be neglected when L/d_p > 120. During our measurements this condition generally was satisfied.

The possible influence of heat and mass transfer between fluid and particle on the kinetic measurements may be estimated according to the procedure of Yoshida et.al. (67) and of Satterfield and Sherwood (68). The calculations have shown that when α-Bi_2O_3 is applied as an oxidant the temperature difference across the boundary layer during the kinetic measurements only amounts to 0.1 °C, while the ratio of the concentration drop and the average bulk concentration only has a value of 0.02. A second factor that supports the conclusion of negligible heat and mass transfer across the boundary layer is the fact that the activation energies for the chemical reactions amount to 85-125 kJ mol^{-1}. Reactions in which film diffusion is important generally have activation energies in the order of 4-8 kJ mol^{-1}.

The effects of heat and mass transfer inside the catalyst particle can be expressed by the effectiveness factor, which

is defined as the ratio of the reaction rate under the experimental conditions and the reaction rate when no pore diffusion or heat effect is involved. Calculation of the effectiveness factor according to the procedure outlined by Weisz and Hicks (69) has shown that in all cases this parameter has a value close to one. Moreover, it has been experimentally confirmed that experiments with small particles gave the same results as those with large particles.

4.3.2 OXIDATION OF PROPYLENE

In paragraph 3.5 we have already mentioned that the selectivities for the various products are strongly dependent on the contact time in the reactor. Therefore, we paid in the first place attention to this relation. Thus, at a fixed propylene inlet concentration and at a fixed temperature the concentrations are measured as a function of time for various W/F-values. For each run a fresh oxide sample is used. The course of the product concentrations with time for a typical experiment is shown in figure 4.6.a. The concentrations extrapolated to t=0, i.e. to a fully oxidized oxide sample, are

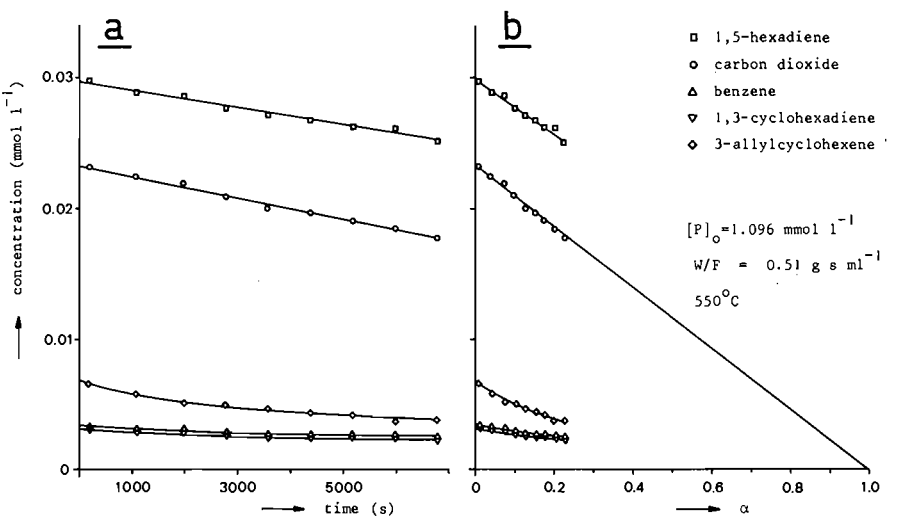

Figure 4.6 Product concentrations as a function of time and of degree of reduction. Reduction of α-Bi_2O_3 with propylene in flow reactor.

plotted in figure 4.7 as a function of the W/F for T=550°C. At W/F = 1 g s ml^{-1} the propylene conversion amounts to 10%. We see that carbon dioxide and 1,5-hexadiene are formed by a parallel reaction from propylene, while benzene and possibly 1,3-cyclohexadiene and 3-allylcyclohexene result from a consecutive reaction from 1,5-hexadiene. The course of the carbon dioxide concentration with W/F points to a zero order propylene dependency. One has to remember, however, that the formed products may be also converted to carbon dioxide and water, so that the carbon dioxide concentrations at higher contact time originate both from propylene and from the formed C_6-C_9 hydrocarbons.

Although the concentration versus duration curves are useful in yielding the concentrations at time zero, they hardly give information about the way in which the oxygen is consumed from the oxide. For this purpose curves in which the concentrations or rate of reactions are plotted against the degree of reduction of the oxide are more suitable. In figure 4.6.b

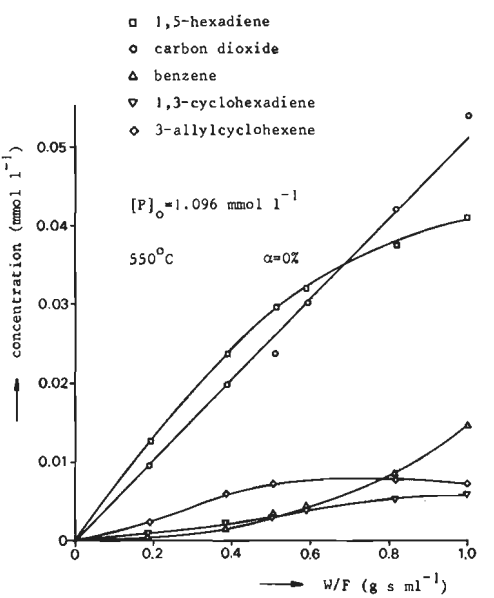

Figure 4.7 Reduction of α-Bi_2O_3 with propylene in flow reactor. Product concentrations as a function of contact time.

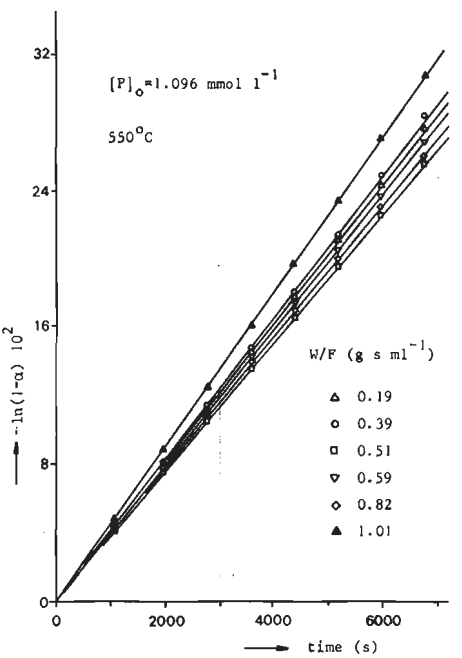

Figure 4.8 Reduction of α-Bi_2O_3 with propylene in flow reactor. Check of first order volumetric reaction model for the overall reduction.

the concentrations of the experiment described by figure 4.6.a are replotted against the degree of reduction, calculated from the analysis results as outlined in paragraph 3.5. We see that for carbon dioxide the concentration decreases linearly with the degree of reduction. Since in this case the concentration in the exit stream has a direct relation to the rate of oxygen depletion this indicates that the oxygen consumption for the aselective reaction proceeds according to equation (10) i.e. the volumetric reaction model with first order bulk oxygen dependence. For the other products no such single relation between concentration and degree of reduction is found. The 1,5-hexadiene concentration decreases less than linear with the degree of reduction, which may indicate that reduced sites play a role in this reaction.

In figure 4.8 we have plotted $-\ln(1-\alpha)$, α being the degree of reduction calculated from a total product analysis, versus time for all our W/F values. It turns out that the overall oxygen depletion of α-Bi_2O_3 up to α=30% may be well described by the volumetric reaction model. It has to be realized in this connection that for the conversion of 1 mole propylene to carbon dioxide and water 18 times as much oxygen has to be supplied by the oxidant than for the conversion of 1 mole propylene to 1,5-hexadiene. Consequently, even when the selectivity for 1,5-hexadiene is in the order of 90%, as is the case for the experiments described by figure 4.7, the oxygen consumption for the CO_2-formation will be two times that for the 1,5-hexadiene formation. The total degree of reduction will, therefore, be primarily determined by the oxygen consumption of the aselective reaction. Further, it follows from figure 4.8 that the oxygen depletion is almost independent of the contact time. This agrees quite well with figure 4.7, which shows that at low contact time the decrease in rate of 1,5-hexadiene formation is compensated by an increase of the other C_6-hydrocarbons.

Since according to figure 4.7 only carbon dioxide and 1,5-hexadiene are formed directly from propylene we decided to study the kinetics of these two reactions in a differential reactor. All measurements are carried out at W/F-values

between 0.07 and 0.085 g s ml^{-1}. Under these conditions propylene conversions are always less than 2%. Reaction rates for carbon dioxide and 1,5-hexadiene formation as a function of the degree of reduction for various inlet concentrations of propylene are depicted in figures 4.9.a and 4.9.b, respectively. Since at a fixed degree of reduction the following relations can be assumed to hold fairly accurately:

$$\frac{d[HD]}{dW/F} = k_{HD}\,[P]^m \quad \text{and} \quad \frac{d[CO_2]}{dW/F} = k_{CO_2}\,[P]^n \tag{13}$$

or

$$\ln r_{HD} = \ln k_{HD} + m \ln[P] \tag{14}$$

and $$\ln r_{CO_2} = \ln k_{CO_2} + n \ln[P], \tag{15}$$

in which [P] represents the propylene concentration and m and n are reaction orders, we may determine the order of the parallel reactions in propylene from plots of ln (Δ[HD]/ΔW/F) and ln ($\Delta[CO_2]$/ΔW/F) versus the ln of the inlet concentration of propylene $[P]_o$. From figure 4.10 we calculate a reaction order of 1 for the 1,5-hexadiene formation and of 0.9 for the CO_2-formation. Both reaction orders are independent of the degree of reduction up to α=30%. It further turns out from figure 4.11 that again the overall reduction can be described by the first order volumetric reaction model. For the total conversion of propylene to both 1,5-hexadiene and carbon dioxide a reaction order in propylene of 0.96 may be calculated.

The influence of the temperature is studied at various propylene inlet concentrations. Figure 4.12 shows the rates of formation of carbon dioxide and 1,5-hexadiene as function of the degree of reduction at a propylene mole fraction of 0.182 and the temperature as variable. Similar curves have been obtained for other propylene inlet concentrations. From figure 4.13 we can conclude that also at different temperatures the first order volumetric reaction model holds for the overall reduction of α-Bi_2O_3.

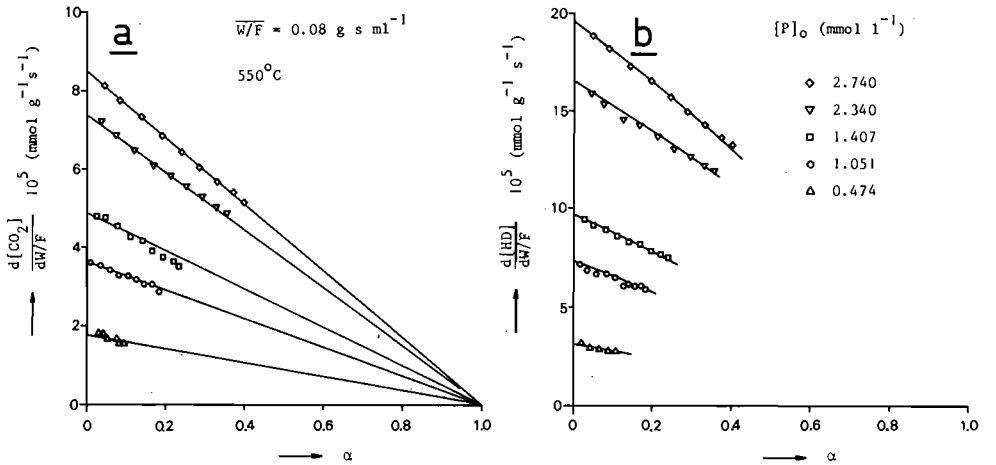

Figure 4.9 Rate of formation of carbon dioxide (a) and 1,5-hexadiene (b) as a function of the degree of reduction. Reduction of α-Bi_2O_3 with propylene in flow reactor at various inlet concentrations.

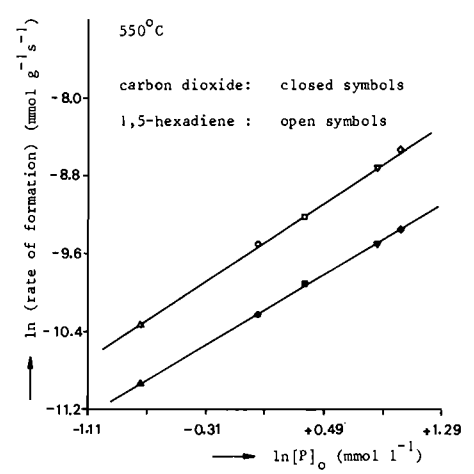

Figure 4.10 Rate of formation of 1,5-hexadiene and carbon dioxide at α=0% as a function of the propylene inlet concentration. Flow reactor.

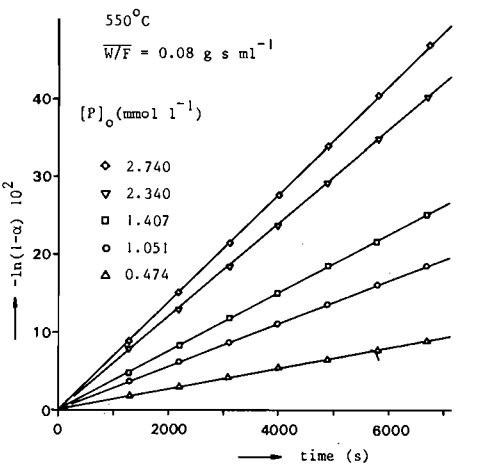

Figure 4.11 Check of first order volumetric reaction model for the reduction of α-Bi_2O_3 with propylene at various inlet concentrations. Flow reactor.

The temperature dependence of the rate constants k_{HD} and k_{CO_2} at α=0% calculated with equation (14) and (15) is shown in figure 4.14. For the 1,5-hexadiene formation the Arrhenius plot yields a value of 93 kJ mol^{-1}, while for the carbon dioxide formation a value of 129 kJ mol^{-1} is found. At higher degrees of reduction these energies of activation hardly undergo a change.

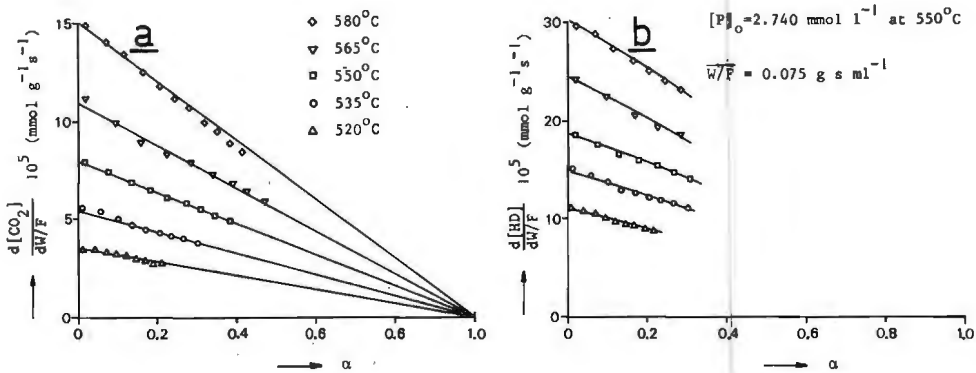

Figure 4.12 Rate of formation of carbon dioxide (a) and 1,5-hexadiene (b) as a function of the degree of reduction. Reduction of α-Bi_2O_3 with propylene in flow reactor at various temperatures (x_{prop}=0.182).

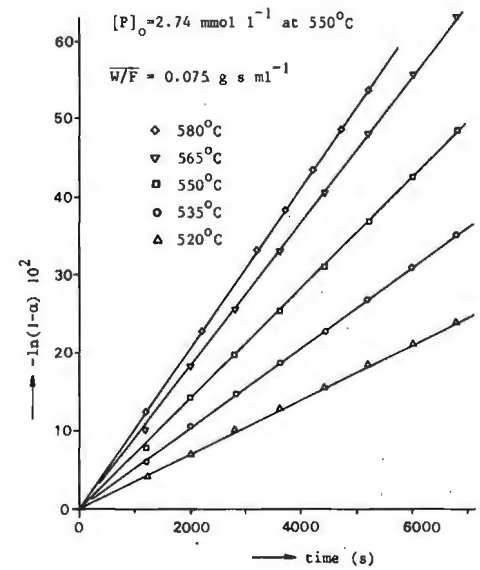

Figure 4.13 Check of first order volumetric reaction model for the reduction of α-Bi_2O_3 with propylene at various temperatures. Flow reactor (x_{prop}=0.182).

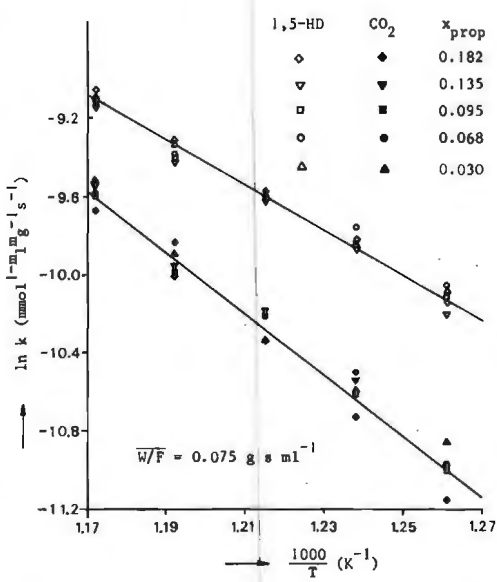

Figure 4.14 Arrhenius plot for the rate of formation of carbon dioxide and 1,5-hexadiene at α=0%. Flow reactor.

Sofar we have dealt only with the experiments in which α was lower than ∿30%. This procedure has been chosen since further reduction was expected to cause problems in view of the formation of bismuth metal. A high degree of reduction would also mean an extremely long duration of the experiment. For both a qualitative and quantitative description of the role

which the degree of reduction plays in the 1,5-hexadiene formation it is desired to know how this formation takes place in a further stage of the reduction. Therefore, we continued some experiments till very high degrees of reduction, an example of which is depicted in figure 4.15. We see that indeed the carbon dioxide formation obeys equation (10), i.e. the volumetric reaction model with first order oxygen dependence, over the whole traject. The dependence of the 1,5-hexadiene formation on the degree of reduction, on the other hand, may be well described by an expression of the form:

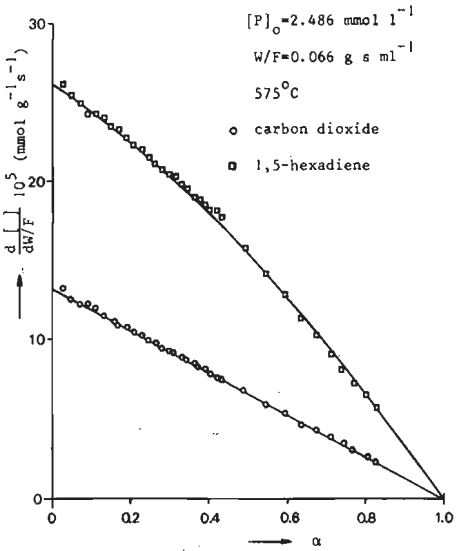

Figure 4.15 Rate of formation of 1,5-hexadiene and carbon dioxide as a function of the degree of reduction. Reduction of α-Bi_2O_3 with propylene in flow reactor.

$$\frac{d[HD]}{dW/F} = k_{HD}(\alpha_o+\alpha)(1-\alpha)\ [P] \qquad (16)$$

This equation can be derived as follows. When the adsorption mode of propylene resulting in 1,5-hexadiene involves the dissociation in a hydrogen atom and an allyl species, the hydrogen atom likely will be bonded to an oxygen ion of the surface leading to the formation of a hydroxylgroup. Further, when all oxygen ions at the surface have equal tendency to bind a hydrogen atom the number of oxygen ions will be proportional to $(1-\alpha)$, assuming the degree of reduction in the surface layer to be equal to that of the bulk. The latter will be the case as diffusion of oxygen through the lattice is fast compared to the chemical reaction. In addition to the adsorption of the hydrogen atom also the allyl has to be bonded to the surface. We assume that for this a surface vacancy is required. As the reduction proceeds the number of vacancies also will increase. If we put

N_1 : number of active vacancies originally present on the

surface,

N_2 : number of oxygen ions originally present on the surface,

α_o : N_1/N_2,

α : fraction of the N_2 sites that is reduced,

then the number of reduced and oxidized sites at a certain degree of reduction will be given by $N_2\ (\alpha_o+\alpha)$ and $N_2\ (1-\alpha)$, respectively. The number of combinations of vacancies and oxygen ions at the surface will then be proportional with $N_2^2\ (\alpha_o+\alpha)(1-\alpha)$, so that for the rate of 1,5-hexadiene formation, which is proportional with this number of combinations of vacancies and oxygen ions as well as with the propylene concentration equation (16) is obtained. Experimentally for α_o a value of 2.8 is found, which means that originally there are more active vacancies on the surface than oxygen ions.

Since for the formation of 1,5-hexadiene two allyl species are required one should expect an order in propylene for this reaction greater than one, assuming the reaction between two allyl species to be the rate determining step. It appears, however, that in a broad range of propylene partial pressures the reaction order in propylene is one. Various reasons may be put forward for this behaviour. The reaction between a strongly adsorbed propylene molecule and a propylene molecule from the gas phase, for instance, yields a first order propylene dependence (Eley-Rideal mechanism). However, the fact that the adsorption study indicates a weak propylene adsorption while a first order behaviour in the substrate concentration has also been found for reactions involving only one molecule does not support this mechanism. The supposition that the adsorption of propylene and in particular the abstraction of hydrogen atom from the propylene molecule, determines the rate of 1,5-hexadiene formation, however, is more appropriate:

1. Adsorption

$$\square_s + C_3H_6 \rightleftharpoons (C_3H_6)_{ads}$$

2. Abstraction of hydrogen atom

$$(C_3H_6)_{ads} + O_s \rightleftharpoons \overset{C_3H_5}{\square_s} + \overset{H}{O_s}$$

3. Chemical reaction

$$\begin{matrix} H \\ | \\ O_s \end{matrix} + \begin{matrix} C_3H_5 \\ | \\ \square_s \end{matrix} + \begin{matrix} C_3H_5 \\ | \\ \square_s \end{matrix} + \begin{matrix} H \\ | \\ O_s \end{matrix} \xrightarrow{\text{fast}} C_6H_{10} + H_2O + 3\square_s + O_s$$

The observed activation energy applies to step (2), i.e. the abstraction of the hydrogen atom.

The fact that the rate of carbon dioxide formation decreases linearly with the degree of reduction also can be interpreted in terms of propylene adsorption. When we assume in this case that the oxygen ions in the surface act as adsorption sites the rate will be first order in the oxygen density of the surface and will decrease linearly with the degree of reduction.

The reaction order in propylene of 0.9 for the aselective reaction may be described with a Langmuir-Hinshelwood model:

$$r_{CO_2} = \frac{k_1[P]}{1+k_2[P]}, \qquad (17)$$

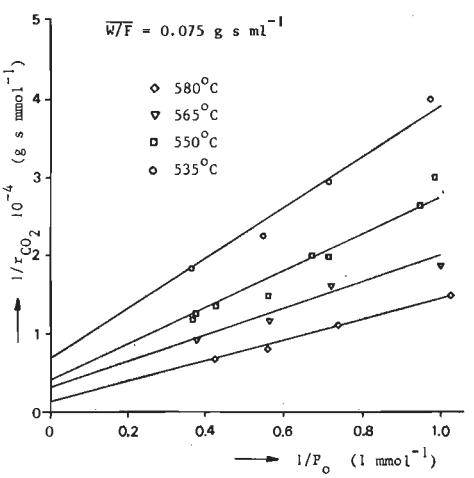

Figure 4.16 Plot of $1/r_{CO_2}$ versus $1/P_o$. Check of equation (17) for the aselective reaction.

as is illustrated by figure 4.16 where a plot of $1/r_{CO_2}$ versus $1/P_o$ yields straight lines at various temperatures. For the apparent activation energy a value of 124 kJ mol^{-1} is found from this figure.

If we now compare the model discussed so far with the results of the experiments described in paragraph 3.6 it looks as if both studies complete each other. Thus, from the adsorption experiments it follows that upon reduction of α-Bi_2O_3 the amount of adsorbed propylene increases, while from the rate studies we conclude that vacancies are important for 1,5-hexadiene formation. We, therefore, suggest that the

adsorption of propylene leading to 1,5-hexadiene is initiated in the first instance on vacancies. At the reaction temperatures this adsorbed propylene splits off a hydrogen atom resulting in the adsorbed allyl species necessary for 1,5-hexadiene formation.

4.3.3 OXIDATION OF 1,5-HEXADIENE

In the oxidation of propylene, benzene is formed from 1,5-hexadiene by a consecutive reaction. The role of the products 1,3-cyclohexadiene and 3-allylcyclohexene in this reaction did not become clear from the experiments described so far. Therefore, we decided to investigate the oxidation of 1,5-hexadiene in more detail.

The study of the kinetics of the 1,5-hexadiene oxidation reaction is, however, complicated by the fact that in the temperature range of interest (500-600^{o}C) 1,5-hexadiene undergoes also thermal reactions, mainly under the influence of allyl radicals (70). Products that are formed are besides monoolefins (ethylene, propylene, 1-butene, 1-pentene), diolefins, and triolefins also 1,3-cyclohexadiene, benzene and 3-allylcyclohexene. The latter products are also formed during the catalytic reaction. The course of the concentrations of the most important products as a function of the contact time when the reactor is filled with 2 g silicon carbide is given in figure 4.17. Products that are formed in high concentration are 3-allylcyclohexene, propylene, 1,3-cyclohexadiene and benzene. Figure 4.18 is obtained by correction of the product concentrations measured in the effluent of the reactor filled with α-Bi_2O_3 and silicon carbide for the homogeneous contribution measured when the reactor is filled with silicon carbide only. It is assumed in this case that the products which are formed when the reactor is only filled with silicon carbide are not converted by the α-Bi_2O_3. When we compare figure 4.18 with figure 4.17 it appears that as far as the hydrocarbons are concerned the difference amounts only a factor two. From figure 4.18 it follows directly that carbon dioxide, 3-allyl-

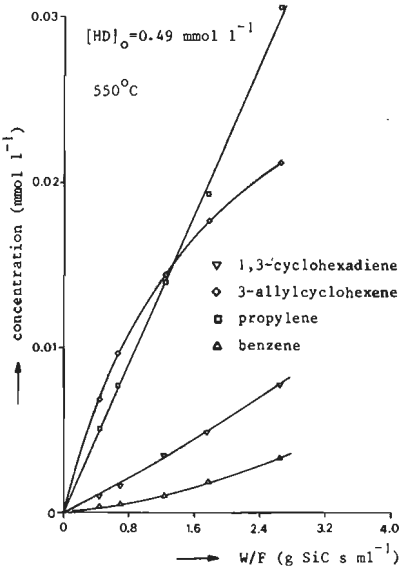

Figure 4.17 Reaction of 1,5-hexadiene in flow reactor filled with 2 g silicon carbide. Product concentrations as a function of contact time.

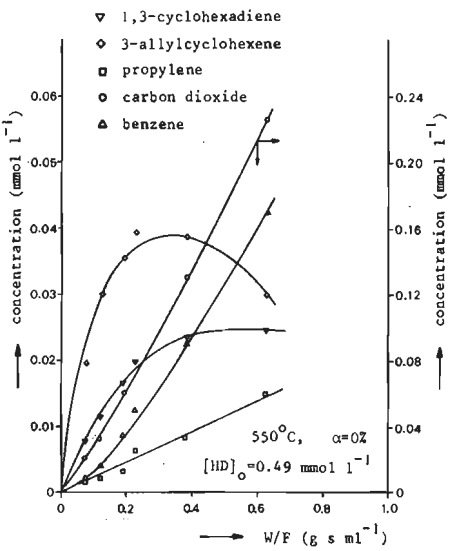

Figure 4.18 Reduction of α-Bi_2O_3 with 1,5-hexadiene in flow reactor. Product concentrations as a function of contact time.

cyclohexene, propylene and 1,3-cyclohexadiene originate by way of parallel reactions from 1,5-hexadiene. The more than linear increase of the carbon dioxide concentration with the contact time may be interpreted in terms of combustion of the formed C_6/C_9-hydrocarbons at higher contact times. Since a strong increase of the propylene concentration at high W/F due to abstraction of the allyl group from 3-allylcyclohexene is not observed, we suggest that this product is oxidized in a consecutive reaction to carbon dioxide. Finally the course of the benzene concentration with contact time presumes that this product besides being formed directly from 1,5-hexadiene also originates at high W/F-values by a consecutive reaction from 1,3-cyclohexadiene.

In figure 4.19 for a typical experiment the concentrations are plotted versus the degree of reduction. From this figure we see that the dependence of the benzene formation on the degree of reduction resembles strongly that of 1,3-cyclohexadiene, which points to a similar mechanism for both products. Moreover, it could be another indication that 1,3-cyclohexadiene is converted by a consecutive reaction to benzene. The

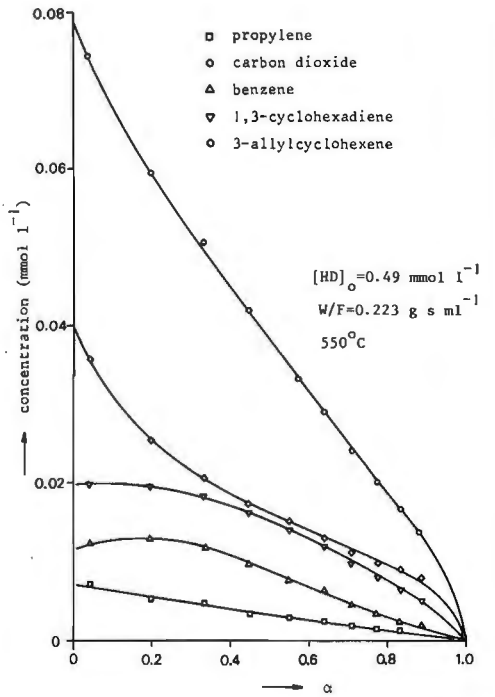

Figure 4.19 Product concentrations as a function of the degree of reduction. Reduction of α-Bi_2O_3 with 1,5-hexadiene in flow reactor.

course of the 3-allylcyclohexene and carbon dioxide concentration with the degree of reduction is less straightforward and it looks as if this α-dependence can not be explained by a simple mechanism. However, we may conclude from the fast decrease of the 3-allylcyclohexene concentration at low values of α that for the formation of this product an ensemble containing several oxygen sites is required. The to a more linear behaviour tending course at high values of α maybe indicates that this product originates by way of various mechanisms. This is also valid for the formation of carbon dioxide. Finally it appears that for the formation of propylene the first order volumetric reaction model is applicable, which means that this product is not or only to a minor extent formed by the reaction:

$$2C_6H_{10} \rightarrow C_9H_{14} + C_3H_6,$$

since then the formation of both products with the degree of

reduction, α, in broad outline should have shown the same picture.

Summarizing we propose that for the oxidation of 1,5-hexadiene over α-Bi_2O_3 the following qualitative reaction model is applicable:

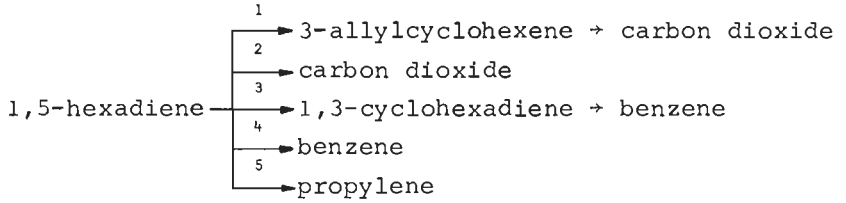

The kinetics of the parallel reactions (1) - (5) are next studied in a differential reactor at W/F values of 0.05-0.08 g s ml^{-1}. For each measurement a new oxide sample is used. Moreover, each experiment is repeated in a reactor only filled with silicon carbide, allowing to correct the kinetic experiments for the homogeneous contribution. It is clear that this procedure is not beneficial to the accuracy of the measurements, the more as presumably the products formed in the gas phase will be converted by α-Bi_2O_3.

The effect of varying the 1,5-hexadiene inlet concentration upon the rate of formation of the various products is determined at 550°C. The dependence of the rates on the degree of reduction is given in figures 4.20 a,b,c and d for 1,3-cyclohexadiene, benzene, 3-allylcyclohexene and carbon dioxide, respectively. As far as propylene is concerned we did not measure the formation of this product in more detail, since firstly propylene is produced only in small amounts and secondly the 1,5-hexadiene used for the kinetic experiments appeared to be slightly contaminated with propylene.

Assuming that at zero degree of reduction the reactions may be described by a rate expression of the form

$$r = k[HD]^n, \qquad (18)$$

the order of the parallel reactions in 1,5-hexadiene at α=0% may be determined from a plot of ln r versus ln[HD]. From figure 4.21 we see that the formation of benzene, 1,3-cyclo-

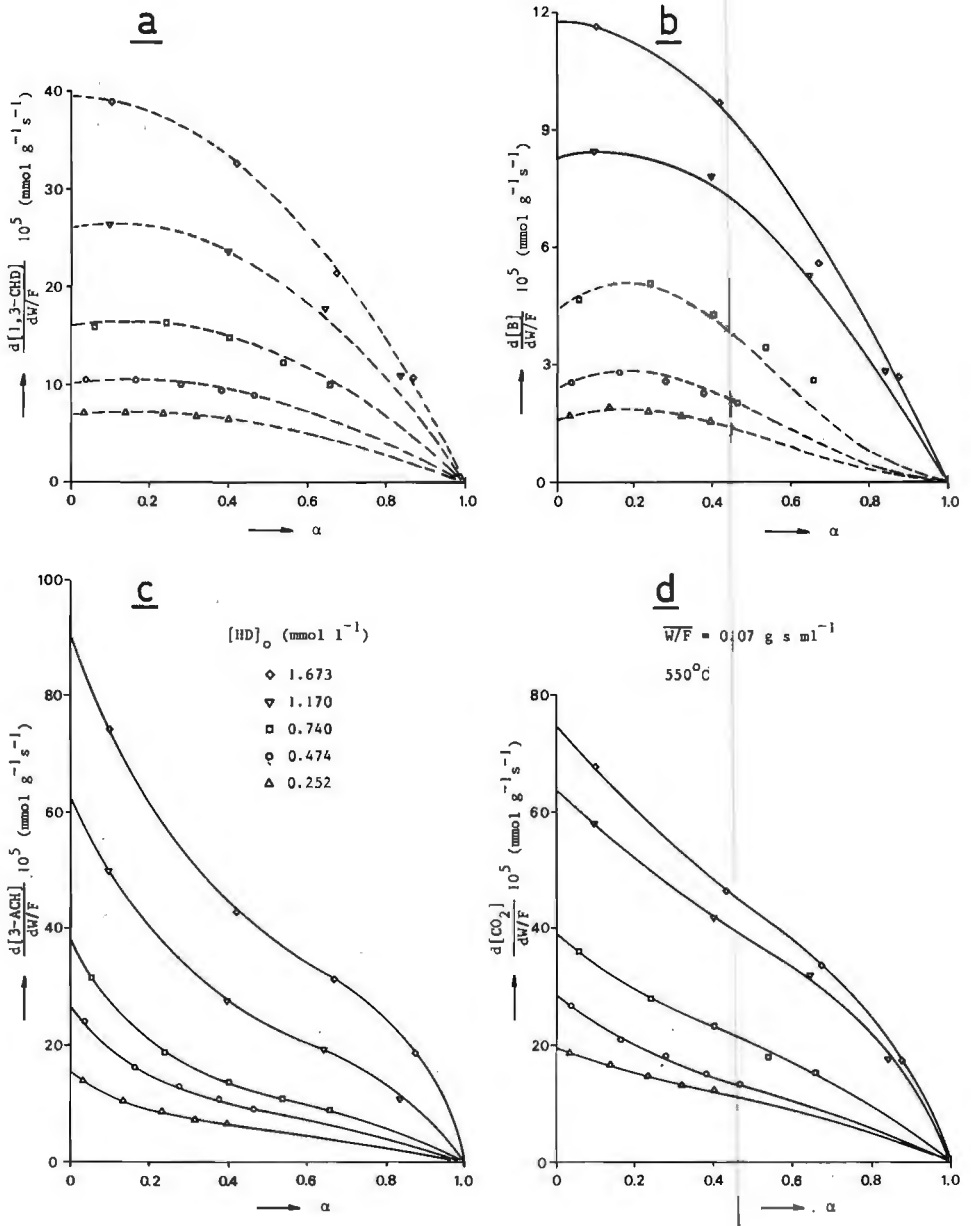

Figure 4.20 Rate of formation of 1,3-cyclohexadiene (a), benzene (b), 3-allylcyclohexene (c) and carbon dioxide(d) as a function of the degree of reduction. Reduction of α-Bi_2O_3 with 1,5-hexadiene in flow reactor at various inlet concentrations.

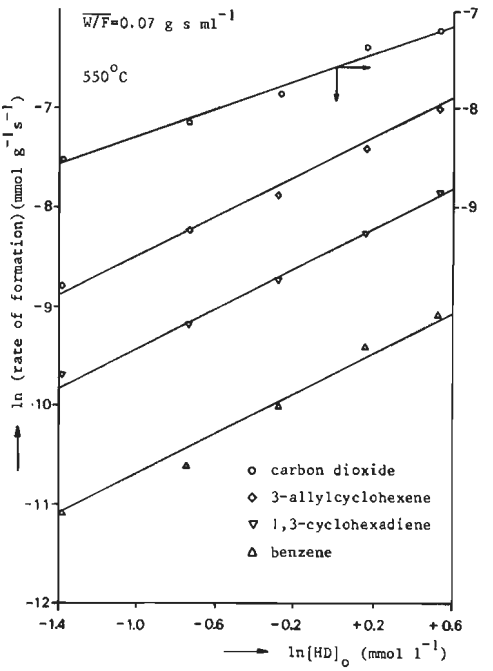

Figure 4.21 Rates of formation as a function of the 1,5-hexadiene inlet concentration at α=0%. Flow reactor.

hexadiene and 3-allylcyclohexene all possess a first order 1,5-hexadiene dependence, while the carbon dioxide formation has an order in 1,5-hexadiene of 0.9.

The influence of the temperature upon the rate of formation of the various products is depicted in figure 4.22 a,b,c and d. We see that the rates show the same dependence on the degree of reduction as is the case for changing the 1,5-hexadiene concentration. Extrapolation of the curves to α=0% offers again the possibility to estimate the temperature dependence of the rate constant k in equation (18). The results, which are given in figure 4.23, yield activation energies of 67 kJ mol^{-1} for 1,3-cyclohexadiene, 148 kJ mol^{-1} for benzene, and 88 kJ mol^{-1} for 3-allylcyclohexene. The apparent activation energy for carbon dioxide formation amounts to 125 kJ mol^{-1} at high temperatures and drops to 70 kJ mol^{-1} at low temperatures.

In the preceding paragraph on the reduction of α-Bi_2O_3 with propylene we saw that the degree of reduction of the bulk directly reflects the degree of reduction of the surface, as

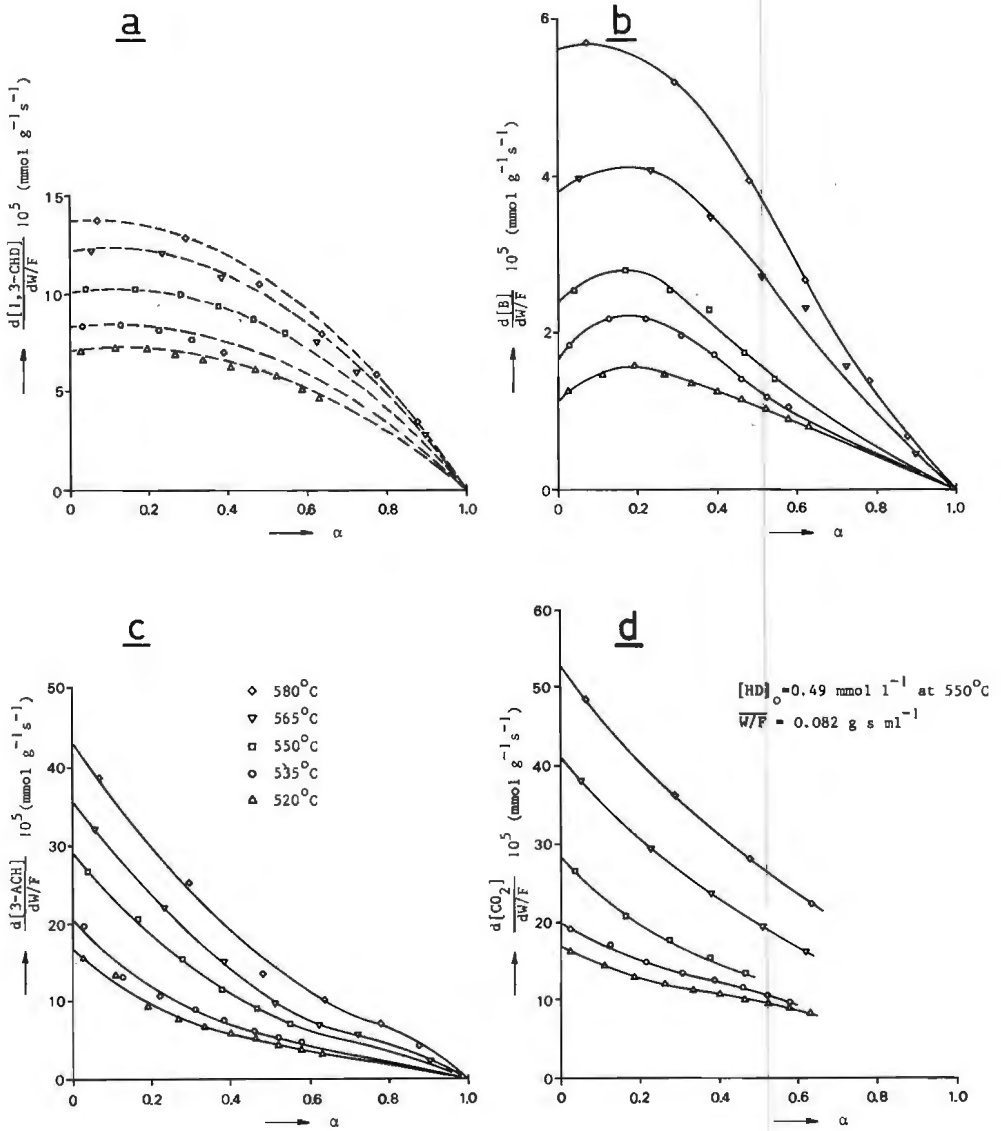

Figure 4.22 Rate of formation of 1,3-cyclohexadiene (a), benzene (b), 3-allylcyclohexene (c) and carbon dioxide (d) as a function of the degree of reduction. Reduction of α-Bi_2O_3 with 1,5-hexadiene in flow reactor at various temperatures (x_{HD}=0.033).

diffusion of oxygen through the lattice is fast compared to the chemical reaction. Since for 1,5-hexadiene oxidation the reaction rates are of the same order of magnitude we may assume that also in this case the diffusion of oxygen ions through the lattice is not rate determining. Therefore, when for the various

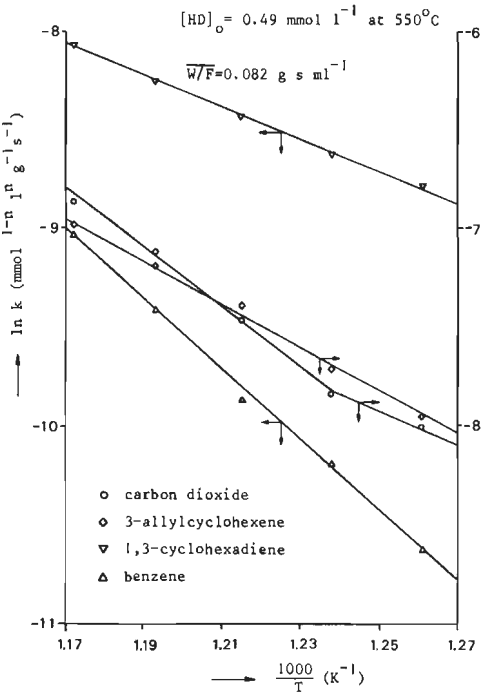

Figure 4.23 Arrhenius plot for product formation during 1,5-hexadiene oxidation at α=0%. Flow reactor (x_{HD}=0.033).

reactions occuring in 1,5-hexadiene oxidation combinations of vacancies and oxygen atoms in the surface are important as adsorption sites for 1,5-hexadiene, this also will appear in the course of the rates with the degree of reduction in the bulk.

When we first consider the formation of 1,3-cyclohexadiene it turns out that at a fixed temperature and 1,5-hexadiene concentration the rate may be well described by a relation of the form

$$\frac{d[1,3\text{-CHD}]}{dW/F} = k_{CHD}(\alpha_o+\alpha)(1-\alpha)[HD] \qquad (19)$$

The underlying mechanism for this expression is similar to that for 1,5-hexadiene formation from propylene, i.e. the formation of 1,3-cyclohexadiene takes place after adsorption of 1,5-hexadiene on a combination of a vacancy and an oxygen atom at the surface. This may be illustrated as follows:

1. Adsorption

2. Hydrogen atom abstraction

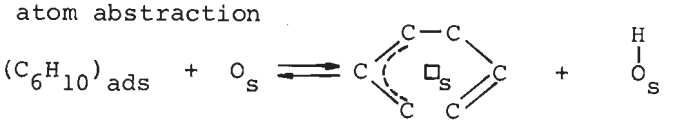

3. Reaction

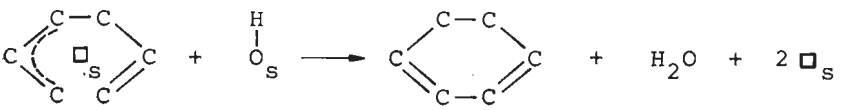

After adsorption of 1,5-hexadiene on a surface vacancy a hydrogen atom is abstracted and adsorbed on a surface oxygen. Abstraction of a second hydrogen atom simultaneously followed by ring closure in a concerted process yields 1,3-cyclohexadiene.

For the formation of 1,5-hexadiene from propylene we proposed as the rate determining step the abstraction of a hydrogen atom from the propylene molecule, a process that was found to have an activation energy of 93 kJ mol^{-1}. This value is of the same order of magnitude as that found for the 1,3-cyclohexadiene formation from 1,5-hexadiene, i.e. 67 kJ mol^{-1}. Therefore, it looks appropriate to suppose that also for the formation of 1,3-cyclohexadiene from 1,5-hexadiene the abstraction of the hydrogen atom is the rate determining step.

The broken lines in figure 4.20a and 4.22a are those theoretically calculated according to equation (19). We see that they agree quite well with the experimental points. The validity of the model further follows from table 4.1, which shows that both temperature increase and variation of the concentration hardly affects the value of α_o. The average value of α_o amounts to 0.77, indicating that originally there are more oxygen ions present on the surface than vacancies active for 1,5-hexadiene adsorption.

With regard to benzene it turns out that the rate of formation of this product may be described within reasonable limits by an expression like:

$$\frac{d[B]}{dW/F} = k_B(\alpha_o+\alpha)\ (1-\alpha)^2\ [HD]. \qquad (20)$$

Table 4.1 Influence of mole fraction 1,5-hexadiene and temperature on α_o for rate of formation of 1,3-cyclohexadiene.

x_{HD}	0.017	0.033	0.050	0.079	0.113	0.033	0.033	0.033	0.033
T (^oC)	550	550	550	550	550	520	535	565	580
α_o	0.78	0.78	0.73	0.77	0.76	0.76	0.78	0.81	0.80

The interpretation of this formula is that for the direct formation of benzene a 1,5-hexadiene adsorption is required in which one vacancy and two oxygen species at the surface are involved. This adsorption mode is possible when simultaneously two hydrogen atoms are abstracted from 1,5-hexadiene, which each are bonded as hydroxyl groups to surface oxygen ions, while adsorption of the remaining carbon chain takes place on one surface vacancy:

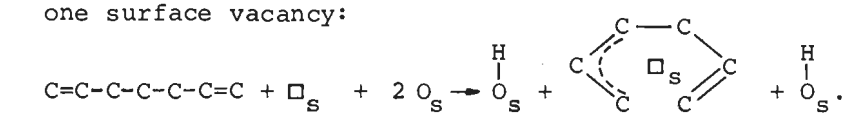

The abstraction of two hydrogen atoms obviously will be attended by a higher activation energy. Ring closure of the adsorbed carbon species and abstraction of two more hydrogen atoms now easily gives benzene and water.

The broken lines of figure 4.20b are calculated according to formula (20) with a value of α_o of 0.24. We see that a reasonable agreement exists with the experimental measured rates. The value for α_o is also in this case less than 1, which implies that there are originally more oxygen ions present than vacancies active for 1,5-hexadiene adsorption. At higher concentrations and higher temperatures the agreement becomes worse, probably due to inaccuracy of the measurements.

With respect to the formation of 3-allylcyclohexene and carbon dioxide the picture is more complicated. Nevertheless, we may derive some qualitative parameters from the kinetic parameters at α=0% and the change of the rates of formation with α. If we consider the latter relation first we note immediately that the rate of formation of 3-allylcyclohexene and to a small extent that of carbon dioxide decreases rather fast in the region $0 < \alpha < 30\%$. When for the formation of both

products also an adsorption site made up from certain combinations of vacancies and oxygen ions is required it appears that the S-shaped form of the curves can not be explained by a simple combination of vacancies and/or oxygen ions. If, however, we suppose that both products originate by more than one mechanism then also the experimental curves will be composed of two or more curves, which each have their own specific relation to the degree of reduction. When, for instance, adsorption of 1,5-hexadiene is possible involving only an ensemble of oxygen ions, a strong decrease of the rate with the degree of reduction will result. The more convex part of the curve at higher degrees of reduction may then be caused for example by an adsorption mode of 1,5-hexadiene, that increases with the degree of reduction. This interpretation of the experimental results is supported by the fact that the rate constants for CO_2-formation at α=0% in figure 4.23 show different temperature dependencies at low and high temperature, which could mean a change from one mechanism to another. The fact that for the formation of 3-allylcyclohexene a constant activation energy is found as well as the first order behaviour in 1,5-hexadiene for this product indicates that in this case the various mechanisms possess the same rate determining step, but that for the addition of the allyl alternative routes are possible.

4.4 REDUCTION OF α-Bi_2O_3 IN THE THERMOBALANCE

4.4.1 THE THERMOBALANCE AS A CHEMICAL REACTOR

In the Dupont 900/950 thermoanalyzer the sample bucket is placed in a horizontal position while the feed gases are passed over the sample. This means that the reactants are transported by diffusion into the layer of oxide particles in the sample bucket. To assure an optimum mass transport across the gas film around the particles a high gas flow through the reactor part of the balance is required, since at high gas flows the thickness of the film is small. The gas flow through the

reactor, however, can not be increased unlimitedly since at high flows the stability of the measurement will be affected. The maximum allowable gas flow amounts to about 325 ml NTP min^{-1}, which corresponds to a linear velocity of about 3 cm s^{-1} under reaction conditions. If we compare this with the gas flow which applies to the experiments in the differential reactor (150 ml NTP min^{-1}, corresponding to 25 cm s^{-1} at 550°C) it turns out that the conditions for film diffusion limitation are in the thermobalance more favourable than in the flow reactor. An other phenomenon that one has to consider concerns the non uniformity of the radial concentration profile. A non uniform concentration profile may arise when the chemical reaction is fast compared to the diffusion transport. In this case the concentration close to the oxide surface does not correspond with the bulk gas phase concentration, which may mask the kinetic results.

Experimentally the existence of concentration gradients in radial direction has been established by Tielen (71) for the oxidation of ethylene in honeycomb afterburner catalysts. From this study it became clear that the cup mix concentration is only half of the wall concentration. Although at first sight this comparison with the active wall reactor may go too far, the thermobalance reactor nevertheless may be visualized as a tube in which a catalytically active plate with thickness δ is situated. The active plate is composed of the catalyst particles which are spread in a uniform layer over the sample boat. Experimentally it has been confirmed that calculations similar to that of the active wall reactor are also valid for a catalytically active flat plate placed in a tube (72,73).

The influence of possible film diffusion was studied by repeating an experiment carried out under extreme conditions (high temperature, high concentration) at various gas flows (150, 200, 250, 300 ml NTP min^{-1}). On account of these measurements, which did not show great differences between each other, we decided to carry out all experiments with a gas flow of 250 ml NTP min^{-1}.

The effect of pore diffusion was investigated by varying

the particle diameter of the oxide particles from d < 0.05 mm to 0.15 < d < 0.25 mm. It turned out that with all reducing agents the particle diameter did not influence the overall rate of reduction. Unless otherwise stated most experiments were carried out with the sieve fraction 0.105 - 0.15 mm or 0.15 - 0.25 mm (H_2).

In performing the experiments it turned out that in raising the temperature to that of the reaction the α-Bi_2O_3 sample gives off carbon dioxide. Since the amount is rather small quantitative determination in the thermobalance is difficult. We, therefore, decided to study this phenomenon in the volumetric adsorption apparatus. It appeared that a fresh oxide sample looses an amount of 0.4 cm^3 NTP CO_2 $(g\ kat)^{-1}$. This CO_2 release probably is due to the fact that when α-Bi_2O_3 is exposed for long time in the air bismutite is formed, a product that decomposes at higher temperature. The formation of this product also has been observed by Levin and Roth (48). Since decomposition of bismutite will result in some reduction of the sample it is conceivable that α-Bi_2O_3 will absorb oxygen after a high temperature treatment. Experimentally we measured an amount of 0.08 cm^3 NTP O_2 $(g\ kat)^{-1}$.

When from the measurements in the thermobalance the overall rate of reduction is calculated we assume that the measured weight loss only represents the oxygen depletion. It may occur, however, that during the reduction process highly unsaturated products are formed which stay adsorbed on the surface. Analysis of samples reduced with various hydrocarbons showed, however, that carbon deposition did not mask the degree of reduction as determined from the weight loss.

4.4.2 OXIDATION OF HYDROGEN

The reduction of α-Bi_2O_3 with hydrogen was studied for two reasons. Firstly, in the reduction with hydrogen only one product is formed in contrast with reduction with hydrocarbons. Secondly, only a limited number of adsorption modes for hydrogen are possible, of which the adsorption on oxygen as hydroxyl

groups is the most probable. The latter, therefore, offers preeminently the opportunity to study the reactivity of surface oxygen.

From figure 4.24, in which the influence of the hydrogen mole fraction at 550°C upon the reduction is shown, it follows that the reduction process may be well described by the volumetric reaction model with first order oxygen dependence.

$$-\frac{d\alpha}{dt} = k_{H_2}(1-\alpha)\,[H_2]^n \quad \text{or} \quad -\ln(1-\alpha) = k_{H_2}\,[H_2]^n\, t \qquad (21)$$

The order of the reduction in hydrogen is determined from a plot of $\ln \beta (\beta = k'_{H_2}\, x_{H_2}^{\,n})$ versus $\ln x_{H_2}$.

$$\ln \beta = \ln k'_{H_2} + n \ln x_{H_2} \qquad (22)$$

The order appears to be one (Figure 4.25).

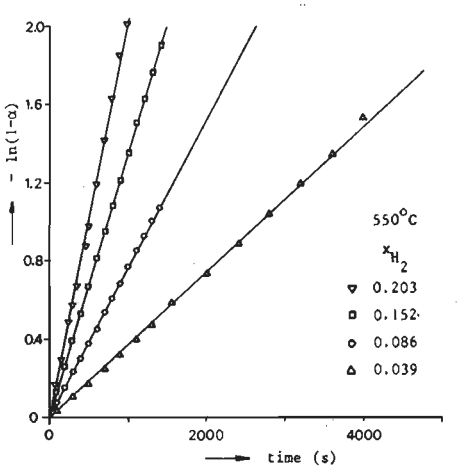

Figure 4.24. Check of the first order volumetric reaction model for the reduction of α-Bi_2O_3 with hydrogen at various mole fractions. Thermobalance.

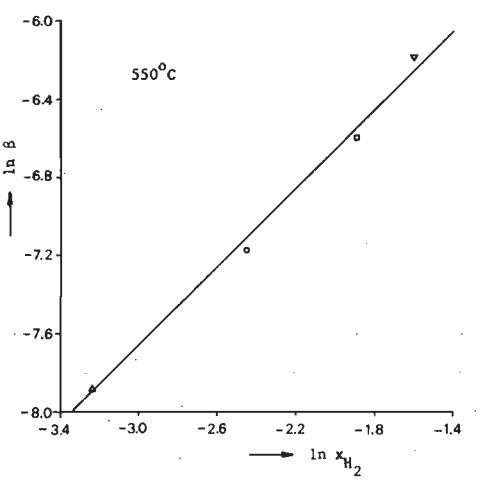

Figure 4.25 Reduction rate at α=0% as a function of the hydrogen mole fraction. Thermobalance.

The temperature dependence of the hydrogen reduction is shown in figure 4.26. It appears that the model described by equation (22) is applicable in the whole investigated temperature traject. For the activation energy calculated from the ln β versus 1000/T plot given in figure 4.27 a value of 92 kJ mol^{-1} is found.

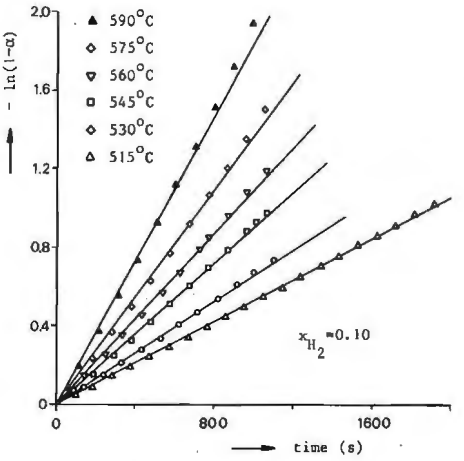

Figure 4.26 Check of the first order volumetric reaction model for the reduction of α-Bi_2O_3 with hydrogen at various temperatures. Thermobalance.

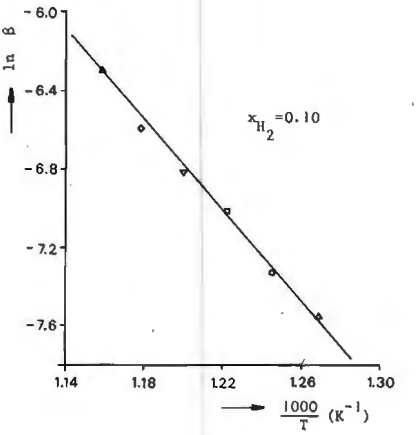

Figure 4.27 Arrhenius plot for the rate of reduction at α=0%. Reduction of α-Bi_2O_3 with hydrogen in thermobalance.

From these results we may describe the reduction with hydrogen by:

$$O_s + H_2 \rightarrow H_2O + \square_s .$$

This mechanism implies that the rate of reduction depends on the concentration of oxygen ions at the surface as well as on the hydrogen mole fraction. When, analogous to the propylene oxidation, we assume that also here the transport of oxygen ions from the bulk to the surface is fast as compared to the chemical reaction, the concentration of oxygen atoms at the surface will decrease with the bulk degree of reduction. For the case that the adsorption as hydroxyl groups is rate determining always a combination of two oxygen ions have to be present and the rate of reduction will decrease with $(1-\alpha)^2$. Since experimentally a first order oxygen dependence is observed only one oxygen ion at the surface will be involved in the rate determining step. This means that the measured activation energy of 92 kJ mol^{-1} is concerned to some degree with the oxygen bond strength in the oxide.

The reduction of α-Bi_2O_3 with hydrogen has also been studied by Beres et.al. (74) in a closed circulation apparatus

in the temperature range 350 - 500°C. These investigators found also a first order behaviour in hydrogen, while their activation energy of 90 kJ mol^{-1} agrees quite well with that found in our study. In contrast with our measurements, however, they found a linear relation between the degree of reduction and time, which points to a constant oxygen concentration at the surface. The maximum degrees of reduction in their study, however, were only 2 or 8%, so that it is questionable whether they were able to measure the activity decrease.

4.4.3 OXIDATION OF PROPYLENE

Since in the reduction of α-Bi_2O_3 with propylene various products may arise it is necessary to analyse the exit stream from the thermobalance to determine the contribution of the rate of formation of these products to the overall rate of oxygen depletion. The analysis showed that besides carbon dioxide and 1,5-hexadiene only very small amounts to hydrocarbons are formed. Therefore, with a quantitative analysis of carbon dioxide and the weight decrease measured by the thermobalance the oxygen consumption of both parallel reactions can be determined, as at each degree of reduction the following relation holds:

$$\left(-\frac{dO}{dt}\right)_{HD} = \left(-\frac{dO}{dt}\right)_{\text{thermobalance}} - \left(-\frac{dO}{dt}\right)_{CO_2,\ \text{measured by } CO_2 \text{ analysis}} \qquad (23)$$

The kinetic parameter for the oxygen depletion due to 1,5-hexadiene formation, however, can also be determined from the peak heights of 1,5-hexadiene in the GLC analysis, which are proportional to the rate of oxygen depletion.

In figure 4.28a the overall rate of reduction is given as a function of the degree of reduction at various mole fractions while figure 4.28b contains the corresponding rates of oxygen depletion as a result of carbon dioxide formation. We see that analogous to the measurements in the flow reactor

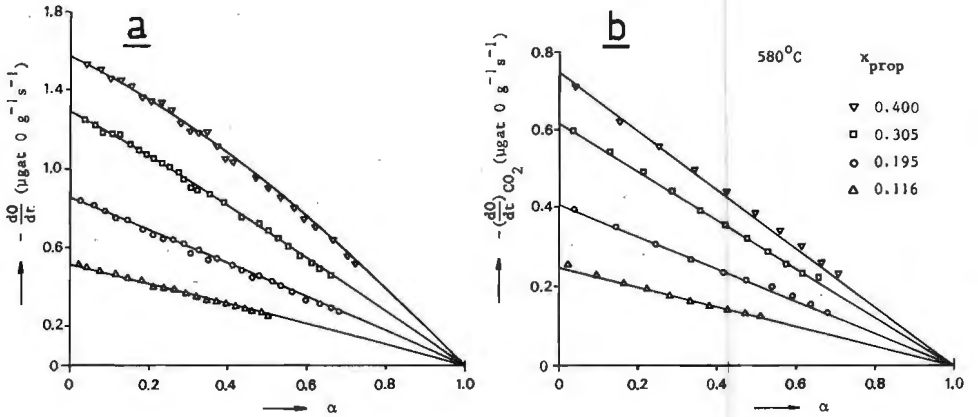

Figure 4.28 Overall of rate of reduction (a) and rate of oxygen depletion due to carbon dioxide formation (b) as function of the degree of reduction at various propylene mole fractions. Thermobalance.

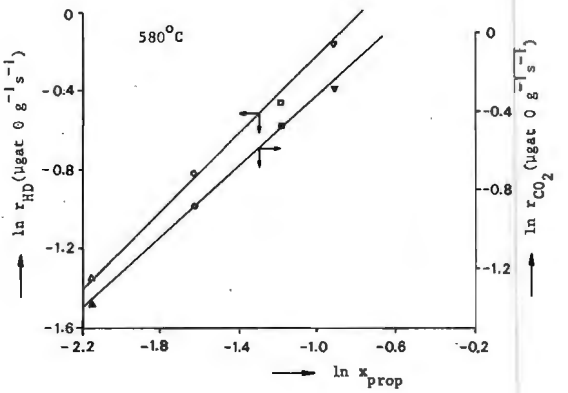

Figure 4.29 Rate of oxygen depletion due to carbon dioxide and 1,5-hexadiene formation at α=0% as a function of the propylene mole fraction. Thermobalance.

the rate of carbon dioxide formation can be described by the volumetric reaction model with first order oxygen dependence. The rate of oxygen release due to 1,5-hexadiene formation, as calculated with formula (23), can again be described by equation (16), of which the interpretation already has been given in paragraph 4.3.2. For α_o values of 2.4 ÷ 2.7 are found, which agrees quite well with those of the flow reactor. This also applies to the reaction orders in propylene for both reactions, i.e. 0.9 for carbon dioxide and 1 for 1,5-hexadiene.

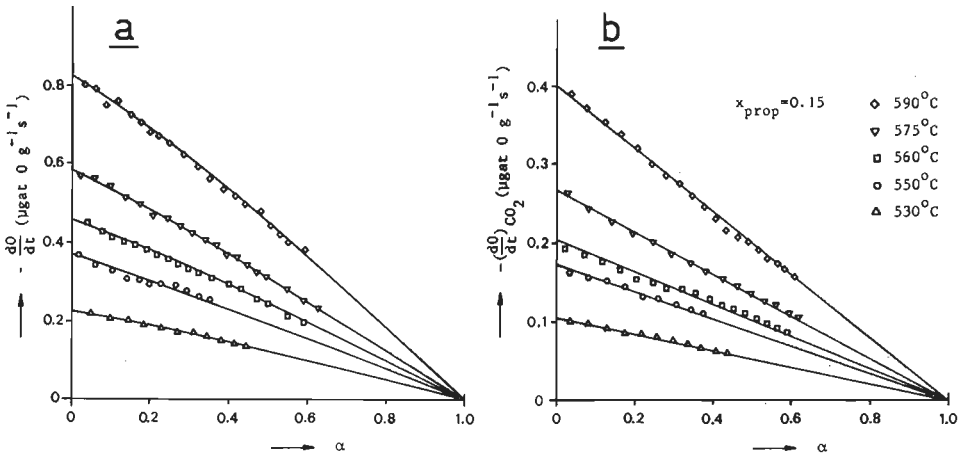

Figure 4.30 Overall rate of reduction (a) and rate of oxygen depletion due to carbon dioxide formation (b) as a function of the degree of reduction at various temperatures. Reduction of α-Bi_2O_3 with propylene in thermobalance.

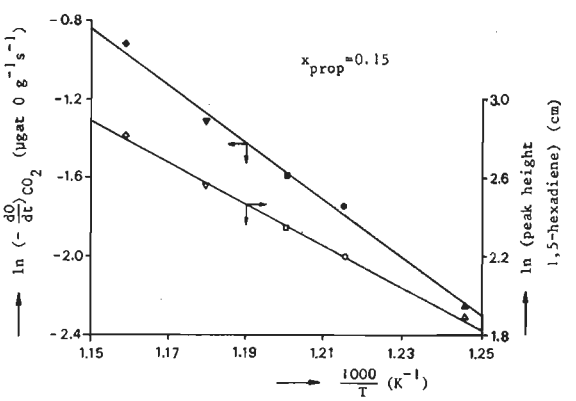

Figure 4.31 Arrhenius plot for the rate of oxygen depletion due to carbon dioxide and 1,5-hexadiene formation at α=0%. Reduction of α-Bi_2O_3 with propylene in thermobalance.

See figure 4.29.

The effect of varying the temperature upon the overall rate of reduction as well as the corresponding rates for carbon dioxide formation is shown in figure 4.30a and b. From the temperature dependence of the reduction rates at α=0%, shown in figure 4.31, an activation energy of 123 kJ mol^{-1} can be calculated for the carbon dioxide formation and 88 kJ mol^{-1} for the 1,5-hexadiene formation. These values agree quite well with

those obtained in the flow reactor experiments. See page 63.

In paragraph 4.3.2 we saw already that at low conversions the influence of the contact time upon the overall oxygen depletion is rather small. Since the conversion levels in the thermobalance are very low it looks appropriate to compare the overall oxygen depletion measured with both techniques. From figure 4.32 it appears that the results obtained in the thermobalance correspond quite well with the flow reactor measurements. This means that the thermobalance, indeed, may be considered as a differential reactor and that the relation between surface concentration and bulk concentration is identical to that of a fixed bed reactor.

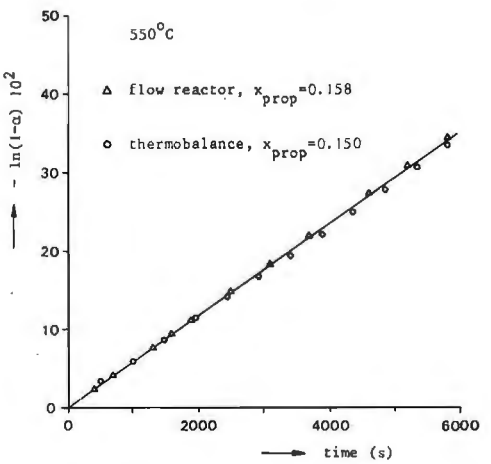

Figure 4.32 Comparison between results obtained in thermobalance and flow reactor.

The reduction of α-Bi_2O_3 with propylene in the thermobalance also has been studied by Massoth and Scarpiello (75). These authors described the kinetics of the overall reduction with a model in which initially the chemical reaction is rate determining followed by a diffusion limited region. Both rates appeared to be first order with respect to propylene, while for the activation energy of the chemical and diffusion steps values of 113 and 84 kJ mol^{-1} were reported, respectively. Analogous to our results they also found that 1,5-hexadiene is the major hydrocarbon formed. With regard to the formation of

carbon oxides they assumed that its presence could be ignored in view of earlier results of Swift et.al. (23) obtained in a fixed bed reactor. From our investigation under comparable conditions it has become clear that this supposition was not justified.

4.4.4 OXIDATION OF 1,5-HEXADIENE

For the oxidation of 1,5-hexadiene in the fixed bed reactor described in paragraph 4.3.3 the degree of reduction has been calculated from a quantitative analysis of the product gas. This means that at high reduction rates and long analysis time only a few samples can be analyzed, which will not benefit the accuracy of the measurements. We, therefore, repeated these experiments in the thermobalance.

It appeared, however, that the amount of hydrocarbons formed by interaction of 1,5-hexadiene with the oxide was much less than the amount formed as a result of the homogeneous gas phase reactions. This is probably due to the large empty volume of the thermobalance as compared with the flow reactor. From the course of the hydrocarbon concentration with the degree of reduction, therefore, no reliable conclusions can be drawn. For determination of the kinetic parameters of the aselective oxidation of 1,5-hexadiene, however, the measurements are more useful.

In figure 4.33 the effect of varying the 1,5-hexadiene mole fraction upon the rate of oxygen consumption due to carbon dioxide formation is shown. Analogous to the experiments in the flow reactor the curves are S-shaped. Compared to the overall rates of oxygen depletion it appears that more than 3/4 of the oxygen is consumed by the aselective reaction. For the order of the carbon dioxide formation in 1,5-hexadiene at α=0% a value of 0.95 is found from figure 4.34, which agrees quite well with the results obtained in the flow reactor.

The change of the rate of formation of carbon dioxide with temperature is shown in figure 4.35. Extrapolation of the

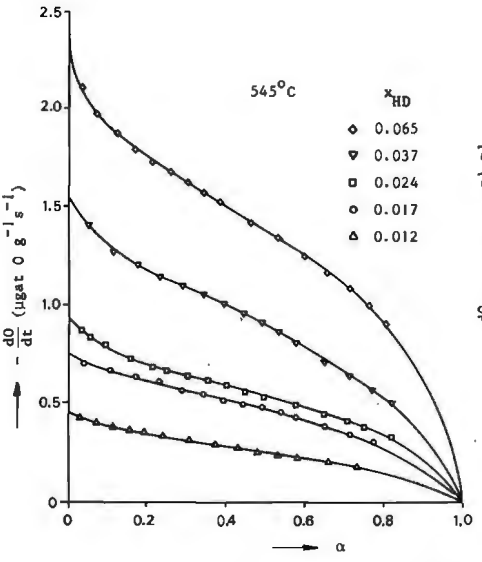

Figure 4.33 Rate of oxygen depletion due to carbon dioxide formation as a function of the degree of reduction at various 1,5-hexadiene mole fractions. Thermobalance.

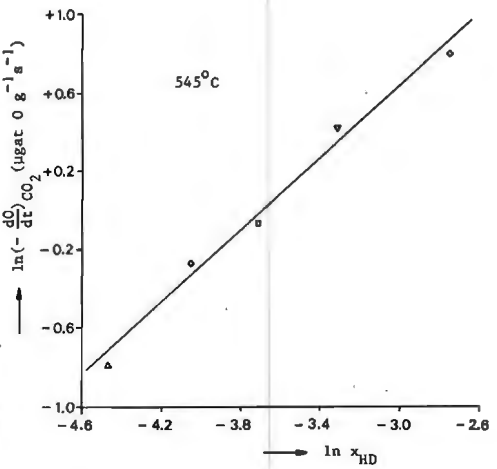

Figure 4.34 Rate of oxygen depletion due to carbon dioxide formation at α=0% as a function of the 1,5-hexadiene mole fraction. Thermobalance.

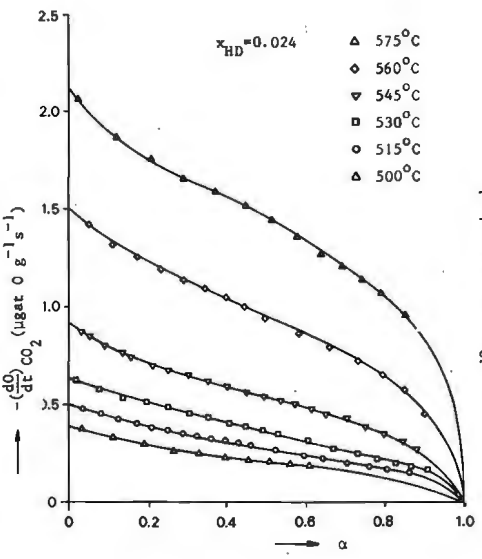

Figure 4.35 Rate of oxygen depletion due to carbon dioxide formation as a function of the degree of reduction at various temperatures. Reduction of α-Bi_2O_3 with 1,5-hexadiene in thermobalance.

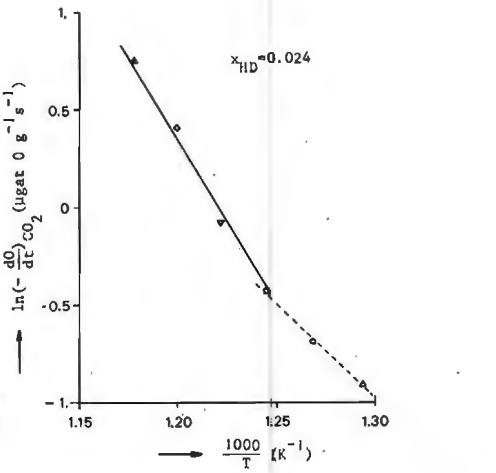

Figure 4.36 Arrhenius plot for the rate of oxygen depletion due to carbon dioxide formation at α=0%. Reduction of α-Bi_2O_3 with 1,5-hexadiene in thermobalance.

rates to α=0% yields the Arrhenius plot of figure 4.36. We see that a change in temperature dependence occurs, i.e. from 143 kJ mol^{-1} at high temperature to 82 kJ mol^{-1} at low temperature. This also corresponds with the experiments described in paragraph 4.3.3 and likely stands for a change in mechanism in going from high to low temperature.

4.4.5 OXIDATION OF BENZENE

The oxidation of benzene was studies to check how far this product is combusted in a consecutive reaction to carbon oxides. From the experiments it turned out that more than 80% of the oxygen consumed can be ascribed to the formation of carbon dioxide. Since gas chromatographic analysis of the product gas showed that no hydrocarbons are formed in the reduction reaction we believe that formation of carbon monoxide accounts for the rest of the oxygen, which has not been determined by us.

The overall rate of oxygen depletion as a function of the degree of reduction at various mole fractions is shown in figure 4.37. It appears that the rate of reduction can be

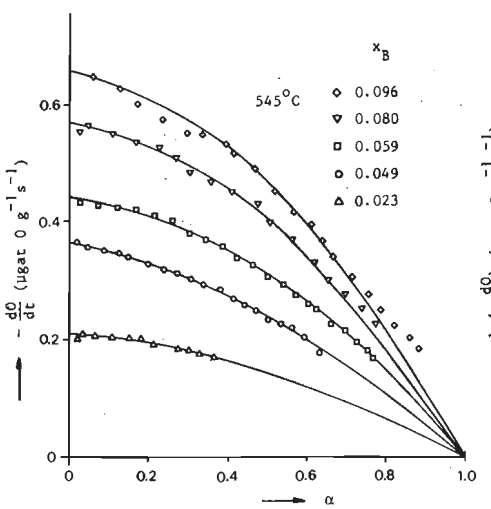

Figure 4.37 Reduction rate as a function of the degree of reduction at various benzene mole fractions. Thermobalance.

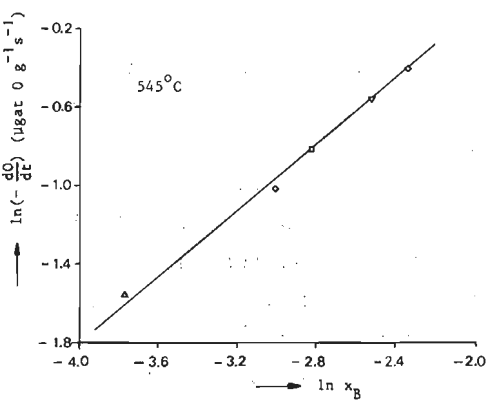

Figure 4.38 Reduction rate at α=0% as a function of the benzene mole fraction. Thermobalance.

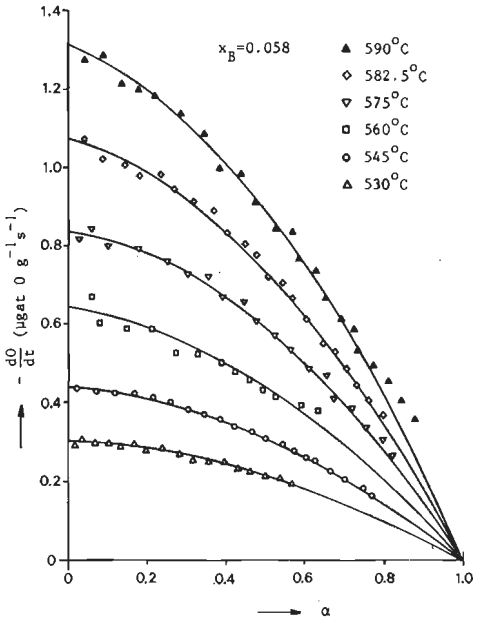

Figure 4.39 Reduction rate as a function of the degree of reduction at various temperatures. Reduction of α-Bi_2O_3 with benzene in the thermobalance.

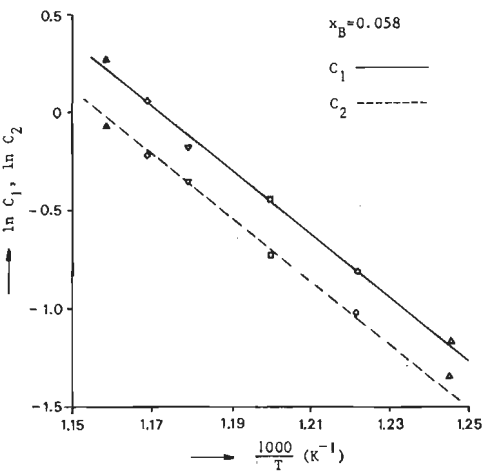

Figure 4.40 Arrhenius plot for the reduction of α-Bi_2O_3 with benzene. Thermobalance.

described by an expression similar to equation (19), i.e. for the combustion of benzene the catalytic site is made up by a vacancy and an oxygen ion in the surface. The solid lines in the figure are those calculated theoretically. The average value of α_o amounts to 1.24. The order of the reduction reaction in benzene follows from figure 4.38 and is found to be close to one, i.e. 0.84.

Figure 4.39 gives the reduction rates as a function of α for a number of temperatures. It turns out that the relation described by equation (19) holds in the whole investigated temperature region. The value of α_o is independent of the temperature. This is illustrated by figure 4.40, which shows that the Arrhenius plot for the constants $C_1 (=k_B \alpha_o x_B)$ and $C_2 (=k_B x_B)$ possess the same activation energy, i.e. 124 kJ mol^{-1}.

4.5 *REDUCTION-REOXIDATION STUDY OF* α-Bi_2O_3

Reoxidation of α-Bi_2O_3 samples reduced to various degrees has been briefly studied by Massoth and Scarpiello (75). These authors found that when α-Bi_2O_3 samples are reduced less than 60%, complete reoxidation was achieved. Above this degree of reduction the percentage reoxidation that could be reached decreased with the degree of reduction. They also reported that when a sample is reduced to 30%, the initial activity can not be restored anymore, but a 27% loss in activity is found. Since for possible application of α-Bi_2O_3 as a technical catalyst knowledge about the degree of restoration of the initial activity is important, we decided to study the regeneration process in more detail.

The parameter that we shall use as a measure for the activity loss is the rate constant for overall reduction of α-Bi_2O_3 as described by equation (11), i.e. the volumetric reaction model with first order oxygen dependence. It is appropriate to assume that the degree of restoration of the original activity will be dependent of reduction, the reduction temperature, and the substrate concentration.

Table 4.2 Dependence of rate constant for overall reduction of α-Bi_2O_3 with propylene (x_{prop}=0.15) on number of reductions and on percentage reduction.

% reduction	10	20	30
k'*in first reduction (s^{-1})	$1.43\ 10^{-4}$	$1.44\ 10^{-1}$	$1.43\ 10^{-4}$
k' in second reduction (s^{-1})	$1.43\ 10^{-4}$	$1.33\ 10^{-4}$	$1.26\ 10^{-4}$
k' in third reduction (s^{-1})	$1.43\ 10^{-4}$	$1.21\ 10^{-4}$	$1.08\ 10^{-4}$

*k' is rate constant for $-\ln(1-\alpha)=k't$

Table 4.2 gives values for k' obtained after three reduction cycles at 590°C with a propylene mole fraction of 0.15. Reoxidation of the oxide sample was always carried out with air at 450°C. From this table it follows that after reduction to 10% the original activity can still be regained. Reduction to higher degrees, however, results in activity loss. In all cases, the percentage reoxidation as measured by weight

increase after propylene reduction was 100%.

The reoxidation of the sample takes place in two steps, i.e. a fast reoxidation followed by an oxygen adsorption which decreases logarithmically with time. See figure 4.41. The logarithmic reoxidation step is independent of the number of reoxidations, as follows from figure 4.42, which applies to reoxidation of α-Bi_2O_3 after reduction to 30%. Similar figures are found for reoxidation after reduction to 10% and 20%. It further turns out that the rate constant for the slow reoxidation in the region α=0-30% decreases linearly with the degree of reduction. After reduction to higher degrees the logarithmic relation remains valid, but the reoxidation rate constant decreases more than linearly.

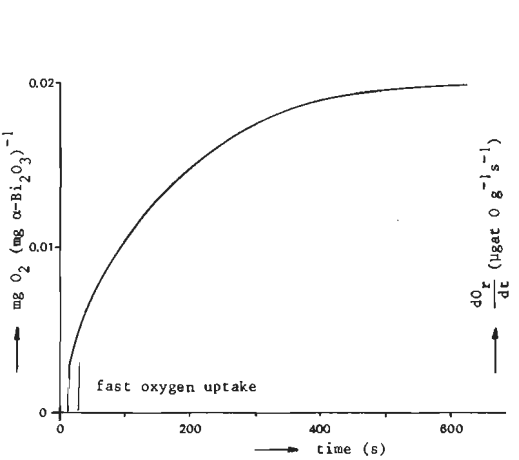

Figure 4.41 Oxygen uptake of α-Bi_2O_3 at 450°C after reduction with propylene (x_{prop}=0.15) at 590°C. Thermobalance.

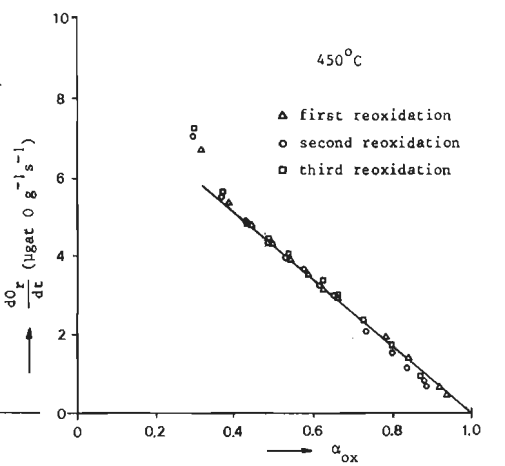

Figure 4.42 Reoxidation of α-Bi_2O_3 with air after reduction with propylene (x_{prop}=0.15) at 590°C to α=30%. Thermobalance.

From table 4.3 we conclude that the percentage fast oxygen uptake decreases with the degree of reduction. This agrees quite well with the investigation of Muira et.al. (76), who studied the reoxidation-reduction of α-Bi_2O_3 by the Temperature Programmed Reoxidation (TPR) method. These authors found that α-Bi_2O_3 prereduced at 350°C to α=4.9% with hydrogen only gives a single peak at 180°C in the TPR curve, while a sample prereduced at 450°C to 3% with hydrogen gives two peaks, i.e. one at 180°C and one at 230°C. By increasing the

Table 4.3 Percentage fast oxygen uptake at 450°C after reduction of α-Bi_2O_3 with propylene (x_{prop} = 0.15) at 590°C.

degree of reduction (%)	10	20	30	60
percentage fast O_2-absorption	18.75	16	15	7.75

degree of reduction the intensity of the second peak increases. These results were interpreted by assuming that the reoxidation taking place in the first stage concerns finely dispersed bismuth, while the second peak in the TPR curve, i.e. the logarithmic reoxidation applies to agglomerated particles of metallic bismuth, which are formed to a larger extent at higher degrees of reduction.

The logarithmic relation between the rate of oxygen consumption and time can be described by the following model also given by Miura et.al. (76). If we assume that the rate of reoxidation, r_{ox}, is proportional to the number of oxygen vacancies introduced in the crystal by reduction and the oxygen pressure P_{O_2} the rate of reoxidation can be expressed by

$$r_{ox} = \frac{dO_r}{dt} = k_{ox}(O_{r,o}-O_r)P_{O_2}^{\ n} \qquad (24)$$

where:

$O_{r,o}$: number of oxygen atoms to complete reoxidation
O_r : number of oxygen atoms consumed for reoxidation after time t.

Equation (24) may be rearranged to

$$\frac{dO_r}{dt} = k_{ox}O_{r,o}(1-\alpha_{ox})P_{O_2}^{\ n} \text{ with } \alpha_{ox} = \frac{O_r}{O_{r,o}} \qquad (25)$$

i.e. the rate of reoxidation increases linearly with the number of oxygen atoms required to complete reoxidation. Since in our measurements the reoxidation rate is independent of the degree of reduction it follows that the rate constant

in equation (25) decreases linearly with the degree of reduction. This probably is due to loss of surface area. That agglomerated particles of Bi-atoms arise already at a degree of reduction of 20% is illustrated by figure 4.43, which shows electron micrographs of α-Bi_2O_3 samples reduced to various degrees of reduction. These pictures show that conglomerates of bismuth atoms are present in all samples, except the one reduced to α=5%.

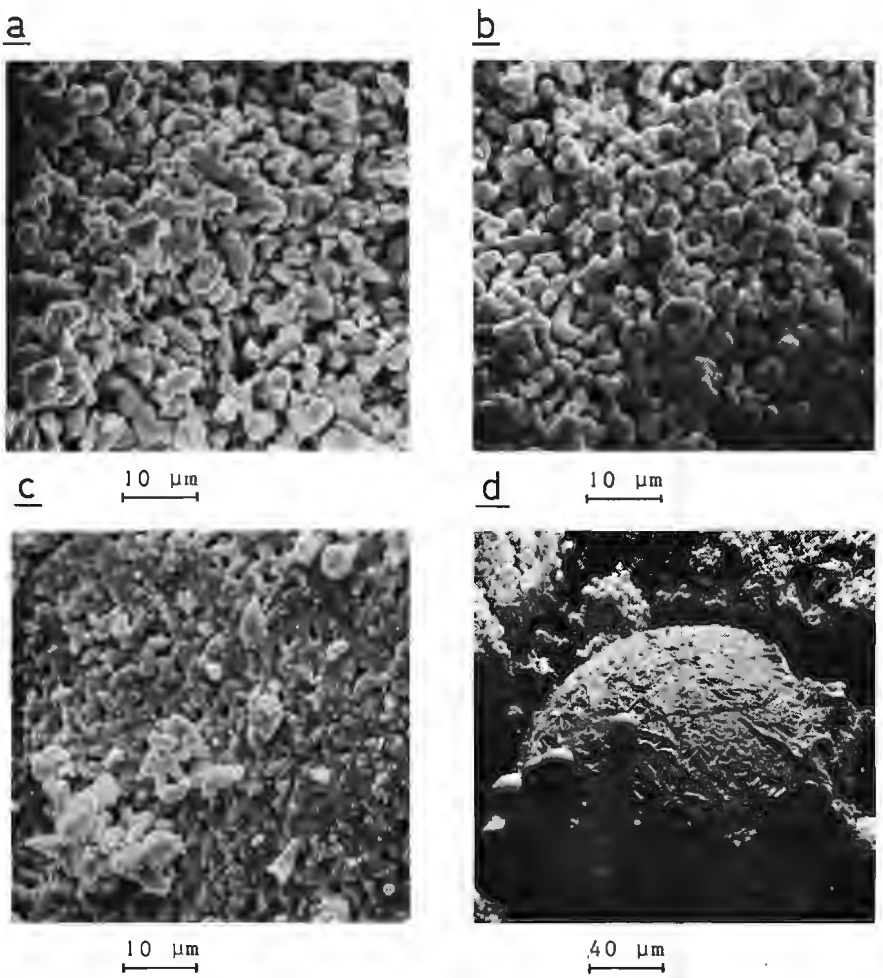

Figure 4.43 Electron micrographs of α-Bi_2O_3 reduced to various degrees of reduction.
(a) non reduced
(b) reduced with propylene at 550°C to α=5%
(c) reduced with propylene at 590°C to α=20%. Reoxidized with air at 400°C.
(d) reduced with 1,5-hexadiene at 530°C to α=80%. Reoxidized at 450°C with air.

As far as the effect of the propylene concentration on the reoxidation rate of α-Bi_2O_3 is concerned it appears that when oxide samples are reduced to the same degree of reduction, reduction with high propylene mole fractions yields high reoxidation rates. This is not surprising since at higher propylene mole fractions the time necessary to reach a certain degree of reduction will be shorter, so that clustering of bismuth atoms will have taken place to a lesser extent. The opposite effect is observed with increasing the reduction temperature. At high temperatures a certain degree of reduction will be reached faster, but higher temperatures will also result in a higher mobility of the bismuth atoms. The net result will depend on the relative rates of both processes. In the case of α-Bi_2O_3 it is found that when the temperature of reduction increases, the rate of reoxidation decreases.

Finally we determined the influence of the temperature upon the reoxidation rate. In figure 4.44 the reoxidation rate is shown as a function of the degree of reoxidation after reduction with propylene (x_{prop}=0.15) at 590°C to α=20%. From the slope of these lines we determined an activation energy of 100 kJ mol^{-1}.

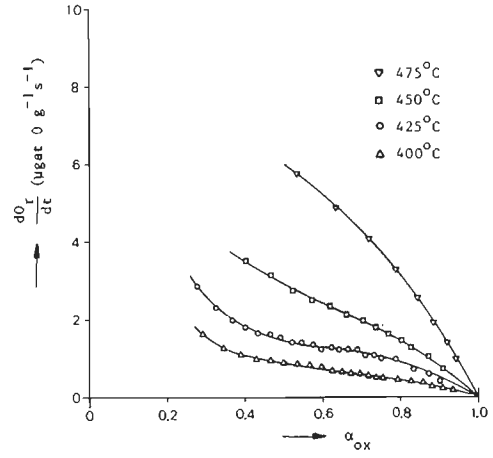

Figure 4.44 Reoxidation of α-Bi_2O_3 with air at various temperatures after reduction with propylene (x_{prop}=0.15) at 590°C to α=20%. Thermobalance.

CHAPTER 5

Reaction Kinetics Part two - Bismuth Oxide as Catalyst

5.1 INTRODUCTION

The experiments described in the previous chapter have all been carried out without oxygen in the feed. For industrial operation this means that one of the following three types of reactors has to be used, i.e. either a two step discontinuous process or a reactor system with two fluid beds between which the solid circulates or a single fluid-bed reactor in which reduction and reoxidation are carried out in one bed. In the former reactor propylene and air are passed alternately over α-Bi_2O_3. With the dual fluidized bed system, on the contrary, one deals more or less with a continuous process. In the first bed of this system the oxidation reactions take place, while in the second bed the reduced α-Bi_2O_3 is regenerated with air. The single fluid-bed reactor, which has been described by Callahan (77), has a separate oxidation and reduction zone, between which the solid circulates. This is brought about by introducing hydrocarbon and oxygen at different places. All systems, however, have the disadvantage that during the reaction the activity of the α-Bi_2O_3 decreases continuously. Moreover, one seriously has to account for activity loss after a large number of reoxidation-reduction cycles due to evaporation of bismuth metal, which originates when the reduction goes too far. This activity loss, however, may be restricted to some degree when α-Bi_2O_3 is brought on a suitable carrier (75). For these reasons it is clear that in industry one prefers to carry out the reactions in a single reactor system where the oxygen necessary for the oxidation is supplied directly with the feed.

In the preceding chapters it has already been mentioned that the addition of oxygen to the system normally results in

lower selectivities for hydrocarbon formation. To elucidate the reasons for this lower selectivity we decided to study the kinetics of the reactions taking place when a mxiture of propylene and oxygen in a stream of inert gas are passed over α-Bi_2O_3. In contrast to the case that only propylene is passed over α-Bi_2O_3, we then call α-Bi_2O_3 an oxidant, we now consider α-Bi_2O_3 to act as a catalyst. Herewith we are aware of the fact that when the oxidation takes place by way of the Mars-van Krevelen oxidation-reduction model (20) in fact α-Bi_2O_3 also acts more or less as an oxidant. However, since in this case oxygen is supplied continuously by the feed the degree of reduction in the steady state will be constant and rather low. Consequently we are not dealing with a real gas-solid reaction in the proper sense.

Besides the kinetics of the propylene oxidation we also paid some attention to the oxidation of 1,5-hexadiene.

Regarding limitations due to mass and heat transport calculations analogous to those mentioned in paragraph 4.3.1 showed that these effects are negligible.

5.2 OXIDATION OF PROPYLENE

5.2.1 PRELIMINARY EXPERIMENTS

Firstly we investigated how the addition of oxygen to the feed mixture affects the formation of the various products as well as how far a contribution has to be expected either from the silicon carbide present in the reactor either from homogeneous gas phase reactions. Both contributions will be called non catalytic. It appeared that only for the reaction to carbon dioxide one has to take into account the contributions due to silicon carbide and to homogeneous reactions. From experiments with an empty reactor it further turned out that this CO_2 formation is mainly (over 90%) caused by the silicon carbide. To correct for this non catalytic carbon dioxide formation we repeated each experiment in a reactor filled with

silicon carbide only.

The effect of varying the contact time on the product distribution when a mixture of oxygen, propylene and helium is passed over α-Bi_2O_3 is shown in figure 5.1. Similar curves are obtained for other oxygen/propylene ratios. The carbon dioxide concentration in this figure has already been corrected for the non catalytic contribution. We see that analogous to the experiments without oxygen in the feed both 1,5-hexadiene and carbon dioxide are formed by parallel reactions from propylene, while the formation of benzene takes place according to a consecutive scheme from 1,5-hexadiene. 1,3-cyclohexadiene is formed in such small concentrations that we cannot decide in what way this product is formed, while 3-allylcyclohexene is hardly detectable in the product mixture.

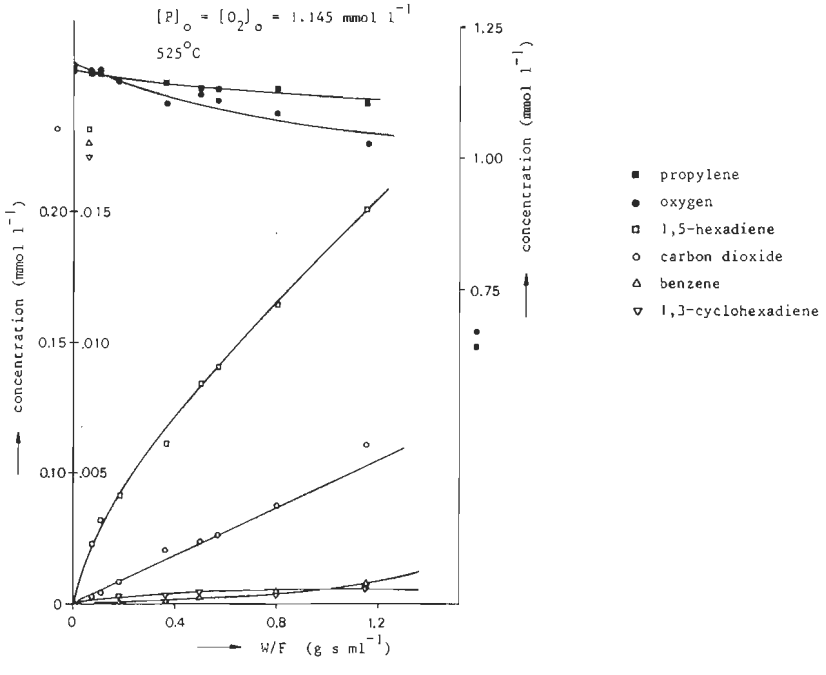

Figure 5.1 Product concentration as a function of contact time. Oxidation of propylene with α-Bi_2O_3 in flow reactor.

5.2.2 KINETICS

Like the experiments without oxygen in the feed we used the differential method for determination of the kinetic parameters. According to the concentration distribution described in figure 5.1 we are here solely dealing with the dimerization reaction to 1,5-hexadiene and the aselective reaction to carbon dioxide:

$$C_3H_6 + O_2 \begin{cases} \xrightarrow{(1)} C_6H_{10} + H_2O \\ \xrightarrow{(2)} CO_2 + H_2O. \end{cases}$$

The average W/F value amounted to about 0.1 g s ml^{-1}.

For the interpretation of the kinetic measurements we used in the first instance rate equations based upon the power rate law:

$$\frac{d[HD]}{dW/F} = r_{HD} = k_{HD}\,[P]^m\,[O_2]^n \qquad (1)$$

and

$$\frac{d[CO_2]}{dW/F} = r_{CO_2} = k_{CO_2}\,[P]^p\,[O_2]^q \qquad (2)$$

where: [P] and $[O_2]$ represent the concentration of propylene and oxygen respectively and m, n, p and q are reaction orders. The order of both reactions in propylene can be determined by varying the propylene concentration at a fixed oxygen concentration and at a fixed temperature. Since the measurements are carried out in a differential reactor we then may write:

$$r_{HD} = \frac{\Delta[HD]}{\Delta W/F} = k'_{HD}\,[P]_o^m \qquad (3)$$

$$r_{CO_2} = \frac{\Delta[CO_2]}{\Delta W/F} = k'_{CO_2}\,[P]_o^p. \qquad (4)$$

The reaction orders can now easily be obtained from plots of ln r versus $\ln[P]_o$, $[P]_o$ being the entrance concentration of propylene. An analogous procedure can be applied for determination of the reaction orders in oxygen. Experiments are then carried out at a fixed propylene concentration.

Since from the preliminary experiments it has emerged that with regard to the CO_2-formation one has to account for contributions from other sources we decided firstly to determine the kinetics of this formation in more detail. This offers the possibility to correct the experiments carried out with α-Bi_2O_3 for the non-catalytic contribution to the CO_2-formation and makes it redundant to repeat all experiments carried out for determining the kinetic parameters.

The results of these measurements which were carried out with a reactor filling of 2 g SiC, are depicted in figures 5.2 - 5.4. The reaction orders in propylene and oxygen are 0.7 and 0, respectively, while for the apparent activation energy a value of 126 kJ mol^{-1} is found.

Next we studied the kinetics of the α-Bi_2O_3 catalyzed reactions to 1,5-hexadiene and carbon dioxide. The dependence of the rates of formation on the propylene concentration was firstly investigated at an oxygen mole fraction of 0.075 and

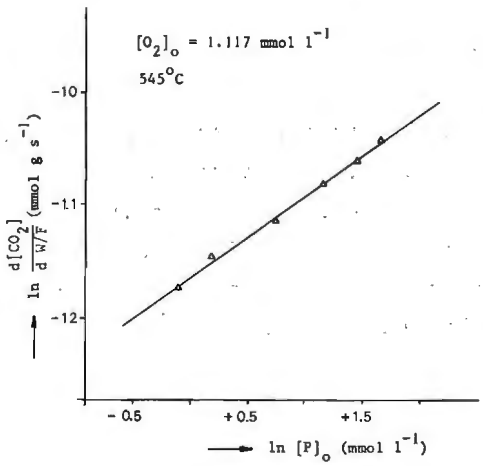

Figure 5.2 Rate of formation of carbon dioxide as a function of the propylene inlet concentration.Flow reactor filled with silicon carbide.

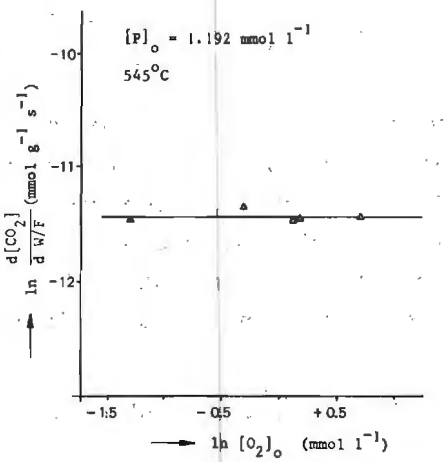

Figure 5.3 Rate of formation of carbon dioxide as a function of the oxygen inlet concentration.Flow reactor filled with silicon carbide.

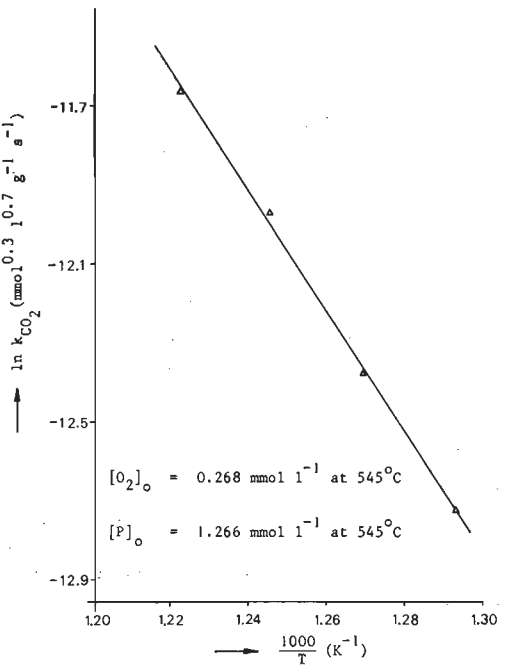

Figure 5.4 Arrhenius plot for the oxidation of propylene to carbon dioxide in reactor filled with silicon carbide (x_{O_2}=0.018, x_{prop}=0.085).

various temperatures. The results are depicted in figure 5.5. The reaction order in propylene for the 1,5-hexadiene formation appears to be independent of the temperature and has over the whole range of investigated propylene concentrations a value of 1.2. The reaction order in propylene for CO_2-formation, on the contrary, turns out to be dependent on the temperature. Going from high to low temperature the reaction order changes from 0.8 at 545°C to 1 at 500°C.

Varying the oxygen concentration at a fixed propylene mole fraction of 0.08 has the effect illustrated in figure 5.6. We see that at all temperatures the order in oxygen for the carbon dioxide formation has a constant value of 0.7. The effect of the oxygen concentration on the rate of formation of 1,5-hexadiene, on the contrary, shows a different picture. At low oxygen concentration there exists a region in which the rate of

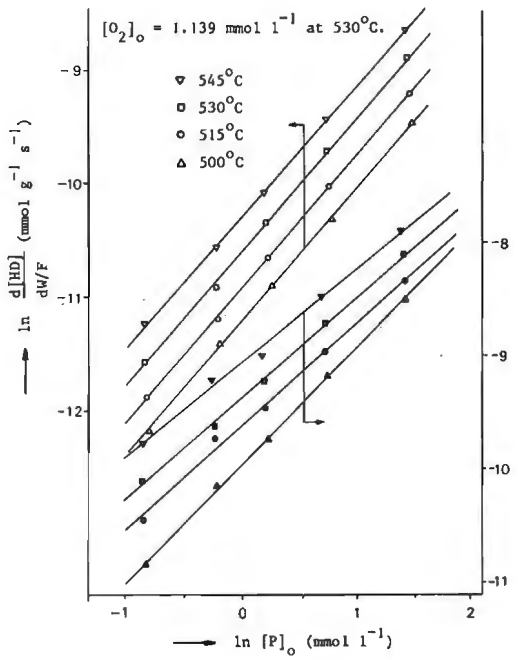

Figure 5.5 Rates of formation of 1,5-hexadiene and carbon dioxide as a function of the propylene inlet concentration at various temperatures. Catalyst α-Bi_2O_3. x_{O_2}=0.075.

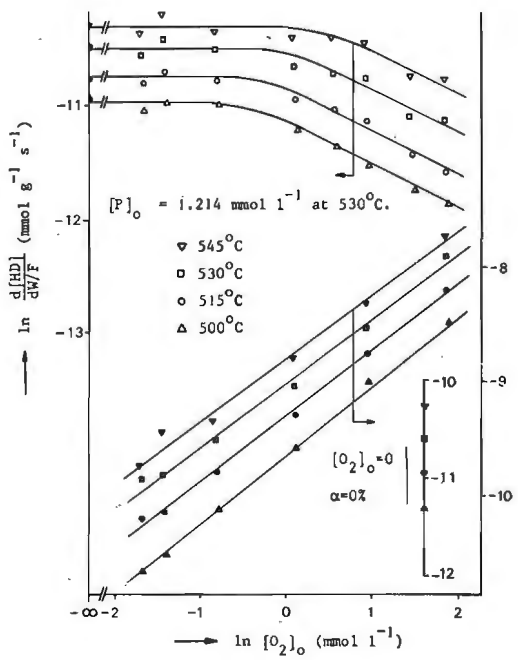

Figure 5.6 Rates of formation of 1,5-hexadiene and carbon dioxide as a function of the oxygen inlet concentration at various temperatures. Catalyst α-Bi_2O_3. x_{prop}=0.08.

formation for 1,5-hexadiene is independent of the oxygen concentration. The width of this region further depends on the temperature. At 545°C the region extends to an oxygen concentration of 1.11 mmol l^{-1}, while at 500°C this zero order behaviour only covers the range of oxygen concentrations from 0 to 0.45 mmol l^{-1}. At high oxygen concentration the reaction order changes to -0.4 at all temperatures, i.e. increasing the oxygen concentration decreases the 1,5-hexadiene rate of formation.

To check how far the experiments without oxygen in the feed described in chapter 4 are linked with these measurements, we carried out at each temperature an experiment without oxygen in the feed. The results of these measurements are given in figure 5.6 at $\ln[O_2]_o = -\infty$. It appears that an initial addition of oxygen to the feed does not affect the rate of formation of 1,5-hexadiene. As the amount of carbon dioxide formed in the experiments with $[O_2]_o=0$ is very small we calculated the CO_2 concentrations in this case with the aid of the kinetic parameters determined in the flow reactor experiments, described in paragraph 4.3.2. The results indicate that addition of oxygen to the feed causes an increase of the rate of carbon dioxide formation as compared with the experiments without oxygen in the feed. The above means that in the region of low oxygen concentrations the decrease in selectivity is caused by an increase of the aselective reaction.

If we compare the measurements depicted in figure 5.5 with those given in figure 5.6 it appears that the reaction order in propylene for the CO_2 and 1,5-hexadiene formation is determined at an oxygen concentration which as far as 1,5-hexadiene is concerned is situated in the transition region from zero to negative order. Since a change in reaction order indicates a change in reaction mechanism or a change in emphasis between two cocurrently operating mechanisms we decided to determine the reaction orders in propylene also at a high and low oxygen concentration. The results of these measurements are given in figure 5.7 and 5.8. It appears that at high oxygen concentration ($[O_2]_o = 3.5$ mmol l^{-1})the reaction order in propylene for carbon dioxide formation has a value of 1, while the 1,5-hexadiene formation still possesses a reaction

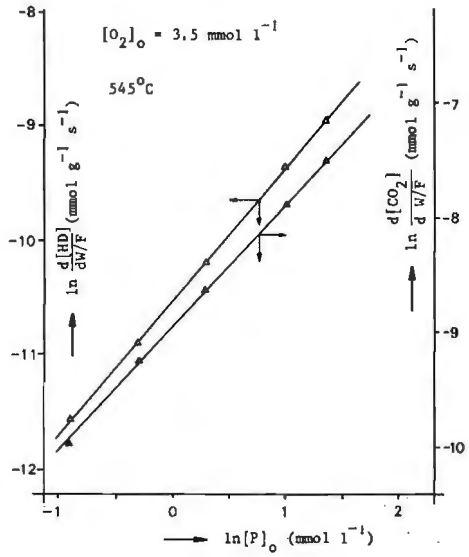

Figure 5.7 Rates of formation of 1,5-hexadiene and carbon dioxide as a function of the propylene inlet concentration at high oxygen concentration. Catalyst α-Bi_2O_3.

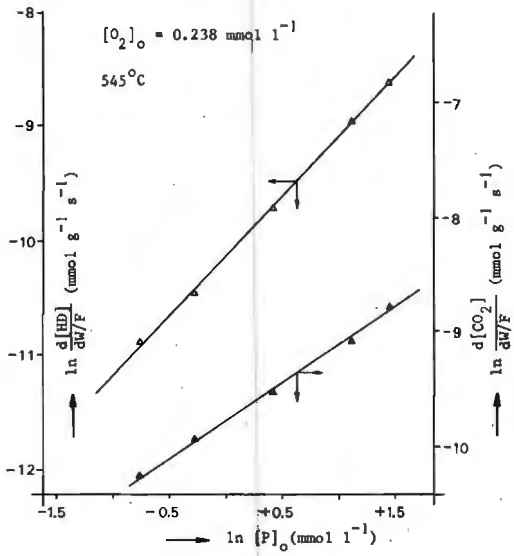

Figure 5.8 Rates of formation of 1,5-hexadiene and carbon dioxide as a function of the propylene inlet concentration at low oxygen concentration. Catalyst α-Bi_2O_3.

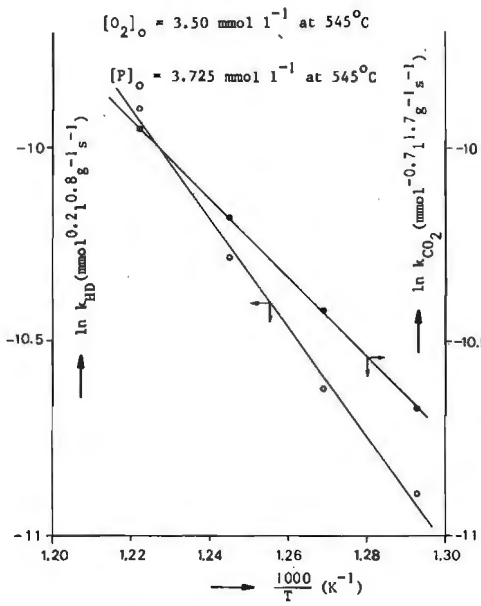

Figure 5.9 Arrhenius plot for oxidation of propylene with α-Bi_2O_3 at high oxygen mole fraction (x_{O_2}=0.235, x_{prop}=0.25).

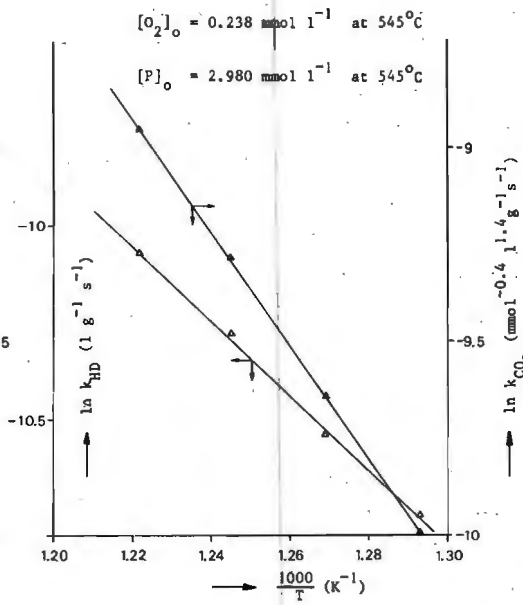

Figure 5.10 Arrhenius plot for oxidation of propylene with α-Bi_2O_3 at low oxygen mole fraction (x_{O_2}=0.016, x_{prop}=0.20).

order of 1.2. Assuming the reaction orders in oxygen for 1,5-hexadiene and carbon dioxide formation to be -0.4 and 0.7, respectively, we calculate apparent activation energies of 82 kJ mol^{-1} and 118 kJ mol^{-1} for the aselective and selective reaction, respectively. See figure 5.9. These values agree well with the measurements given in figure 5.6 at high oxygen concentration, from which activation energies of 88 kJ mol^{-1} and 126 kJ mol^{-1} are obtained for carbon dioxide and 1,5-hexadiene formation, respectively.

At low oxygen concentration ($[O_2]_o$=0.238 mmol l^{-1}),on the contrary, a quite different picture is obtained. Figure 5.8 shows that the reaction order in propylene for 1,5-hexadiene formation now amounts to one, while the reaction order for carbon dioxide possesses a value of 0.7. Assuming a zero order oxygen dependence for 1,5-hexadiene and a reaction order in oxygen of 0.7 for carbon dioxide the rate constants at various temperatures were calculated with equation (1) and (2). The results are depicted in figure 5.10. It turns out that the activation energies have interchanged, i.e. the aselective reaction possesses an apparent activation energy of 122 kJ mol^{-1} while for the formation of 1,5-hexadiene a value of 80 kJ mol^{-1} is obtained. These values also agree well with the results shown in figure 5.6 at low oxygen concentration. From this figure values of 126 and 88 kJ mol^{-1} are calculated for the reaction to carbon dioxide and 1,5-hexadiene, respectively.

5.2.3 DISCUSSION

To facilitate the interpretation of the kinetic results described in the preceding paragraph the reaction orders and apparent activation energies obtained at the various conditions have been summarized in table 5.1. From this table as well as from the figures it is clear that for both reactions a distinction has to be made between the kinetics at low oxygen concentration (region I, $[O_2]_o$ < 0.4 mmol l^{-1}), intermediate

Table 5.1 Reaction orders and activation energies at various reaction conditions for the oxidation of propylene with α-Bi_2O_3 as catalyst. Differential measurements.

Feed composition		Temp. °C	CO_2-formation			1,5-HD formation		
			reaction order in		E_{act}	reaction order in		E_{act}
x_{O_2}	x_{prop}		oxygen	propylene	kJ mol^{-1}	oxygen	propylene	kJ mol^{-1}
0.01-0.04	0.08	500						
		515						
		530	0.7		126	0		88
		545						
0.04-0.15	0.08	500						
		515						
		530	0.7			0- -0.4		
		545						
0.15-0.30	0.08	500						
		515						
		530	0.7		88	-0.4		126
		545						
0.016	0.03-0.30	545		0.7	122		1	80
0.075	0.02-0.30	500		1.0				
		515		0.9	109		1.2	97
		530		0.9				
		545		0.8				
0.23	0.03-0.25	545		1	82		1.2	118

oxygen concentration (region II, $[O_2]_o$=0.4-1.65 mmol l^{-1}) and high oxygen concentration (region III, $[O_2]_o$ > 1.65 mmol l^{-1}) in the feed. Before we discuss these three regions we first shall go further in some features of oxidation reactions that might be responsible for formation of 1,5-hexadiene and carbon dioxide.

It is generally accepted nowadays that in the oxidation of propylene over oxide catalysts allyl species play a role (15,19). We also saw this to be the case in chapter four for the formation of 1,5-hexadiene with α-Bi_2O_3 acting as an oxidant. The centers active for allyl formation appeared to be anion vacancies. We shall call these sites V sites. Besides V sites the surface also

contains sites on which only combustion of propylene takes place. For the carbon dioxide formation with α-Bi_2O_3 acting as an oxidant the oxygen atoms in the surface were assumed to be the active centers. These sites will, therefore, be called O sites. When we assume that upon addition of oxygen to the feed these two sites will remain responsible for the oxidation of propylene the reaction sequences A and B in the following scheme are possible.

A. V site

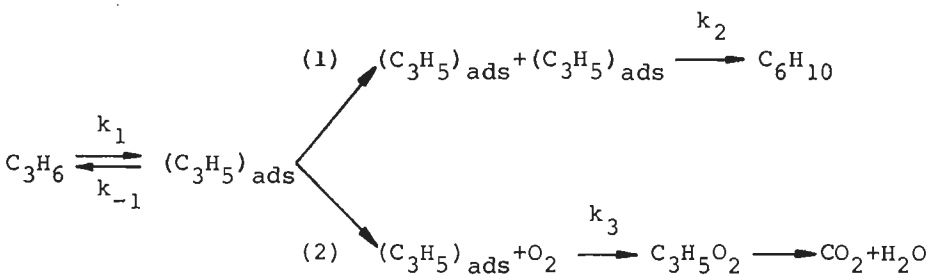

B. O site

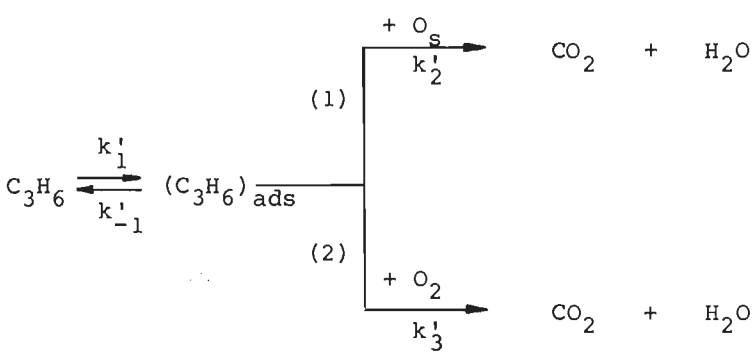

In contrast with 1,5-hexadiene, which is formed by reaction between two allyl species adsorbed on the surface (A1), carbon dioxide may arise by 3 reaction paths, i.e. either by disintegration of allyl peroxides (A2) or by reaction of propylene adsorbed on the O site with either oxygen from the oxide surface (B1) (described in chapter 4) or from the gas phase (B2) (Eley-Rideal mechanism). The allyl peroxy radicals

in reaction A2 may be formed by reaction between gas phase oxygen with either desorbed or adsorbed allyl species.

So far we have supposed that the reactions take place by only one mechanism. When a product is formed by various mechanisms the reaction order and activation energy that have been determined experimentally not necessarily need to be the parameters that characterize one rate determining step exclusively. This is a.o. the case when the contributions for the various processes are of the same order of magnitude. When, on the other hand, one of the processes determines the overall rate, experimentally the kinetic parameters of this reaction will be determined.

From chapter 4 it became clear that when no oxygen is present in the feed, the formation of 1,5-hexadiene is first order in propylene, while the carbon dioxide formation takes place by a Langmuir-Hinshelwood reaction model. With this in mind we shall develop the general kinetic expressions for the formation of 1,5-hexadiene and carbon dioxide according to reaction path A and B.

REACTION PATH A

For the experiments without oxygen in the feed as well as at low oxygen concentration we found that the rate of 1,5-hexadiene formation is first order in propylene. This is consistent with a model in which the adsorption of propylene as allyl species determines the overall rate of reaction. We see this if we derive the equation for the steady state coverage of the surface with propylene on the V sites (θ_v). The reactions that have to be accounted for are:

$$\sigma_v + P \underset{k_{-1}}{\overset{k_1}{\rightleftharpoons}} \sigma_v P \qquad (\sigma_v = \text{vacancy } (\square_s) + \text{oxygen ion } (O_s);\ \sigma_v P = (\text{allyl})_{ads} + (H)_{ads})$$

$$2\sigma_v P \xrightarrow{k_2} 1,5\text{-HD} + H_2O + 3\,\square_s + O_s.$$

For the steady state we get:

$$\frac{d\theta_v}{dt} = 0 = k_1(1-\theta_v)[P] - k_{-1}\theta_v - k_2\theta_v^2 \qquad (5)$$

If we assume that:

$$k_2\theta_v >> k_{-1} \qquad (6)$$

the steady state coverage is given by:

$$\theta_v = \frac{k_1[P]}{k_2\ 2}\left(\sqrt{1 + \frac{4k_2}{k_1[P]}} - 1\right) \qquad (7)$$

Two special cases can be discerned. When

$$\frac{4k_2}{k_1[P]} << 1, \qquad (8)$$

θ_v will be very close to one, i.e. the surface will be fully covered with propylene and the 1,5-hexadiene formation will be independent of the propylene partial pressure. When, on the other hand,

$$\frac{4k_2}{k_1[P]} >> 1 \qquad (9)$$

equation (7) may be rearranged to:

$$\theta_v = \sqrt{\frac{k_1}{k_2}[P]} \qquad (10)$$

For the rate of 1,5-hexadiene formation:

$$r_{HD} = k_2\theta_v^2 \qquad (11)$$

we then get:

$$r_{HD} = k_1[P] \qquad (12)$$

We see that a first order propylene behaviour emerges when

$k_2 >> k_{-1}, k_1[P]$. The adsorption of propylene will then determine the overall rate of reaction.

When oxygen is added to the feed also reaction A2 takes place:

$$\sigma_v P + O_2 \xrightarrow{k_3} CO_2 + H_2O$$

We assume that this reaction is first order in oxygen. The steady state surface coverage now follows from:

$$\frac{d\theta_v}{dt} = 0 = k_1(1-\theta_v)[P] - k_{-1}\theta_v - k_2\theta_v^2 - k_3\theta_v[O_2] \qquad (13)$$

At low oxygen concentration

$$k_3\theta_v[O_2] << k_2\theta_v^2 \qquad (14)$$

and, provided that still $k_2 >> k_{-1}, k_1[P]$, equation (10) will result. Upon increasing the oxygen concentration, however, this condition will cease to be fullfilled. Assuming $k_2\theta_v >> k_{-1}$, the steady state coverage will now be given by

$$\theta_v = \frac{k_1[P] + k_3[O_2]}{2k_2}\left(\sqrt{1 + \frac{4k_1k_2[P]}{(k_1[P] + k_3[O_2])^2}} - 1\right) \qquad (15)$$

At high oxygen concentration, i.e.

$$\frac{4k_1k_2[P]}{(k_1[P] + k_3[O_2])^2} << 1, \qquad (16)$$

equation (15) simplifies to:

$$\theta_v = \frac{k_1[P]}{k_1[P] + k_3[O_2]} \qquad (17)$$

For oxygen concentrations where the second term in the denominator of (17) is much larger that the first one, equation (17) reduces to:

$$\theta_v = \frac{k_1[P]}{k_3[O_2]} \qquad (18)$$

When we substitute this result in equation (11) we see that raising the oxygen concentration results in an increase of the propylene reaction order, while a negative order in oxygen shows up. For the rate of carbon dioxide we find under these conditions:

$$r_{CO_2} = k_1[P], \qquad (19)$$

i.e. first order in propylene and zero order in oxygen. In this case almost all allyl species are consumed by the aselective reaction A2.

REACTION PATH B

For the formation of carbon dioxide by reaction B2 we also assume first order kinetics in oxygen. The steady state coverage of the surface by propylene adsorbed on the O sites (θ_o) is then given by:

$$\theta_o = \frac{k_1'[P]}{k_1'[P] + k_{-1}' + k_2' + k_3'[O_2]}, \qquad (20)$$

while for the rate of carbon dioxide formation we find:

$$r_{CO_2} = \frac{k_2'k_1'[P]}{k_1'[P] + k_{-1}' + k_2' + k_3'[O_2]} + \frac{k_3'k_1'[P][O_2]}{k_1'[P] + k_{-1}' + k_2' + k_3'[O_2]} \qquad (21)$$

When we now return to the three regions of oxygen concen-

trations in which both reactions express different kinetics, we could interpret the experimental results in the light of the reaction scheme discussed and kinetic expressions derived so far.

a. REGION I (low oxygen concentration)

For 1,5-hexadiene it turns out that addition of oxygen to the feed has no effect on the rate measured when no oxygen is present in the gas phase at α=0%. The reaction order of one as well as the activation energy of 80-88 kJ mol^{-1} and the value of the rate constant further agree well with the kinetic parameters determined for the dimerization reaction under reducing conditions. We, therefore, conclude that at low oxygen concentration in the feed the 1,5-hexadiene formation takes place by a mechanism in which the formation of allyl species is the rate determining step. We further conclude that all the allyl species that are formed are consumed by reaction A1, the formation of 1,5-hexadiene.

The formation of carbon dioxide is in this region characterized by a reaction order in propylene and oxygen of 0.7 and an apparent activation energy of 122 kJ mol^{-1}. This can be visualized as follows. Since at low oxygen concentration carbon dioxide is mainly formed by reaction path B the rate will be described by equation (21). It further appears that in this region the rate of carbon dioxide formation is primarily determined by the reaction of propylene with oxygen from the surface, i.e. path B1. This is illustrated by figure 5.11, which shows the initial rates measured at low oxygen concentration (i.e. depicted in figure 5.8) and those calculated with the kinetic parameters obtained in chapter 4. In fact the contribution of path B1 will be somewhat lower than shown in figure 5.11, as the decrease in carbon dioxide formation according to the chapter 4 mechanism (B1) is somewhat reduced by the other oxidation step (B2). It also is now clear that the measured activation energy for carbon dioxide formation in this region is very close to

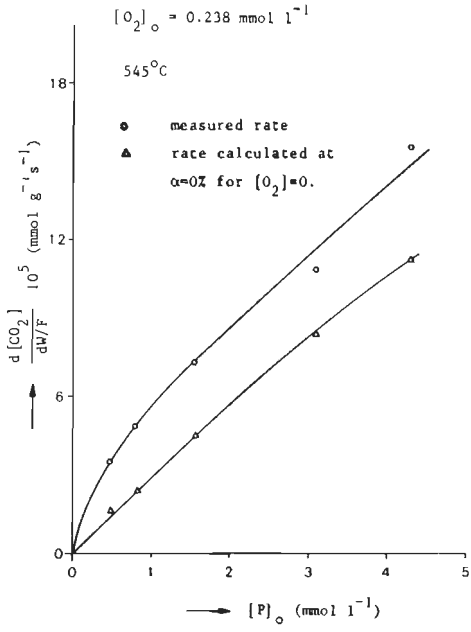

Figure 5.11 Rate of formation of carbon dioxide as a function of the propylene inlet concentration. Comparison between measured rate and rate calculated for $[O_2]_o$=0 at α=0% with parameters given in chapter 4. Catalyst α-Bi_2O_3.

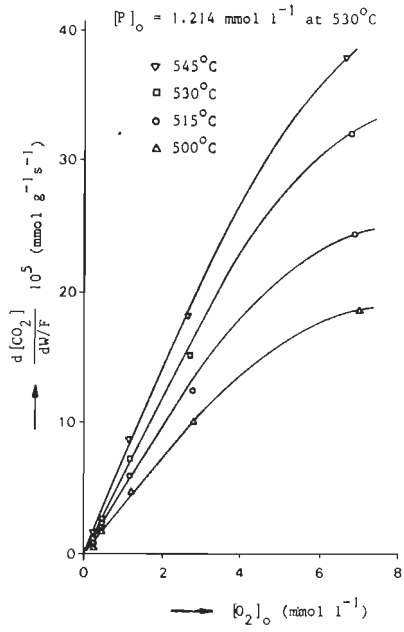

Figure 5.12 Rate of formation of carbon dioxide as a function of the oxygen inlet concentration after correction for the contribution due to mechanism B1 at α=0%. Catalyst α-Bi_2O_3. (x_{prop}=0.08).

that measured when no oxygen is present in the feed.

Equation (21) also predicts that at low oxygen concentration the rate of carbon dioxide formation has to be first order in oxygen. At high oxygen concentration, however, the kinetics have to change to a zero order oxygen behaviour, as then the term $k_3'[O_2]$ in the nominator of equation (21) will become important. This zero order oxygen dependence at high oxygen concentration also applies to equation (19). If we assume in first approximation the CO_2 formation by reaction B1 to be independent of the oxygen concentration and substract the rates due to B1 at α=0% from the experimental measured rates we get the picture shown in figure 5.12. It turns out that at low oxygen concentration the rate is first order in oxygen, while at high oxygen concentration a change to a zero order behaviour takes place.

b. REGION III (high oxygen concentration)

At high oxygen concentration a negative order in oxygen is found, i.e. addition of oxygen decreases the formation of 1,5-hexadiene. Simultaneously the reaction order in propylene changes from 1 to 1.2, while the activation energy increases from 80-88 to 117-122 kJ mol^{-1}. We suppose that the decrease of the rate of 1,5-hexadiene formation is caused by the fact that allyl species now react with oxygen present in high concentration in the gas phase to form allyl peroxy radicals, i.e. besides reaction A1 also reaction A2 takes place. This also explains a change in activation energy for 1,5-hexadiene formation, since in stead of k_1 we now measure the temperature dependence of the rather complicated form $k_2\theta_v^2$, θ_v being expressed by equation (15). The change in reaction order from 1 to 1.2 may also be explained in terms of CO_2 formation by reaction A2.

With regard to carbon dioxide formation in this region it turns out that this product is formed according to a scheme which is first order in propylene and has an activation energy of 82 kJ mol^{-1}. Since at high oxygen concentration carbon dioxide is primarily formed by reaction B2 and A2, the rate expression will be given by

$$r_{CO_2} = k_1 [P] + k_1' [P], \qquad (22)$$

i.e. first order in propylene. Since k_1 has an activation energy of 80-88 kJ mol^{-1} the experimental measured temperature dependence of 82 kJ mol^{-1} indicates that the activation energy for k_1' has to be of the same order of magnitude, as reaction B2 contributes for the most part to the CO_2 formation in this region.

c. REGION II (intermediate oxygen concentration)

In this region the rate of formation of 1,5-hexadiene is characterized by an apparent activation energy of 96 kJ mol^{-1} and a reaction order of propylene of 1.2. Regarding the reaction

order in propylene this increase also may be explained by the occurrence of carbon dioxide formation by reaction path A2. From figure 5.6 we see that the width of the transition region further depends on the temperature. Since increasing the temperature results in a wider zero order region k_2 must increase faster than k_3 with temperature increase.

Finally, the CO_2 formation in this region can be interpreted in terms of the models described above. It appears, however, that fitting of the rates of figure 5.5 according to a Langmuir-Hinshelwood model gives straight lines at all four temperatures, which intersect at one point. The reason for this behaviour becomes clear when we consider figure 5.6. From this figure we see that at the lowest temperature (500°C) the contribution to CO_2 formation by path A2 is highest, which means that the rate of carbon dioxide formation at this temperature has to be corrected most. In the $1/r_{CO_2}$ versus $1/P_o$ plot this will result in the largest lift of the low temperature line.

5.3 OXIDATION OF 1,5-HEXADIENE

To investigate the effect of gas phase oxygen on the consecutive oxidation of 1,5-hexadiene we first studied the relation between product concentration and contact time both in a reactor filled with silicon carbide only and in a reactor filled with a layer silicon carbide and α-Bi_2O_3. When we compare the results obtained for the case that the reactor is only filled with SiC with figure 4.17, which gives the product concentrations as a function of W/F in a solely with silicon carbide filled reactor and no oxygen in the feed, it appears that the same products are formed. The relative amounts of the products, however, have changed. Thus, the concentration of 3-allylcyclohexene and propylene are now lower than that of benzene and 1,3-cyclohexadiene,while the C_9H_{14} concentration now is considerably lower than the propylene concentration. From some experiments with an empty reactor it further became clear that this non catalytic contribution is made up by homogeneous reactions ($\sim$ 30%) and reactions initiated by the

silicon carbide. In contrast to propylene oxidation, however, now also hydrocarbons are formed homogeneously.

When the reactor is filled with silicon carbide and α-Bi_2O_3 it turns out that the non catalytic contribution is three times as high as product formation due to α-Bi_2O_3. This will not benefit the accuracy of the measurements. From the measurements, however, we may conclude that carbon dioxide, 3-allylcyclohexene and 1,3-cyclohexadiene are formed by parallel reactions from 1,5-hexadiene, while benzene is formed by a consecutive reaction. However, it is not clear from which hydrocarbon the benzene is formed, which illustrates the inaccuracy of the method. For this reason as well as from the fact that at short contact time in a reactor filled with silicon carbide or empty reactor the steady state hardly is to be reached, we decided not to continue the kinetic study on this point.

CHAPTER 6

Reaction Kinetics Part three - Influence of Zinc Oxide on the Oxidation of Propylene with Bismuth Oxide

6.1 INTRODUCTION

In chapter 3 we mentioned that the $Bi_2O_3(ZnO)_{1.36}$ binary oxide, provided it is not reduced further than α=15%*, showed no activity loss even after 40 reduction-reoxidation cycles. Compared with α-Bi_2O_3 this indeed is a real improvement. It also appeared that under reducing conditions the sum of the selectivities for 1,5-hexadiene and benzene did not change to a large extent when the binary oxide Bi_2O_3-ZnO was used instead of α-Bi_2O_3. At first sight one may, therefore, suppose that zinc oxide only acts as a carrier for α-Bi_2O_3. From the literature (40), however, it is known that zinc oxide itself also possesses dehydroaromatization properties. Moreover, zinc oxide stabilizes the γ-phase of bismuth oxide, which may have other dimerization characteristics than α-Bi_2O_3. We, therefore, decided to study briefly the influence of zinc oxide on the kinetics of the propylene oxidation.

The measurements, which were all carried out without oxygen in the feed, were performed both in the flow system and in the thermobalance apparatus. As from paragraph 3.5 it turned out that all Bi_2O_3-ZnO samples showed the same behaviour when no oxygen is present in the feed, we carried out all experiments with the same oxidant sample, i.e. $Bi_2O_3(ZnO)_{1.36}$. To characterize the oxygen activity of the oxide we also reduced $Bi_2O_3(ZnO)_{1.36}$ with hydrogen in the thermobalance.

*α for these experiments is defined on page 40

6.2 OXIDATION OF PROPYLENE IN THE FLOW REACTOR

The product concentrations as a function of the contact time have already been given in figure 3.7. If we compare this figure with figure 4.7, which shows the results for α-Bi_2O_3, it appears that addition of zinc oxide does not result in a great change of the product distribution, i.e. carbon dioxide and 1,5-hexadiene are formed in parallel reactions, while benzene originates by a consecutive reaction from 1,5-hexadiene.

For the kinetic study we used the differential method, analogous to the experiments described in the preceding chapters. The average W/F values amounted to 0.05-0.12 g s ml^{-1}. Experiments with variable gas flow at constant W/F showed that film diffusion could be ignored. The influence of pore diffusion on the rate of reaction could be excluded, as experiments with variable particle diameters showed no difference between each other.

Since in the flow reactor experiments the oxide sample is reoxidized after each run, reduction may not be continued beyond α=10-15%, as then irreversible activity loss will occur. This makes the flow reactor less suitable for a study of the relation between the rates of formation and the degree of reduction. In this paragraph the kinetics will, therefore, always refer to α=0%, i.e. when the oxide sample is in its fully oxidized state.

The rate of formation of 1,5-hexadiene is shown in figure 6.1 as a function of the propylene inlet concentration at four different temperatures. The observed relation points to a reaction order in propylene greater than one. Fitting of these results by a second order Langmuir-Hinshelwood model, in which the surface reaction between two adsorbed allyl species is the rate determining step, appears not to be succesful. However, the initial rates can be conveniently described by the following relation:

$$r_{HD} = C_1[P]_o + C_2[P]_o^2 \qquad (1)$$

$[P]_o$ being the inlet concentration of propylene. This model is based on the assumption that the oxide surface contains

two kinds of adsorption sites for propylene resulting in 1,5-hexadiene, i.e. X and Y sites. When on the X sites the adsorption of propylene is the rate determining step a first order behaviour in propylene will result:

$$r_{HD,X} = k_1[P] \qquad (2)$$

If we further assume that on the Y sites a weak propylene adsorption is involved, while the chemical reaction between two allyl species is now thought to be rate determining, then the rate expression for 1,5-hexadiene formation on this site becomes:

$$r_{HD,Y} = \frac{k_2(K[P])^2}{(1+K[P])^2}. \qquad (3)$$

With $K[P] \ll 1$ this simplifies to

$$r_{HD,Y} = k_2K^2[P]^2 \qquad (4)$$

and the final rate expression will be identical to equation (1).

The solid lines in figure 6.1 are those calculated theoretically with values for $C_1 (=k_1)$ and $C_2 (=k_2K^2)$ shown in figure 6.2. From this figure we calculate an activation energy of 87 kJ mol^{-1} for k_1, while for C_2 an apparent activation energy of 39 kJ mol^{-1} is obtained. This low value for C_2 is due to the fact that the heat of adsorption for propylene on the Y site is not yet accounted for.

The initial rates of carbon dioxide formation are depicted in figure 6.3. It appears that these results may be well described by a single site Langmuir-Hinshelwood model, i.e.

$$r_{CO_2} = \frac{k_3K'[P]}{1+K'[P]}, \qquad (5)$$

since the $1/r_{CO_2}$ versus $1/P_o$ plot shows straight lines for all temperatures. See figure 6.4. The apparent activation energy amounts to 109 kJ mol^{-1}.

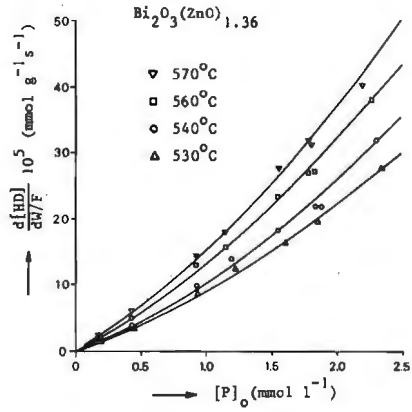

Figure 6.1 Rate of 1,5-hexadiene formation at α=0% as a function of the propylene inlet concentration at various temperatures. Flow reactor.

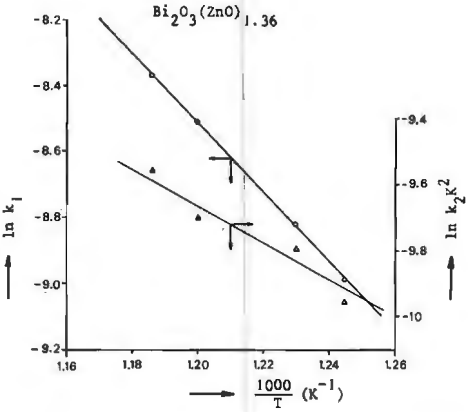

Figure 6.2 Arrhenius plot for 1,5-hexadiene formation at α=0%. Flow reactor.

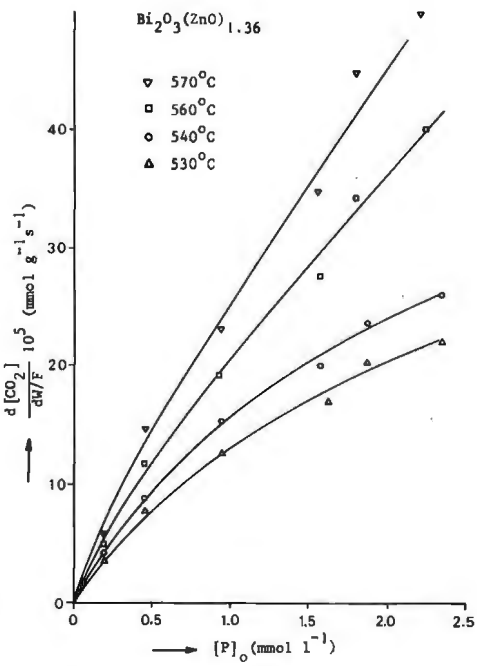

Figure 6.3 Rate of carbon dioxide formation at α=0% as a function of the propylene inlet concentration at various temperatures. Flow reactor.

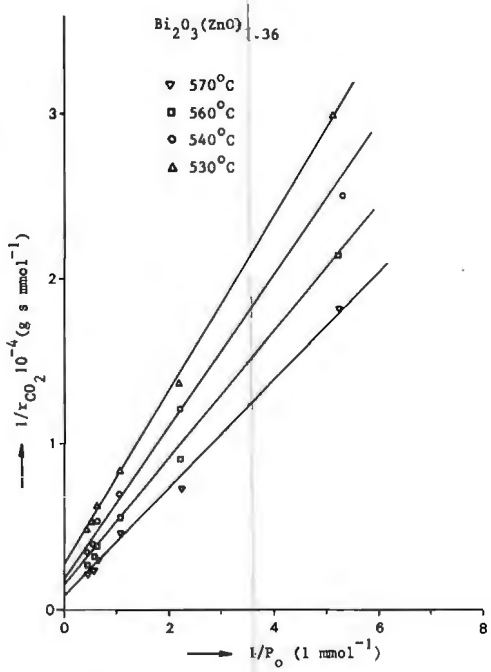

Figure 6.4 Plot of $1/r_{CO_2}$ versus $1/P_o$. Check of equation (5) for the aselective reaction.

6.3 *REDUCTION OF $Bi_2O_3(ZnO)_{1.36}$ IN THE THERMOBALANCE*

The experiments described in this paragraph are all carried out under the same conditions as described in paragraph 4.4. For the hydrogen reduction we used the sieve fraction 0.15-0.30 mm, while for the reduction with propylene the fraction with particle diameters between 0.075 and 0.05 mm was used.

6.3.1 *OXIDATION OF HYDROGEN*

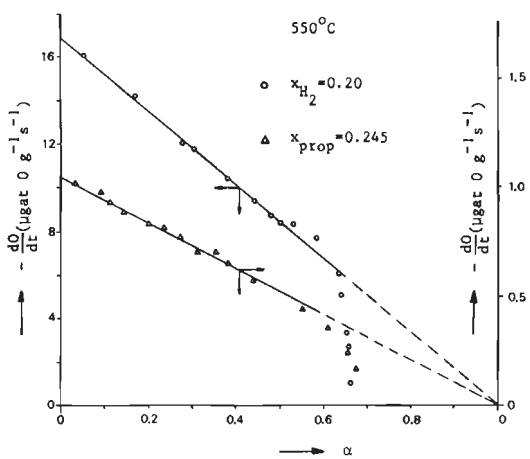

Figure 6.5 Reduction of $Bi_2O_3(ZnO)_{1.36}$ with hydrogen and propylene. Thermobalance.

Figure 6.5 shows for a typical experiment the rate of reduction as a function of the degree of reduction. We see that the reduction continues to α=66-67%, which corresponds with the amount of oxygen bonded in the form of bismuth oxide. Moreover, the observed relation indicates that the hydrogen reduction of the bismuth oxide-zinc oxide sample may be described by the volumetric reaction model with first order oxygen dependence (see paragraph 4.2).

The influence of the hydrogen mole fraction on the reduction is shown in figure 6.6 at 550°C. As the lines in this figure are described by

$$-\ln(1-\alpha) = k\, x_{H_2}^{n}\, t, \qquad (6)$$

the order of the reduction reaction in hydrogen can be obtained from a plot of ln β ($\beta = k\, x_{H_2}^{n}$) versus ln x_{H_2}. From figure 6.7 the reaction order in hydrogen appears to be one.

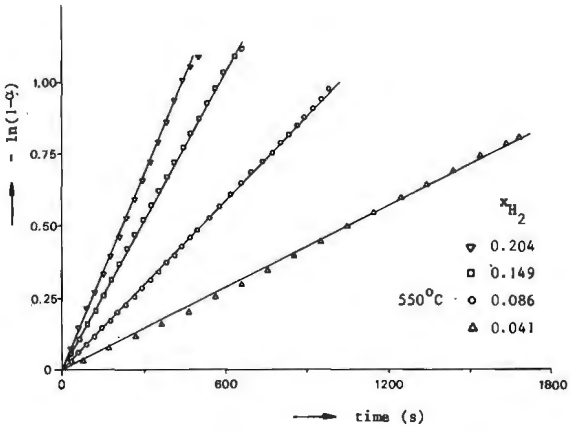

Figure 6.6 Validity of the first order volumetric reaction model for the reduction of $Bi_2O_3(ZnO)_{1.36}$ with hydrogen at various mole fractions. Thermobalance.

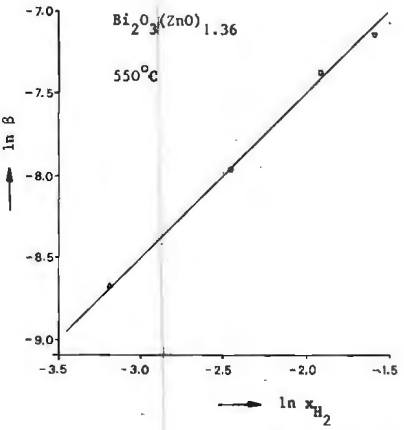

Figure 6.7 Reduction rate at α=0% as a function of the hydrogen mole fraction. Thermobalance.

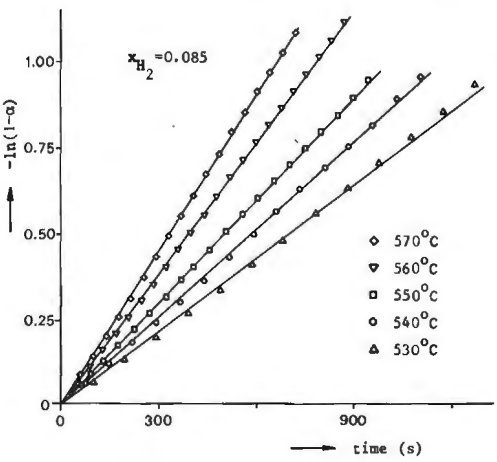

Figure 6.8 Validity of the first order volumetric reaction model for the reduction of $Bi_2O_3(ZnO)_{1.36}$ with hydrogen at various temperatures.

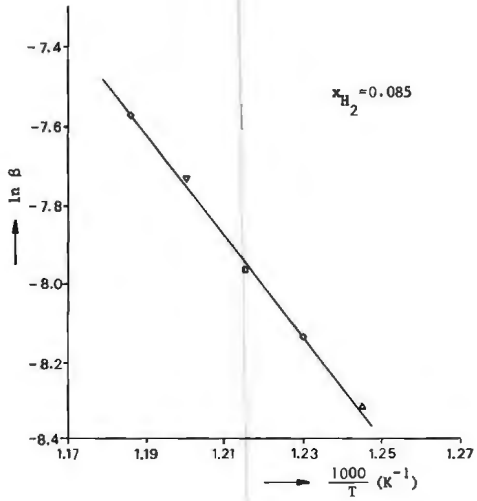

Figure 6.9 Arrhenius plot for the reduction of $Bi_2O_3(ZnO)_{1.36}$ with hydrogen. Thermobalance.

Changing the temperature at constant hydrogen mole fraction has the effect shown in figure 6.8. From a plot of ln β versus 1/T, an activation energy of 106 kJ mol^{-1} is calculated. See figure 6.9.

6.3.2 *OXIDATION OF PROPYLENE*

Since at the time these experiments were carried out the thermobalance was not yet equipped with the gas chromatographic system and the carbon dioxide monitor, we only get information about the total rate of oxygen depletion, i.e. due to formation of both 1,5-hexadiene and carbon dioxide. Nevertheless, these measurements give us some idea of the way in which zinc oxide affects the relation between the rate of reduction and the degree of reduction compared with α-Bi_2O_3.

From figure 6.5, which shows the rate of reduction as a function of α at 550°C and x_{prop}=0.245, we see that also in the case of propylene the reduction only can be continued to α=66-67%, i.e. till all the oxygen bonded to bismuth is consumed. Moreover, like α-Bi_2O_3 the overall reduction process can be described in this α-region by the volumetric reaction model with first order oxygen dependence.

Varying the propylene mole fraction at constant temperature has the effect shown in figure 6.10. From the slope of these lines the order in propylene for the overall oxygen depletion may be calculated. This results in a value of one. See figure 6.11.

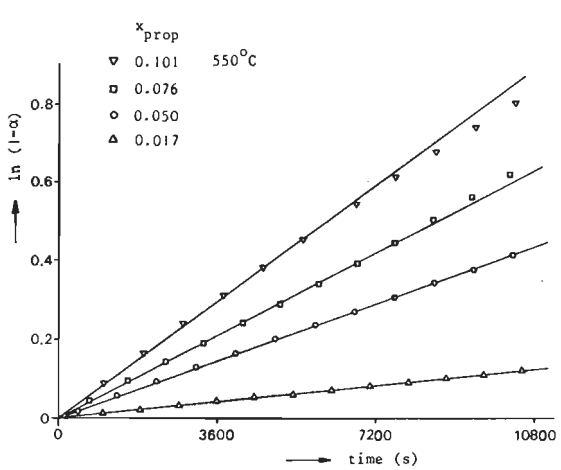

Figure 6.10 Validity of the first order volumetric reaction model for the reduction of $Bi_2O_3(ZnO)_{1.36}$ with propylene at various mole fractions. Thermobalance.

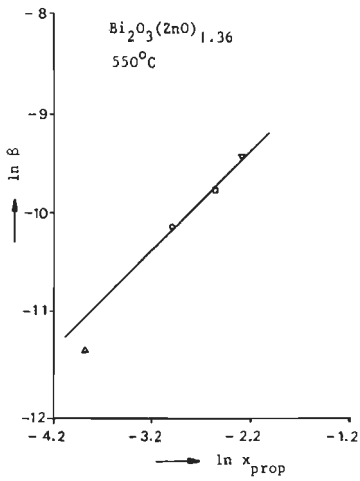

Figure 6.11 Reduction rate at α=0% as a function of the propylene mole fraction. Thermobalance.

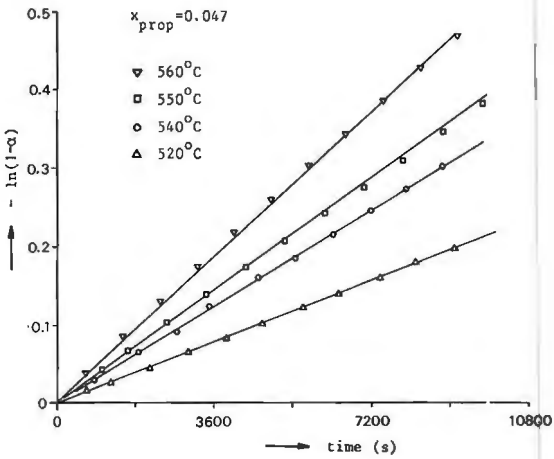

Figure 6.12 Validity of the first order volumetric reaction model for the reduction of $Bi_2O_3(ZnO)_{1.36}$ with propylene at various temperatures. Thermobalance.

The temperature dependence for the propylene reduction of $Bi_2O_3(ZnO)_{1.36}$ is depicted in figure 6.12. From the slope of the lines an apparent activation energy of 108 kJ mol^{-1} may be calculated for the overall rate of oxygen depletion. This agrees quite well with the observation made with the flow reactor that most oxygen is consumed by the aselective reaction.

6.4 DISCUSSION

The results described in this chapter indicate that the addition of zinc oxide to α-Bi_2O_3 has two effects. First, zinc oxide acts more or less as a stabilizing agent for bismuth oxide, while secondly the kinetics of the propylene oxidation are influenced. Further, the relation between the rate of oxygen depletion and the degree of reduction, which is identical to that of α-Bi_2O_3, points to a mechanism for propylene oxidation with the binary oxide system similar to that of α-Bi_2O_3.

The stabilizing effect of ZnO follows i.e. from the fact that no appreciable loss in activity takes place after 40 reduction-reoxidation cycles. An electron micrograph picture of a sample that had been used in 40 cycles is shown in figure

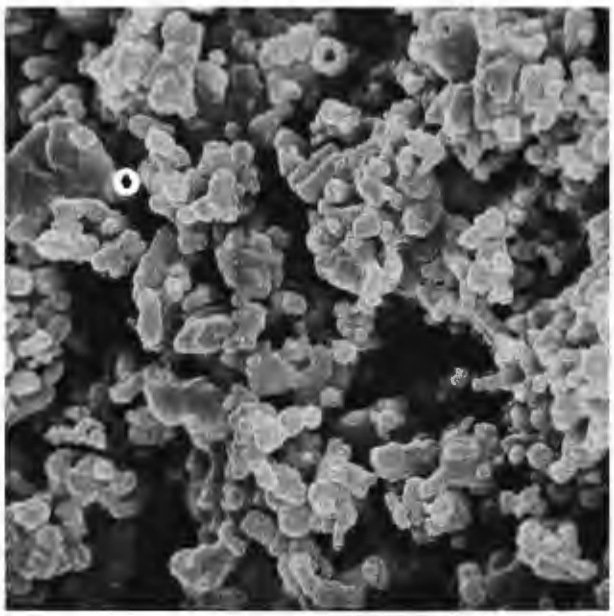

Figure 6.13 Electron micrograph of $Bi_2O_3(ZnO)_{1.36}$ used in 40 reduction-reoxidation cycles.

6.13. In contrast with the photographs depicted in figure 4.43 no reoxidized bismuth clusters can be observed in this picture. The stabilizing effect is also supported by the reduction experiments in the thermobalance, which showed that only the oxygen bonded to bismuth may be taken from the oxide sample.

As far as the kinetics of the oxidation of propylene are concerned it turns out that for the formation of carbon dioxide the Langmuir-Hinshelwood model that applies to α-Bi_2O_3 also described well the results in the case of $Bi_2O_3(ZnO)_{1.36}$. The rate of carbon dioxide formation is, however, roughly three to four times higher than in the case of α-Bi_2O_3, which may be interpreted in terms of the higher surface area for the binary oxide. The kinetics of the dimerization reaction, on the other hand, show a different picture. As shown in paragraph 6.2 the initial rates of 1,5-hexadiene formation can be interpreted by assuming the existence of two sites, X and Y, on which the dimerization reaction takes place, showing first and second order kinetics, respectively. When we consider the activation energy for the dimerization on the X sites it appears that the

observed value of 87 kJ mol^{-1} is very close to those measured for α-Bi_2O_3 (88 kJ mol^{-1} for the thermobalance measurements; 93 kJ mol^{-1} for the flow reactor experiments). Therefore, as on the X sites the dimerization also shows a first order behaviour in propylene, we suppose that they are very similar to the active sites on α-Bi_2O_3. Further, if we compare the initial rate of 1,5-hexadiene formation on the X site with that on α-Bi_2O_3 it turns out that in the former case a higher rate is found. This may also be explained by the higher surface area of the binary oxide. Regarding the reaction on the Y sites the possibility exists that either zinc oxide or a combination of zinc and bismuth is responsible for the reaction on this site. The measurements do not point to a preference for one of the possibilities. However, in the light of the stabilizing effect of the zinc oxide, which is consistent with the existence of two independent sites, a light preference should be given to zinc oxide.

Finally, the change of the activation energy for the hydrogen reduction, which is somewhat higher than that for α-Bi_2O_3, indicates that the addition of zinc oxide also changes the oxygen reactivity to some degree as compared with α-Bi_2O_3. We have to remember, however, that in the binary oxide system the γ-phase of Bi_2O_3 is present. The lattice oxygen in this compound may have a different reactivity in view of its different structure. For the dimerization reaction the activation energy remains almost constant upon addition of zinc oxide. This indicates that the rate determining step for this reaction is hardly influenced by changes in the reactivity of the lattice oxygen. This is in agreement with our previous conclusion that reduced sites play an important role for the dimerization reaction.

CHAPTER 7

Final Discussion

The main aim of this chapter is to evaluate the results described in the preceding chapters in the light of the studies that have already been published on the subject reaction as well as to establish the place of α-Bi_2O_3 in the group of oxide catalysts as far as its catalytic properties are concerned.

First of all, however, we shall deal with the parameters that make an oxide catalyst selective either for carbon dioxide or acrolein or 1,5-hexadiene and benzene.

Subjects that subsequently will be discussed are:
- kinetics of propylene dimerization and aromatization,
- reaction mechanism,
- oxygen mobility in α-Bi_2O_3 as compared to other oxide systems.

7.1 PRODUCT DISTRIBUTION IN THE OXIDATION OF PROPYLENE

As outlined in chapter 1 there exist three main routes for oxidation of propylene with oxide catalysts, i.e. either to acrolein or to 1,5-hexadiene and benzene or to carbon dioxide. Starting from the observation that many of these oxidation reactions occur by an oxidation-reduction mechanism it is not surprising that one has tried to correlate the catalytic activity of oxide catalysts with parameters, which refer to the bond strength of oxygen in the oxide. As in the oxidation step the oxygen-catalyst bond has to be broken, one may expect that a correlation will be found between the catalytic activity and the metal-oxygen bond strength in the oxide. Besides the bond strength, which according to Moro-oka and Ozaki (5) is represented by the "heat of formation of the oxide divided by the number of oxygen atoms in the oxide molecule (ΔH_o)", also the activation energy for isotopic exchange with molecular oxygen is used as a parameter.

For the formation of carbon dioxide from propylene indeed a correlation has been found by Moro-oka and Ozaki (5) between the catalytic activity of a number of metal oxide catalysts (Pt, Pd, Ag, Cu, Co, Mn, Cd, Ni, Fe, V, Cr, Ce, Al, Th) and ΔH_o of the oxides. The correlation showed that the higher the value of ΔH_o, the lower the activity of the oxide was for complete combustion. A similar conclusion derived Gelbshtein et.al. (78) for the butene oxidation with oxide catalysts. They found a correlation between the activation energy for butene combustion and the activation energy for the isotopic oxygen exchange.

For a number of oxides (In, Ni, Cu, Co, Mn, Sn, Cd, Ge, Fe, Zn, Ga, Cr, Si, Ca, Ti) it appears that the metal-oxygen bond strength is not only important for the activity for complete oxidation, but also for allylic oxidation, i.e. the oxidation that occurs after abstraction of an α-hydrogen atom and the formation of the symmetrical allylic intermediate:

$$C_3H_6 \longrightarrow (\overset{1}{C}H_2\cdots\overset{2}{C}H\cdots\overset{3}{C}H_2)^- + H^+.$$

When the allyl species is formed it may react with oxygen from the surface to either partial oxidation products (e.g. acrolein) or carbon dioxide. It is reasonable to assume that the route that is preferred will be correlated to some degree with the metal-oxygen bond strength. A correlation of this nature indeed has been reported by Seiyama et.al. (40), who found a linear relationship between the total selectivity for the allylic oxidation, i.e. to acrolein and 1,5-hexadiene or benzene, and the activation energy for isotopic exchange with molecular oxygen.

There exists, however, a second group of oxides (V, Bi, Sb, Mo, W), which deviate strongly from the correlation found by Moro-oka and Ozaki (5). For this group the abstraction of an α-hydrogen atom has been found to be the important process. The significance of the symmetrical allylic intermediate in the formation of acrolein from propylene has been confirmed by oxidation of propylene samples tagged with radioactive carbon

(79,80). However, as may be concluded from our study, the allylic intermediate also appears to be important for the formation of 1,5-hexadiene. It seems, therefore, appropriate to deal further with the way in which the allyl species may be bonded to the surface, as this may give a better insight in the parameters which determine the reaction of the allyl species to either 1,5-hexadiene or acrolein.

The allyl group which is formed during dissociative adsorption of propylene may be bonded to the metal ion of the surface on two different ways, i.e. by way of

a. a π-allyl complex; the electron can migrate freely over the three carbon atoms:

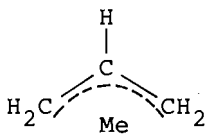

b. a σ-allyl complex; here the metal atom replaces a hydrogen atom of the propylene molecule:

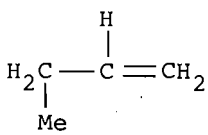

From these two possibilities only in the π-allyl complex both terminal carbon atoms are equivalent. However, by using microwave spectroscopy it recently has been demonstrated by Kondo et.al. (81) that the hydrogen-deuterium exchange reaction of propylene over bismuth molybdate (Bi:Mo=1) takes place by a socalled dynamic σ-allyl intermediate. In this mechanism the reaction intermediate is a complex which oscillates fast between the two σ-allyl structures:

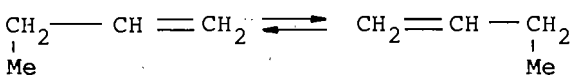

In this case both terminal carbon atoms also will be equivalent. These Japanese investigators further found that the hydrogen exchange reaction between propylene and deuterium over zinc oxide proceeds through the π-allyl intermediate (82). We shall confine ourselves here to a description of the bond between the metal atom and the allyl species by a π-allyl complex, since for our treatment both possibilities do not give different results.

Starting from the simple Hückel molecular orbital (M.O) theory we find for the delocalized π-bond system of an allyl species three orbitals (83), i.e.

$$\psi_B = \tfrac{1}{2}(\phi_1 + \sqrt{2}\,\phi_2 + \phi_3)$$

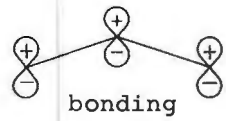

$$\psi_{NB} = \frac{1}{\sqrt{2}}(\phi_1 - \phi_3)$$

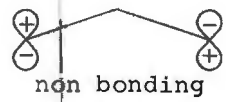

$$\psi_{AB} = \tfrac{1}{2}(\phi_1 - \sqrt{2}\,\phi_2 + \phi_3)$$

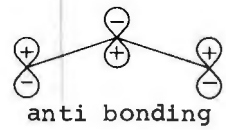

(ϕ_i represents a $2p_z$ orbital on carbon atom i).
The orbital energies and ground state configuration for the allyl radical are given by the following scheme:

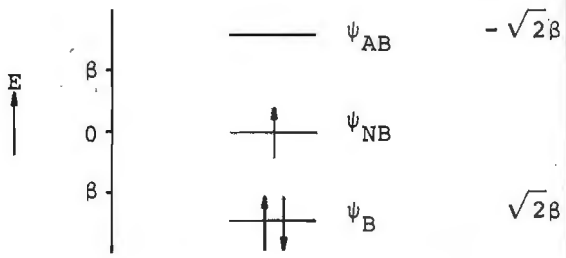

The resonance energy of the allyl radical as compared to the energy of the allyl ion in the canonical form $H_2\overset{\ominus}{C}-CH=CH_2$ amounts

to $(2\sqrt{2}-2)\beta = 67$ kJ mol^{-1} (83).

We now assume that the bonding of the allyl to a metal ion from the surface occurs in a way in which the plane of carbon atoms is roughly parallel to the catalyst surface. This bond likely involves $\sigma\pi$ bonding, i.e. between the filled ψ_B and partly filled ψ_{NB} M.O's from the allyl and the empty or partly filled p and d atomic orbitals (A.O) from the metal cation. Two cases will be considered here, i.e. the bond of the allyl with the MoO_3 surface resulting in the formation of acrolein and the bond between the allyl species and the α-Bi_2O_3 surface, yielding 1,5-hexadiene as the end product. We shall first deal with the MoO_3 catalyst of which the molybdenum ion (Mo^{6+}, $4s^2 4p^6$) at the surface is considered to be the adsorption centre for the allylic intermediate.

According to Peacock et.al. (84) a four centred σ-bonding M.O will be formed between the π-bonding orbital of the allyl (ψ_B) and the initially empty $4d_z2$ A.O of the molybdenum cation, while a three centred π-bonding M.O is formed between the empty d_{xz} or d_{yz} A.O of molybdenum and the non bonding allyl orbital (ψ_{NB}). Electrons that are placed in the π-bonding M.O orbital are symmetrically distributed over the terminal carbon atoms. Since the d orbitals of the metal ion are empty, electrons from the allyl will be donated to this ion, resulting in a partial positive charge on the carbon atoms 1 and 3 of the chemisorbed allyl species. This partial positive charge will promote the interaction of these carbon atoms with the oxygen ions from the surface. Depending on the reactivity of the surface oxygen either acrolein or carbon dioxide will be formed.

When in the case of bismuth oxide the bismuth ion (Bi^{3+}, $6s^2$) is assumed to be the adsorption centre for propylene, the bond will involve the empty p and/or d A.O's from the bismuth ion. If we take the p A.O's a σ-bonding M.O will be formed between the π-bonding M.O from the allyl and the p_z A.O, while a π-bonding M.O will result from the interaction of the ψ_{NB} from the allyl species with either the p_x or p_y A.O from the bismuth ion. Like in the case of molybdenum donation of electrons to the bismuth ions may also take place.

Although the interaction of the terminal partial positive carbon atoms of the allyl with the oxygen from the catalyst surface describes the consecutive formation of acrolein and carbon dioxide in a fairly simple way, this model does not explain the formation of 1,5-hexadiene. Nevertheless, the formation of 1,5-hexadiene also may be explained from the nature of the bond between the allyl species and the surface. This may be visualized as follows. When the adsorption bond is brought about by electrons of both the allyl and the metal ion or when donation of the allyl electrons only takes place in a very limited extent the carbon atoms 1 and 3 will hardly possess a positive charge. This implies that also the interaction between the carbon atoms and the surface oxygen will be less. The allylic intermediate will preserve most of its radical character, the net effect being a preference for coupling of two allyl radicals to form 1,5-hexadiene. For advancing 1,5-hexadiene formation it is therefore necessary to affect the metal ion in such a way that donation of electrons from the allyl to this ion is opposed. A parameter which appears to be of significance in this connection is the electronegativity of the metal ion, which finds expression in the acid-base properties of the oxide. Experimentally Seiyama et.al.(40) indeed have found a relation between the electronegativity (X_i) of the metal ion and the selectivity of the oxide for 1,5-hexadiene and benzene or acrolein. From their results we may conclude that acidic oxides (high X_i) like MoO_3 possess high selectivity for acrolein, while basic oxides (low X_i) like α-Bi_2O_3 primarily are selective for benzene and 1,5-hexadiene. Seiyama et.al. (30) further showed that addition of P_2O_5 and Na_2O to SnO_2 improved selectivity for acrolein and benzene, respectively. We also found that impregnation of a sample $Bi_2O_3(ZnO)_{1.36}$ with a sodium hydroxide solution, evaporating the liquid to dryness and finally calcining the resulting solid at 600°C for 3 h yielded a catalyst which indeed possessed a higher selectivity for 1,5-hexadiene than the untreated sample.

In summary we may state that in the formation of carbon dioxide either directly from propylene or from the allylic intermediate the reactivity of surface oxygen plays an important

role. Furthermore, the formation of acrolein and 1,5-hexadiene occurs by allylic intermediates. Which route ultimately is preferred depends to a large extent on the nature of the adsorption bond between the allyl species and the metal ions.

7.2 KINETICS OF PROPYLENE DIMERIZATION AND AROMATIZATION

From the literature three reports are available, dealing with the kinetics of the propylene dimerization over bismuth oxide (23, 73, 85). One of these has been recently published by Solymosi and Boszo (85). These authors, who studied the formation of 1,5-hexadiene and benzene in a puls reactor, report for the activation energy of the 1,5-hexadiene formation a value of 130 kJ mol^{-1}. From their graphs, however, we calculate a value of 96 kJ mol^{-1}, which is more in agreement with our results given in chapter 4. They also stated that oxygen diffusion from the bulk to the oxide surface had to be fast, although no quantitative results were presented to support this conclusion.

Swift et.al. (23), who studied the dimerization reaction in a flow reactor both with and without oxygen in the feed, found an overall first order conversion of propylene and an activation energy of 115 kJ mol^{-1}, when α-Bi_2O_3 is used as an oxidant. The overall first order behaviour is in agreement with the results presented in chapter 4 of this thesis.Here we found for the formation of 1,5-hexadiene and carbon dioxide reaction orders of 1 and 0.9, respectively. Regarding the activation energy, on the other hand, it is not stated whether their value refers to the overall conversion of propylene or only to the formation of 1,5-hexadiene. Their value, however, is very close to that we found for the aselective combustion of propylene, a reaction which contributes even at high selectivities for a considerable part to the conversion of propylene. In case oxygen is added to the feed Swift et.al. (23) report for the reaction to C_6 hydrocarbons a first order behaviour in propylene and a zero order dependence in gas phase oxygen.These results are also in good agreement with our measurements given

in chapter 5.

Finally, we have to compare our results with those described in the investigation of Massoth and Scarpiello (75), who studied the reduction of α-Bi_2O_3 with propylene in a thermobalance. As we stated already in chapter 4, these authors assumed that the formation of carbon dioxide could be ignored. From our results,however, it follows that this assumption is not justified at all. In contrast to our study they also interpreted their results in an entirely different way. Instead of introducing a model for the surface reaction they described the overall reduction with a model in which initially an undefined surface reaction is rate determining, while in a later stage of the reduction diffusion of propylene through the product layer of molten bismuth, which envelops the bismuth oxide particle, should be rate determining. For these combined effects they derived the following expression:

$$\frac{t}{f_c} = \frac{1}{k_c} + \frac{1}{k_d}\frac{f_d}{f_c} \qquad (1)$$

where

$$f_c = 1 - (1-\alpha)^{1/3} \qquad (2)$$

$$f_d = 3 - 3(1-\alpha)^{2/3} - 2\alpha \qquad (3)$$

k_d apparent rate constant for diffusion $(\sim \frac{M\, ID\, C_{A,s}}{\rho R^2})$

k_c apparent rate constant for chemical reaction $(\sim \frac{M\, k\, C_{A,s}}{\rho R})$

α is the degree of reduction at time t; $C_{A,s}$ is the substrate concentration of A at the reaction interface; ρ is the density of the bismuth oxide particle; R is the radius of the bismuth oxide particle; M is the molecular weight of the oxide particle; ID is the diffusion coefficient of propylene in molten bismuth; k is the chemical rate constant at the Bi-Bi_2O_3 interface. The validity of this model may be tested by plotting t/f_c versus

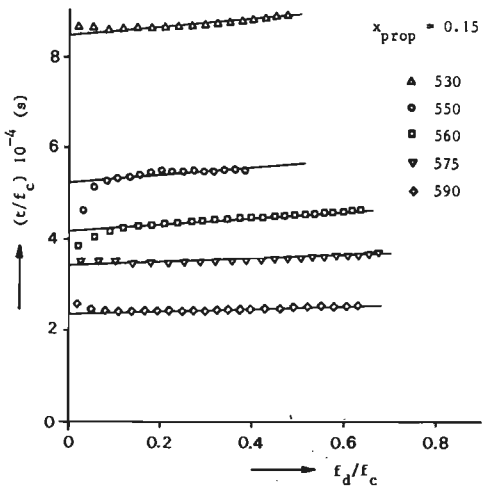

Figure 7.1 Correlation of measurements given in figure 4.30.a according to the combined chemical reaction and diffusion control model of Massoth and Scarpiello (75).

f_d/f_c. Equation (1) only will be valid when both processes, i.e. chemical reaction and diffusion, play a role in the reduction process. For the measurements of Massoth and Scarpiello (75) this indeed turned out to be the case, i.e. at 550°C and x_{prop}=0.22 they found for k_c and k_d values of 3.5 10^{-3} and 3 10^{-3} min^{-1}, respectively. If we plot our measurements according to equation (1) we also get straight lines. As follows from figure 7.1 all lines, however, are almost parallel to the f_d/f_c axis, indicating that diffusion is not significant in our measurements. At 550°C and x_{prop}=0.22 we find values of 1.67 10^{-3} and 10.7 10^{-3} min^{-1} for k_c and k_d, respectively. For the temperature dependence of k_c we calculate an activation energy of 117 kJ mol^{-1}, which agrees fairly well with the value of 115 kJ mol^{-1} reported by Massoth and Scarpiello (75). The values for k_d are too inaccurate to derive a temperature dependence. Over the whole temperature traject, however, the ratio k_d/k_c has an average value of 8.
The lower value for k_c found by us may be partly interpreted in terms of a lower surface area for our sample (0.25 m^2 g^{-1} versus 1.5 m^2 g^{-1} for the sample studied by Massoth and

Scarpiello). As Massoth and Scarpiello make no distinction between formation of 1,5-hexadiene and carbon dioxide we can not explain the difference in terms of either enhanced carbon dioxide or 1,5-hexadiene formation. Further from our electron micrographs of samples reduced to various degrees of reduction it appears that bismuth clusters are present in samples reduced to α=20%. See figure 4.43. We, therefore, doubt whether during the whole reduction process a molten bismuth layer will surround the unreacted bismuth oxide particle. The assumption that agglomerated bismuth particles are formed looks more appropriate.

In summary we may state that although the chemical reaction-product layer diffusion model gives a reasonable description of the overall reduction process the model nevertheless has to be rejected in our case, since:

- it does not take into account the different mechanisms by which carbon dioxide and 1,5-hexadiene are formed;
- it is very doubtful that during the whole process the molten bismuth layer will surround the oxide particle.

Besides for α-Bi_2O_3 kinetic studies have been carried out for Bi_2O_3-SnO_2 by Seiyama et.al. (28), for Mn-Na oxide by Friedli et.al. (86) and for In_2O_3 by Trimm and Doerr (25). Concerning In_2O_3 Trimm and Doerr (25) found that both 1,5-hexadiene and acrolein are produced at short contact times, while benzene is formed in a consecutive reaction from 1,5-hexadiene. In this connection it is interesting to note that the electronegativity of In_2O_3 lies between that of Bi_2O_3 and MoO_3. The experimental measured rates of 1,5-hexadiene formation could be described by a model in which the rate determining step involves the reaction of two adsorbed propylene molecules with dissociatively adsorbed oxygen. A similar mechanism has been proposed by Seiyama et.al. (28) for the formation of 1,5-hexadiene with the Bi_2O_3-SnO_2 catalyst. They found for the 1,5-hexadiene formation a reaction order in propylene of 1.6 and suggested that the conversion of adsorbed olefins into two π-allyl intermediates coordinated to a single active site should be rate determining. In contrast with these studies Friedli et.al. (86) report that with the Mn-Na oxide catalyst the dimerization reaction is

first order in propylene and zero order in oxygen. From these studies we have to conclude that as yet no general rules can be given regarding the participation of one or two propylene molecules in the rate determining step.

7.3 REACTION MECHANISM

The models proposed in chapter 4 for the dimerization of propylene and the cyclization of 1,5-hexadiene all assume the abstraction of a hydrogen atom from either propylene or 1,5-hexadiene as the rate determining step. The observed relation between the rate of formation of 1,5-hexadiene and the degree of reduction further points to a mechanism for the dimerization involving both a reduced site, i.e. an anion vacancy, and an oxygen ion from the surface. Similar relations are found to apply for the cyclization of 1,5-hexadiene. For carbon dioxide formation from propylene, on the other hand, the oxygen ions from the surface are proposed to be the adsorption centres. This agrees with the correlations mentioned in paragraph 7.1 regarding the importance of the metal-oxygen bond strength for the aselective reaction.

Regarding the surface anion vacancies, these always will be present on the surface for electroneutrality reasons. This may be seen as follows. When a crystal is cleft along a plane which contains only either O^{2-} or Me^{n+} ions always one half of these ions will go to the one half of the crystal while the other half will go to the other piece of the crystal. This means that an oxide surface always contains cations, which miss one of their coordinating ligands. These places are well suited as adsorption centres for the allyl species. Normally speaking one should expect that the ratio surface O^{2-}/vacancies amounts to 1. However, the real value of this ratio will be determined by the type of crystallographic planes that form the surface.

When we now recall the α_o values (α_o represents the ratio of the number of active surface vacancies and the number of active oxygen ions at the surface) found for the various reac-

tions described in chapter 4 (see table 7.1) we see a rather large variation in these values. Although at first glance one should expect this ratio to be close to 1, one has to keep in mind that various reactions take place on the oxide surface. Moreover, steric effects also may enter the picture. For propylene dimerization, for instance, the α_o value of 2.8 states that there are more vacancies than active oxygen ions. This, however, becomes clear when we remember that the oxygen ions also act as adsorption centres for propylene resulting in carbon dioxide formation.

Table 7.1 Values for α_o found for reduction of α-Bi_2O_3 with propylene, 1,5-hexadiene and benzene.

reducing agent	reaction	adsorption site	α_o
propylene	$C_3H_6 \rightarrow C_6H_{10}$	□ + O	2.8
1,5-hexadiene	$C_6H_{10} \rightarrow C_6H_8$	□ + O	0.77
1,5-hexadiene	$C_6H_{10} \rightarrow C_6H_6$	□ + O + O	0.25
benzene	$C_6H_6 \rightarrow CO_2$	□ + O	1.24

For the combustion of benzene, on the other hand, the value of α_o is very close to 1, which agrees with the observation that only CO and CO_2 are formed as products. Finally, an interpretation of the values for 1,3-cyclohexadiene and benzene formation from 1,5-hexadiene is hardly possible, since at least 4 products are formed, in which combinations of vacancies and oxygen ions are important. The rather low value for benzene formation may indicate that this product also originates directly from 1,5-hexadiene, since it is appropriate to assume that there are less vacancies which favour the abstraction of two than of one hydrogen atom.

In chapter 4 and 5 it has been assumed that the formation of 1,5-hexadiene takes place by a reaction between two allylic intermediates adsorbed on the α-Bi_2O_3 surface. However, a reaction scheme in which 1,5-hexadiene is formed by coupling

of two desorbed allyl radicals in the gas phase is an alternative route. This reaction also shows first order kinetics in propylene, provided the abstraction of an α hydrogen atom is the rate determining step. Direct evidence for desorption of allyl radicals from a manganese oxide surface at 600°C and a pressure of 10^{-9} bar has been provided by Hart and Friedli (87). Using mass spectroscopy these authors detected in the presence of propylene or propylene/oxygen mixtures only allyl radicals. Since no radicals were produced in the absence of manganese oxide the catalyst is responsible for allyl formation. Conclusive information in our case, however, is not available. The importance of the free allyl stage for the dimerization reaction has been shown also by Dorogova and Kaliberdo (88), who studied the dimerization of propylene tagged with radioactive carbon on a silver catalyst and found that the radioactive carbon atom ends up both in position 1 and 3 of 1,5-hexadiene.

Finally it seems appropriate to consider our results in the light of the mechanisms proposed for the oxidation of propylene to acrolein with a bismuth molybdate catalyst. It has been established that the rate determining step in this reaction concerns the abstraction of an α hydrogen atom, yielding the symmetrical allylic intermediate (79,80). About the metal ion (Bi^{3+} or Mo^{6+}) that acts as the adsorption centre for the allyl after proton abstraction no agreement exists in the literature. According to Peacock et.al. (84) the allyl is bonded to the Mo^{6+} ion. Matsuura and Schuit (89) and Haber and Grzybowska (90), on the contrary, present arguments in favour of Bi^{3+}, the Mo-O polyhedra being responsible for the second hydrogen abstraction, resulting finally in the formation of acrolein. Qualitatively the importance of the Bi^{3+} for the π allyl intermediate formation has been put forward by Sakamoto et.al. (29) on basis of the activity of bismuth containing oxides for 1,5-hexadiene formation.

The results described in this thesis point to a mechanism in which the formation of 1,5-hexadiene with α-Bi_2O_3 also proceeds by allylic intermediates. Further, like in the case of the bismuth molybdate catalyst the abstraction of an α hydrogen atom is proposed to be the rate determining step. When in both

catalysts the same ion is involved in the first hydrogen abstraction it looks reasonable to assume that the activation energies for the rate determining step are in both cases of the same order of magnitude. For acrolein formation with bismuth molybdate the reported activation energies generally range from 55-84 kJ mol^{-1} (90-93). If we compare these values with those found in this study for 1,5-hexadiene formation (82, 84, 93 kJ mol^{-1}) we see that they lie in the same range. This provides new evidence in favour of the Bi^{3+} ion as the active centre for the first hydrogen abstraction.

7.4 OXYGEN MOBILITY IN α-Bi_2O_3 COMPARED TO OTHER OXIDE SYSTEMS

The mechanisms proposed in chapter 4 for the formation of carbon dioxide and 1,5-hexadiene from propylene and 1,3-cyclohexadiene and benzene from 1,5-hexadiene are all based on the assumption that diffusion of oxygen ions to the surface is fast compared to the chemical reaction. In this case the degree of reduction of the bulk represents the degree of reduction of the surface layer and we may incorporate this degree of surface reduction in the expression that describes the number of vacancies and oxygen ions at the surface. This high mobility of oxygen both in the bulk and along the surface appears to be a common characteristic of many oxides containing bismuth (94). According to Sleight and Linn (95) this property is likely related to the lone pair character of Bi^{3+}. Since in their model for reoxidation of the catalyst they assume that adsorption of gas phase oxygen is not rate determining one should expect a zero order oxygen dependence. For 1,5-hexadiene formation this, indeed,has been found in a certain range of oxygen concentrations. Moreover, the reoxidation experiments have shown that this process is much faster than the reduction of the catalyst.

Although in our study diffusion of oxygen ions through the solid does not enter the kinetics this picture can not be considered to be the general rule. For the reduction of bismuth molybdate with 1-butene, for instance, Batist et.al. (55) found

that under certain conditions the rate of chemical reaction and of oxygen diffusion are of the same order of magnitude, while the importance of oxygen diffusion in the case of toluene oxidation with bismuth uranate clearly has been demonstrated by Steenhof de Jong (37). In the latter case even diffusion of two oxygen species was found to be important.

Literature

1. Marek, L.F., and Hahn, D.A., "The catalytic oxidation of organic compounds in the vapour phase", Chem.Catalog Co., New York, 1932.
2. Popovskii, V.V., Boreskov, G.K., Muzy Kantor, V.S., Sazanov, V.A., and Shubnikov, S.G., Kinet.Katal., 10, 786 (1969).
3. Roĭter, V.A., Golodetz, G.I., Pyatnitskiĭ,Yu, I., Proceedings Fourth International Congress on Catalysis, Vol.1, Akademia Kiado, Budapest, (1971) p.365.
4. Vol'kenshtein, F.F., Elektronnaya Teoriya Kataliza na Poliprovodnikakh Fizmatgiz, Moscow, (1960) ref.quoted by Margolis (19).
5. Moro-oka, Y., and Ozaki, A., J.Catal., 5, 116 (1966).
6. Moro-oka, Y., Morikawa, Y., and Ozaki, A., J.Catal., 10, 86 (1968).
7. Boreskov, G.K., Kinet.Katal., 11 (2), 312 (1970).
8. Sachtler, W.H.M., Dorgelo, G.J.H., Fahrenfort, J., and Voorhoeve, R.J.H., Repr. Fourth Int. Congr. Catal., Moscow, 1968, p.604.
9. Novakova, J., Cat.Rev., 4, 77 (1970).
10. Parravano, G., Cat.Rev., 4, 53 (1970).
11. Boreskov, G.K., Disc. Farad. Soc., 41, 263 (1966).
12. Berés, J., Brückman, K., Haber, J., and Janas, J., Bull. Acad. Pol. Sci. Sér. Sci. Chem., 20, 813 (1972).
13. Dowden, D.A., Proc. 4th Int. Congr. Catal., Akademia Kiado, Budapest, (1971) p.454.
14. Peacock, J.M., Parker, A.J., Ashmore, P.G., and Hockey, J.A., J.Catal., 15, 387 (1970).
15. Sachtler, W.M.H., Cat. Rev., 4, 27 (1970).
16. Daniel, C., and Keulks, G.W., J.Catal., 24, 529 (1972).
17. Daniel, G., Monnier, J.R., and Keulks, G.W., J.Catal., 31, 360 (1973).
18. Mc Cain, C.C., and Godin, G.W., Nature, (London), 202, 692 (1964).
19. Margolis, L.Ya., Cat. Rev., 8, 241 (1973).
20. Mars, J., and van Krevelen, D.W., Chem.Eng.Sci.Suppl., 3, 41 (1954).
21. Haber, J., International Chemical Engineering, 15, 21 (1975).
22. Buiten, J., J.Catal., 13, 374 (1969).
23. Swift, H.E., Bozik, J.E., and Ondrey, J.A., J.Catal., 21, 212 (1971).
24. Trimm, D.L., and Doerr, L.A., J.Catal., 23, 49 (1971).
25. Trimm, D.L., and Doerr, L.A., J.Catal., 26, 1 (1972).
26. Fattore, V., Fuhrmann, Z.A., Manara, G., and Notari, B., J.Catal., 37, 215 (1975).
27. Seiyama, T., Mochida, J., Uda, T., and Egashira, M., 2nd Japan-Soviet Catalysis Seminar, Tokyo, (1973) p.134.
28. Seiyama, T., Uda, T., Mochida, J., and Egashira, M., J.Catal., 34, 29 (1974).
29. Sakamoto, T., Egashira, M., and Seiyama, T., J.Catal., 16, 407 (1970).
30. Seiyama, T., Egashira, M., Sakamoto, T., and Aso, I., J.Catal., 24, 76 (1972).
31. Centola, P., Mazzocchia, C., Terzaghi, G., and Pasquon, I., Chimica Ind., Milano, 54, 859 (1972).
32. Veatch, F., Callahan, J.L., Milberger, E.C., and Forman, R.W., Proc. 2nd Int. Congr. Cat., Technip, Paris, (1961), p.2647.
33. Callahan, J.L., Graselli, R.K., Milberger, E.C., and Strecker, H.A., Ind.Eng.Chem., Proc.Res.Develop., 9, 134 (1970).
34. Ondrey, J.A., and Swift, H.E., U.S.Pat., 3.655.750 (1972).
35. Moro-oka, Y., Takita, Y., and Ozaki, A., J.Catal., 23, 183 (1971).
36. Ockerbloom, N.E., Hydrocarbon Processing, Nov. 1972, p.117.
37. Steenhof de Jong, J.G., Thesis, Eindhoven (1972).
38. Uda, T., Egashira, M., and Seiyama, T., Nippon Kagaku Kaishi, p.16 (1972).

39. Chemical Engineering News, 23 Sept. 1974, p.18.
40. Seiyama, T., Yamazoë, N., and Egashira, M., Proc. Fifth Int. Congr. Catal., North-Holland Publishing Co., Amsterdam, (1973), p.997.
41. Thomas, J.M., and Thomas, W.J., "Introduction to the principles of heterogeneous catalysis", Academic Press, London, (1967).
42. German, A.L., and Heynen, H.W.G., J.Sci.Instrum., 5, 413, (1972).
43. Adv. Chem. Ser., 22, 428 (1959).
44. Cummings, G.A. Mc D., and Mc Laughlin, E., J.Chem. Soc., p.1391 (1955).
45. Safronov, G.M., Batog, V.N., Stepanyuk, T.V., and Fedorov, P.M., Russ. J. Inorg. Chem., 16, 460 (1971).
46. Levin, E.M., and Roth, R.S., J.Res.Nat.Bur.Stand., Phys. and Chem., 68A, 197 (1964).
47. Sillen, L.G., Arkiv Kemi, Mineralogi och Geologi, 12A, (18), 1 (1937).
48. Levin, E.M., and Roth, R.S., J.Res.Nat.Bur.Stand., Phys. and Chem., 68A, 189 (1964).
49. Gattow, G., and Fricke, H., Z.Anorg. Allgem.Chem., 324, 287 (1963).
50. Batog, V.N., Pakhomov, V.I., Safronov, G.M., and Federov, P.M., Inorganic Materials, 9, 1400 (1973).
51. Batist, Ph.A., Bouwens, J.F.H., and Schuit, G.C.A., J.Catal., 25, 1 (1972).
52. Wolfs, M.W.J., Thesis, Eindhoven, (1974).
53. Kemball, C., Adv.Catal., 2, 233 (1950).
54. Kemball, C., Proc.Roy.Soc.(London), A187, 73 (1946).
55. Batist, Ph.A., Kapteijns, C.J., Lippens, B.C., and Schuit, G.C.A., J.Catal., 7, 33 (1967).
56. Steenhof de Jong, J.G., Guffens, C.H.E., and van der Baan, H.S., J.Catal., 31, 149 (1973).
57. Mantri, V.B., Gokarn, A.N., and Doraiswamy, L.K., Chem.Eng.Sci., 31, 779 (1976).
58. Levenspiel, O., "Chemical reaction engineering", John Wiley and Sons, Inc., New York (1972).
59. Wen, C.Y., Ind.Eng.Chem., 60, 34 (1968).
60. Ishida, M., and Wen, C.Y., Chem.Eng.Sci., 26, 1031 (1971).
61. Papanastassiou, D., and Bitsianes, G.,Metal.Trans., 4, 477 (1973).
62. Szekely, J., and Evans, J.W., Metal. Trans., 2, 1691, 1699 (1971).
63. Ishida, M., and Wen, C.Y., A.I.Ch.E.Journal, 14, 311 (1968).
64. Finlayson, B.A., "The method of weighted residuals and variational principles", Academic Press, New York, (1972).
65. Danckwerts, P.V., Chem.Eng.Sci., 2, 1 (1953).
66. Wicke,E., Adv.Chem.Ser., 148, 75 (1975).
67. Yoshida, F., Ramaswami, D., and Hougen, O.A., A.I.Ch.E. Journal, 8, 5 (1962).
68. Satterfield, C.N., and Sherwood, T.K., "The role of diffusion in catalysis", Addison-Wesley Publishing Company, Inc., Reading (1963).
69. Weisz, P.B., and Hicks, J.S., Chem.Eng.Sci., 17, 265 (1962).
70. Nohara, D., and Sakai, T., Ind.Eng.Chem., Prod.Res.Developm., 12, 322 (1973).
71. Tielen, W.H.M., "An experimental and theoretical study of the active wall reactor", MSc. report, Eindhoven University of Technology, (1976).
72. Brauer, H.W., and Fetting, F., Chemie Ing. Technik, 36, 921 (1964).
73. Mühle, J., Chemie Ing. Technik, 41, 7, (1969).
74. Beres, J., Brückman, K., Haber, J., and Janas, J., Bull.Acad. Polon.Sci. Chim., 20, (8), 813 (1972).

75. Massoth, F.E., and Scarpiello, D.A., J.Catal., 21, 225 (1971).
76. Miura, H., Morikawa, Y., and Shirasaki, T., J.Catal., 39, 22 (1975).
77. Callahan, J.L., and Milberger, E.C., U.S.P., 3, 472, 892 (1969).
78. Gelbshtein, A.J., Stroeva, S.S., Bakshi, Yu.M., and Mischenko, Yu.A., Fourth Int. Congr. Catal., Moscow, 1968, paper 22.
79. Mc Cain, C.C., Gough, G., and Godin, G.W., Nature, (London), 198, 989 (1963).
80. Sachtler, W.M.H., and de Boer, N.H., Proc. Third Int.Congr. Catal., North-Holland Publishing Company, Amsterdam, (1965), p.252.
81. Kondo, T., Saito, S., and Tamaru, K., J.Am.Chem.Soc., 96, 6857 (1974).
82. Naito, S., Kondo, T., Ichikawa, M., and Tamaru, K., J.Phys.Chem., 76, 2184 (1972).
83. Cotton, F.A., "Chemical applications of group theory", Interscience Publishers, New York, (1963).
84. Peacock, J.M., Sharp, M.J., Parker, A.J., Ashmore, P.G., and Hockey, J.A., J.Catal., 15, 379 (1969).
85. Solymosi, F., and Boszo, F., Prep. Sixth Int. Congr. Catal., London, (1976), paper A27.
86. Friedli, H.R., Hart, P.J., and Vrieland, G.E., Symposium on Catalytic Oxidation of Hydrocarbons, Presented before the Division of Petroleum Chemistry, Inc. and the Divisions of Colloid and Surface Chemistry and Physical CHemistry, Am.Chem. Soc., New York, sept. 1969, p. C70.
87. Hart, P.J., and Friedli, H.R., Chem. Commun., (J. Chem.Soc.Sect. D), (1970) p. 621.
88. Dorogova, V.B., and Kaliberdo, L.M., Russ. J. Phys. Chem., 45, 1633 (1971).
89. Matsuura, I., and Schuit, G.C.A., J.Catal., 25, 314 (1972).
90. Haber, J., and Grzybowska, B., J. Catal., 28, 489 (1973).
91. Blasse, G., J. Inorg. Nucl. Chem., 28, 1124 (1966).
92. Serban, S., Revue Chim. (Bucharest), 18, 65 (1967).
93. Gorshkov, A.P., Kolchin, I.K., Gribov, I.M., and Margolis, L.Ya., Kinet. Katal., 9, 1068 (1968).
94. Takahashi, T., and Iwahara, H., J. Appl. Electrochem., 2, 97 (1971); 3, 65 (1973).
95. Sleight, A.W., and Linn, W.J., Ann. New York Acad. Sci., 272, 22 (1976).

APPENDIX I

Numerical Solution of the Equations for a Gas-Solid Reaction with Diffusion

For an oxide particle with spherical shape and radius R a mass balance for gaseous reactant A and solid reactant B in a spherical shell yields the following differential equations for diffusion of gas A into the porous oxide particle and consumption of oxygen from the solid:

$$\varepsilon \frac{\partial C_A}{\partial t} = ID_{eff} \left(\frac{\partial^2 C_A}{\partial r^2} + \frac{2}{r} \frac{\partial C_A}{\partial r} \right) - r_A \qquad \text{(I-1)}$$

$$- r_B = \frac{\partial C_B}{\partial t} , \quad \text{while } r_A = a r_B \qquad \text{(I-2)}$$

When mass transfer across the boundary layer may be neglected the initial and boundary conditions are:

$$C_A = C_{A,o} \qquad \text{at } r = R \qquad \text{(I-3)}$$

$$\frac{\partial C_A}{\partial r} = 0 \qquad \text{at } r = 0 \qquad \text{(I-4)}$$

$$C_B = C_{B,o} \qquad \text{at } t = 0 \quad \text{and } 0 < r < R \qquad \text{(I-5)}$$

The equations can be solved analytically for the case that (1) :

- the pseudo steady state is assumed, i.e. $\varepsilon \, \partial C_A / \partial t = 0$,
- the reaction is zero order in the solid concentration and first order in the substrate concentration.

When the reaction becomes first order in solid concentration B numerical solution methods have to be applied. We shall give

here the solution method for the case that:

- the pseudo steady state may be assumed,
- the reaction is first order in both the solid concentration B and the substrate concentration A.

The following set of equations has then to be solved:

$$\frac{\mathbb{D}_{eff}}{r^2}\frac{\partial}{\partial r}\left(r^2\frac{\partial C_A}{\partial r}\right) - a\,k\,C_B C_A = 0 \qquad \text{(I-6)}$$

$$\frac{\partial C_B}{\partial t} = -k\,C_B C_A \qquad \text{(I-7)}$$

After introducing the dimensionless parameters

$$y=r/R, \qquad S=C_B/C_{B,o}, \qquad A=C_A/C_{A,o},$$

$$\tau=t/3600, \qquad \Phi=\frac{akC_{s,o}R^2}{\mathbb{D}_{eff}}, \qquad \Psi=k\,C_{A,o}\,3600,$$

equation (I-6) and (I-7) change to:

$$\frac{1}{y^2}\left(\frac{\partial}{\partial y}\left(y^2\frac{\partial A}{\partial y}\right)\right) = \Phi\,A\,S \qquad \text{(I-8)}$$

$$\frac{\partial S}{\partial \tau} = -\Psi\,A\,S \qquad \text{(I-9)}$$

with the initial and boundary conditions:

$$A=1 \quad \text{at} \quad y=1 \qquad \text{(I-10)}$$

$$\frac{\partial A}{\partial y}=0 \quad \text{at} \quad y=0 \qquad \text{(I-11)}$$

$$S=1 \quad \text{at} \quad \tau=0 \qquad \text{(I-12)}$$

To solve this set of differential equations we used the orthogonal collocation method. In this method, which was first developed by Villadsen and Stewart (2), the unknown exact solution is expanded in a series of known functions, which are chosen to satisfy as many conditions of the problem as is feasible: symmetry conditions and possibly boundary conditions. The series of functions is called a trial function. For an one-dimensional problem, where the solution only depends on one coordinate, say x, the trial function is defined by

$$\text{trial function} = y^*(x) = \sum_{j=1}^{N} a_j y_j(x)$$

The unknown coefficients in the series are now determined in such a way that the differential equation is satisfied in some "best way". This is done as follows.After substitution of the trial function into the differential equation the result, called the residual, has to be zero throughout space for the exact solution. For the approximate solution the residual is required to be zero at a set of grid points called collocation points. This condition determines the unknown coefficients in the trial function. In the *orthogonal* collocation method the trial functions are orthogonal polynomials and the computer programs are written in terms of the solution at the collocation points $\{y^*(x_i)\}$, rather than the coefficients $\{a_j\}$. The first condition improves the rate of convergence as N(=the number of interior collocation points) increases, while the second condition simplifies the computer programming (3).

In problems which are symmetric about the centre, i.e. where the boundary condition is expressed as in equation (I-11), it often can be shown that the solution is a function of x^2 rather than just x(3). In this case including this symmetry in the trial function will reduce the number of unknowns by a factor of two.

When we now apply orthogonal collocation to equation (I-8) and (I-11) we get (4):

$$\sum_{j=1}^{N+1} B_{i,j} A_j = \Phi A_i S_i, \qquad i = 1,.., N \tag{I-13}$$

where:

$$B = D Q^{-1} \text{ with} \tag{I-14}$$

$$Q_{i,j} = y_i^{2j-2} \qquad i,j = 1,...., N+1 \tag{I-15}$$

$$\text{and} \quad D_{i,j} = \frac{1}{y^2} \frac{d}{dy} \left(y^2 \frac{dQ}{dy}\right)_{y=y_i} \tag{I-16}$$

For $j = 1$

$$D_{i,j} = 0, \text{ while} \tag{I-17}$$

$$D_{i,j} = (2j-2)(2j-1) y_i^{2j-4} \quad \text{for } j=2,..., N+1 \tag{I-18}$$

In these equations y_i are the roots of the Nth polynomial $P_N(y^2)=0$ at y_i. The polynomials $P_1(y^2)....P_N(y^2)$ are defined by:

$$\int_0^1 w(y^2) P_j(y^2) P_i(y^2) y^2 dy = 0, \qquad j=1,...., i-1 \tag{I-19}$$

The first polynomial, $P_o(y^2)$, has the value 1.
The weighting function $w(y^2)$ can be either 1 or $1-y^2$. We used $w(y^2)=1$, since this gave a higher rate of convergence.

Integration of equation (I-9) is carried out by the trapezium rule. Since S and A are also dependent on the radial distance, y, the integration of S in the time is carried out on each radial level, y_i by using:

$$S_i(\tau+\Delta\tau) = S_i(\tau)\left(1- \frac{\Psi\Delta\tau}{2} A_i(\tau)\right)/\left(1+ \frac{\Psi\Delta\tau}{2} A_i(\tau+\Delta\tau)\right) \tag{I-20}$$

with $i = 1,...,N$.

Substitution of boundary condition (I-10) in equation (I-9) gives:

$$y=1 \quad A=1 \quad (j=N+1) : \quad \frac{dS_{N+1}}{d\tau} = -\Psi S_{N+1},$$

or after integration:

$$S_{OP}=S_{N+1} = \exp(-\Psi\tau) \qquad \text{(I-21)}$$

Finally at $\tau=0$ substitution of (I-12) in equation (I-13) results in:

$$\sum_{j=1}^{N+1} B_{i,j} A_j = \Phi A_i, \quad i=1,\ldots,N \qquad \text{(I-22)}$$

Summarizing the solution procedure implies that at $\tau=0$ equation (I-22) has to be solved. At $\tau \neq 0$, however, we have to solve the following set of equations:

$$\sum_{j=1}^{N} B_{i,j} A_j(\tau+\Delta\tau)=\Phi A_i(\tau+\Delta\tau) S_i(\tau+\Delta\tau), \qquad \text{(I-23)}$$

$$\text{with } S_i(\tau+\Delta\tau)=S_i(\tau) \left\{(1-\Omega A_i(\tau))/(1+\Omega A_i(\tau+\Delta\tau))\right\} \qquad \text{(I-24)}$$

with $\Omega = \Psi\Delta\tau/2$

$S_{OP} = \exp(-\Psi\tau)$

$I = 1,\ldots,N.$

Solution of $\underline{A}$ from equation (I-22) at $\tau=0$ has been carried out by using the standard computer procedures known as Croutdecomposition and Croutsolution.

In equation (I-23) $\underline{A}\ (\tau+\Delta\tau)$ and $\underline{S}\ (\tau+\Delta\tau)$ have to be solved from $\underline{A}\ (\tau)$ and $S(\tau)$. Since the reaction term is non linear an iteration process is required to solve this equation. We used the method of Newton, since this method has given satisfactory results in earlier calculations, for the non isothermal active wall reactor (5).

When with the method of Newton we want to solve $\underline{F}(\underline{x})=0$, the matrix equation which has to be solved after k iterations is given by:

$$\underline{F}(\underline{x}_{k-1}) + \underline{F}'(\underline{x}_{k-1}) \{ \underline{x}_k - \underline{x}_{k-1} \} = 0, \qquad \text{(I-25)}$$

$\underline{F}'(\underline{x}_{k-1})$ being the first derivative of $\underline{F}(\underline{x}_{k-1})$ with respect to $\underline{x}_{k-1}$.

We now call the variables in our specific problem at $\tau \neq 0$

at $\tau = \tau$: $\underline{AI}$ and $\underline{SI}$,

at $\tau = \tau + \Delta\tau$: $\underline{AO}$ and $\underline{SO}$: the calculated values after (k-1) iterations,

$\underline{AN}$ and $\underline{SN}$: the values that have to be calculated in the kth iteration.

We then get:

$$\underline{F}(\underline{x}_{k-1}) = B\,\underline{AO} - \underline{b}(\underline{AO}) \qquad \text{(I-26)}$$

$$\underline{F}'(\underline{x}_{k-1}) = B + \frac{\partial b_i(\underline{AO})}{\partial AO_j}, \quad i,j=1,\ldots,N \qquad \text{(I-27)}$$

with

$$\underline{x}_{k-1} = \underline{AO}$$
$$\underline{x}_k = \underline{AN}$$
$$b_i(AO) = \Phi\, AO_i\, SO_i$$

Substitution of (I-26) and (I-27) in equation (I-25) yields after reformulation

$$C\,\underline{AN} = E, \qquad \text{(I-28)}$$

with
$$C_{i,i} = B_{i,i} - \Phi SO_i/(1+\Omega AO_i)$$
$$C_{i,j} = B_{i,j} \text{ for } i \neq j$$
$$E_i = \Omega\Phi AO_i^2\, SO_i/(1+\Omega AO_i) - B_{i,N+1}$$
$$SO_i = SI_i(1-\Omega AI_i)/(1+\Omega AO_i)$$

$i=1,\ldots,N$; $j=1,\ldots,N$

and $S_{OP} = \exp(1-\Psi\tau)$, A=1 for y=1.

The matrix equation (I-28) is solved in each iteration step by the standard procedures Croutdecomposition and Croutsolution. The calculations were performed with 5 internal collocation points.

CALCULATION OF Φ AND Ψ FOR THE REDUCTION OF α-Bi_2O_3 WITH PROPYLENE

For the conditions given in table I.1 we calculate for both Φ and Ψ a value of 0.84. This cooresponds with values of 0.92 and 2.33 10^{-4} sec for Φ and Ψ , respectively. From the results depicted in figure 4.4 it appears that the influence of diffusion can be neglected in our measurements.

Table I.1 Conditions and values of parameters used for calculating Φ and Ψ.

Temperature	580°C
Radius oxide particle	$8\ 10^{-3}$ m
Mole fraction propylene	0.40 ($\sim$ 5.707 mmol l^{-1})
Density α-Bi_2O_3	8.9 g cm^{-3}
Pore volume α-Bi_2O_3	0.12 cm^3 g^{-1}
ID_{eff}(propylene in helium)	$8.6\ 10^{-5}$ m^2 s^{-1}

LITERATURE

1. Ishida, M., and Wen, C.Y., A.I.Ch.E. Journal, 14, 311 (1968).
2. Villadsen, J.V., and Stewart, W.E., Chem.Eng.Sci., 22, 1483 (1967).
3. Finlayson, B.A., Cat.Rev.-Sci.Eng., 10, 69 (1974).
4. Finlayson, B.A., "The method of weighted residuals and variational principles", Academic Press, New York, (1972).
5. Spierts, J.A.M., Internal report, Vakgroep Chemische Technologie, University of Technology, Eindhoven, (1976).

List of Symbols

LATIN SYMBOLS		*units
A	peak area	
	area of 1 molecule	cm^2
C	concentration	$mmol\ l^{-1}$
ID	diffusion coefficient	$m^2\ s^{-1}$
ID_{ax}	axial dispersion coefficient	$m^2\ s^{-1}$
ID_{eff}	effective diffusion coefficient	$m^2\ s^{-1}$
d_p	diameter catalyst particle	m
F	gas flow rate	$ml\ s^{-1}$
f	calibration factor	
$[H_2]$	hydrogen concentration	$mmol\ l^{-1}$
[HD]	1,5-hexadiene concentration	$mmol\ l^{-1}$
K	adsorption constant	bar^{-1}
k	reaction rate constant	$mmol^{1-n}\ l^n\ g^{-1}s^{-1}$
k_m	mass transport coefficient	$m\ s^{-1}$
L	length of catalyst bed	m
M	molecular weight	
m	reaction order	
n	reaction order	
[O]	oxygen concentration in oxide	$\mu gat\ g^{-1}$
$[O_2]$	oxygen concentration in gas phase	$mmol\ l^{-1}$
[P]	propylene concentration	$mmol\ l^{-1}$
P	pressure	bar
p	reaction order	
Q_{ads}	heat of adsorption	$kJ\ mol^{-1}$
q	reaction order	
R	radius catalyst particle	m
r_p	pore radius	Å
r	radial distance	m
r_A	rate of formation of A	$mmol\ g^{-1}\ s^{-1}$
S	entropy of gaseous molecule	$J(mol\ K)^{-1}$
ΔS_{ads}	entropy loss during adsorption	$J(mol\ K)^{-1}$

*unless stated otherwise

T	temperature	^{o}C, K
t	time	s
$\bar{u}$	superficial gas velocity	$m\ s^{-1}$
V	volume actually adsorbed (at STP)	$cm^3\ g^{-1}$
V_m	maximum adsorbable volume at full coverage (at STP)	$cm^3\ g^{-1}$
W	catalyst weight	g
x	mole fraction	
X	electronegativity	

GREEK SYMBOLS

α	degree of reduction	
α_{ox}	degree of reoxidation	
α_o	ratio of number of active vacancies originally present on the surface and the number of oxygen ions originally active on the surface	
ε	porosity	
θ	degree of surface coverage	
μ	dynamic viscosity	$Ns\ m^{-2}$
ρ	density	$kg\ m^{-3}$
ρ	dimensionless radial distance	
σ	catalytic site	
ϕ	Thiele modulus	
ψ	$k.C_{A,o}$	s

SUBSCRIPTS

A,B	component A, B	prop	propylene
CO_2	carbon dioxide	s	reaction interface; surface
CHD	1,3-cyclohexadiene		
HD	1,5-hexadiene	v	V site
H_2	hydrogen		
o	inlet stream; initial value; referring to O site		

Summary

This thesis deals with the conversion of propylene to 1,5-hexadiene and other C_6 hydrocarbons (1,3-cyclohexadiene, 3-allyl-cyclohexene, benzene) with α-Bi_2O_3 and binary oxides of bismuth and zinc. It appears that for all catalysts studied the selectivity for C_6 hydrocarbons is highest ($\sim$60-90%), when no oxygen is present in the feed mixture. In this case the oxygen from the solid is consumed; we then call α-Bi_2O_3 an oxidant. Further, it has been established that addition of zinc oxide to α-Bi_2O_3 hardly improves the selectivity.

The kinetics for the oxidation of propylene and 1,5-hexadiene with α-Bi_2O_3 acting as *oxidant* have been studied both in a differential operating micro flow reactor and in a thermobalance. In the last mentioned system we also investigated the reduction of α-Bi_2O_3 with hydrogen and benzene. The agreement between the results obtained in the micro flow reactor and the thermobalance is very satisfactory. The measurements show that during the reduction of α-Bi_2O_3 with propylene, 1,5-hexadiene and carbon dioxide originate by a parallel scheme, whereas benzene is formed by a consecutive reaction from 1,5-hexadiene. The rate of 1,5-hexadiene formation is first order in propylene and the reaction has an activation energy of 85 kJ mol^{-1}; the formation of carbon dioxide can be described by a single site Langmuir-Hinshelwood model. We conclude that in α-Bi_2O_3 diffusion of oxygen through the lattice is very fast, i.e. the degree of reduction of the bulk represents the degree of reduction in the surface layer. For 1,5-hexadiene formation a model is proposed in which the abstraction of an α hydrogen atom is the rate determining step. The allyl is adsorbed on a vacancy, the hydrogen atom on an oxygen anion. Adsorption measurements on a partly reduced α-Bi_2O_3 sample support this mechanism. For the combustion of propylene to carbon dioxide only oxygen ions are important as adsorption centres for propylene.

When α-Bi_2O_3 is reduced with 1,5-hexadiene, the products 1,3-cyclohexadiene, 3-allylcyclohexene, benzene and carbon dioxide are formed by parallel reactions, whereas 1,3-cyclohexadiene probably also acts as a precursor for benzene. For the 1,5-hexadiene oxidation ensembles of vacancies and surface oxygen ions are also expected to be necessary. For 1,3-cyclohexadiene formation the adsorption of 1,5-hexadiene on a vacancy and a surface oxygen anion is proposed as the rate determining step. Formation of benzene, on the other hand, can best be described by assuming the adsorption of 1,5-hexadiene on one vacancy and two oxygen anions. All reactions are almost first order in propylene.

We paid some attention to the reoxidation of α-Bi_2O_3 after reduction to a certain degree of reduction. It appears that only after reduction to α=5% the original activity can be regained by reoxidation.

Next we studied the kinetics of propylene oxidation with α-Bi_2O_3 acting as a *catalyst*, i.e. with oxygen in the feed. It turns out that at low oxygen concentration the kinetics and the rate of reaction for 1,5-hexadiene formation are identical to the case that no oxygen is present in the feed, i.e. the catalyst is always in its fully oxidized state. At higher oxygen concentrations, however, an increasing part of the allylic intermediates is converted to carbon dioxide. Carbon dioxide is further formed by two other mechanisms, i.e. by reaction of propylene with oxygen from the catalyst surface and by reaction of adsorbed propylene with oxygen from the gas phase.

Finally we studied the influence of zinc oxide on the oxidation of propylene with bismuth oxide. The experiments show that zinc oxide has two important effects. Firstly, it acts as a stabilizing agent for bismuth oxide. This follows from the fact that the activity even after 40 reduction-reoxidation cycles still remains unchanged.Secondly, the dimerization reaction now takes place on two independent sites (X and Y). The kinetics on site X are identical to that of α-Bi_2O_3. The kinetics on site Y, on the contrary, show a second order propylene dependence. We ascribed this site to the action of zinc oxide.

Samenvatting

In dit proefschrift wordt een onderzoek beschreven naar de omzetting van propeen in 1,5-hexadieen en andere C_6 koolwaterstoffen (1,3-cyclohexadieen, benzeen, 3-allylcyclohexeen) met behulp van α-Bi_2O_3 en binaire oxiden van bismuth en zink. Het blijkt dat voor alle onderzochte katalysatoren de selektiviteit voor de C_6 koolwaterstoffen het grootst is (~60-90%), wanneer er zich geen zuurstof in de voeding bevindt. In dit geval wordt de zuurstof uit de vaste stof verbruikt; we zeggen dat het oxide als *oxidant* werkt. Voorts is vastgesteld dat toevoeging van zink oxide aan α-Bi_2O_3 de selektiviteit nauwlijks verbetert.

De kinetiek van de oxidatie van propeen en 1,5-hexadieen met α-Bi_2O_3 werkend als oxidant is bestudeerd in een differentieel werkende microflow reaktor en in een thermobalans. In laatstgenoemd apparaat is tevens de reduktie van α-Bi_2O_3 met waterstof en benzeen bestudeerd. De overeenstemming tussen de resultaten verkregen in de microflow reaktor en de thermobalans is zeer bevredigend. De metingen geven te zien dat in geval van reduktie van α-Bi_2O_3 met propeen, 1,5-hexadieen en kooldioxide ontstaan via een parallel schema, terwijl benzeen via een volgreaktie wordt gevormd uit 1,5-hexadieen. De vorming van 1,5-hexadieen is eerste orde in propeen en heeft een aktiveringsenergie van 85 kJ mol^{-1}. Op de vorming van kooldioxide is een single site Langmuir-Hinshelwood model van toepassing. Geconcludeerd is dat in α-Bi_2O_3 diffusie van zuurstof door het rooster zeer snel is, m.a.w. de reduktiegraad van de bulk is tevens een maat voor die in de oppervlaktelaag. Voor de 1,5-hexadieen vorming wordt een model voorgesteld met als snelheidsbepalende stap de abstraktie van een α waterstof atoom. De allyl rest wordt geadsorbeerd op een vacature, het water-

stof atoom op een zuurstof anion. Adsorptie metingen uitgevoerd met katalysatoren gereduceerd tot een bepaalde reduktiegraad ondersteunen dit mechanisme. Voor de verbrandingsreaktie naar kooldioxide zijn uitsluitend zuurstof ionen van belang.

Indien het α-Bi_2O_3 wordt gereduceerd met 1,5-hexadieen, dan ontstaan 1,3-cyclohexadieen, 3-allylcyclohexeen, benzeen en kooldioxide volgens een parallel schema, terwijl 1,3-cyclohexadieen zeer waarschijnlijk ook als precursor voor benzeen fungeert. Voor de oxidatie van 1,5-hexadieen worden sites bestaande uit ensembles van vacaturen en oppervlakte zuurstof ionen eveneens verwacht noodzakelijk te zijn. Voor de vorming van 1,3-cyclohexadieen wordt als snelheidsbepalende stap de adsorptie van 1,5-hexadieen op een vacature en een oppervlakte zuurstof anion voorgesteld. Benzeen vorming, daarentegen, kan het best beschreven worden door aan te nemen dat adsorptie van 1,5-hexadieen plaatsvindt op een vacature een twee zuurstof anionen. Alle reakties zijn nagenoeg eerste orde in propeen.

Enige aandacht is besteed aan de reoxidatie van α-Bi_2O_3 na reduktie tot een bepaalde reduktie graad. Het blijkt dat alleen na reduktie tot 5% de oorspronkelijke aktiviteit door reoxidatie kan worden teruggewonnen.

Vervolgens is de kinetiek van de propeen oxidatie bestudeerd met α-Bi_2O_3 als *katalysator*, d.w.z. met zuurstof in de voeding. Het blijkt dat bij lage zuurstof concentratie de kinetiek en de reaktiesnelheid voor de 1,5-hexadieen vorming identiek is aan het geval dat er zich geen zuurstof in de gas fase bevindt, d.w.z. de katalysator bevindt zich steeds in de volledig geoxideerde toestand. Bij hoge zuurstof concentraties wordt echter een steeds groter wordend deel van de allyl intermediairen omgezet in kooldioxide. Daarnaast wordt kooldioxide nog op twee andere wijzen gevormd, namelijk door reaktie van propeen met zuurstof uit het katalysator oppervlak en door reaktie van geadsorbeerd propeen met zuurstof uit de gas fase.

Tenslotte bestudeerden wij de invloed van zink oxide op

de oxidatie van propeen met bismuth oxide. De experimenten geven te zien dat zink oxide twee belangrijke effekten heeft. Op de eerste plaats fungeert het als stabilisator voor bismuth oxide, hetgeen volgt uit het feit dat de aktiviteit zelfs na 40 reduktie-reoxidatie cycli nog onveranderd is. Op de tweede plaats blijkt dat de dimerisatie reaktie nu op twee onafhankelijke sites plaatsvindt. De kinetiek op de ene site is identiek aan die van α-Bi_2O_3. De kinetiek op de tweede site, daarentegen, vertoont een tweede orde propeen afhankelijkheid. Deze site is derhalve toegeschreven aan zink oxide.

Levensbericht

De schrijver van dit proefschrift werd op 26 april 1947 geboren te 's-Hertogenbosch. Hij bezocht aldaar het St. Janslyceum, waar hij in 1965 het diploma Gymnasium β behaalde. In september van hetzelfde jaar begon hij met de studie scheikundige technologie aan de Technische Hogeschool te Eindhoven. Het kandidaatsexamen werd in juli 1968 met lof afgelegd. Na o.l.v. Prof. Dr. H. Kloosterziel (vakgroep organische chemie) een afstudeeronderzoek over de stereochemie van de sigmatrope thermische [1,5]-alkyl shift te hebben verricht, behaalde hij in juni 1970 met lof het ingenieursdiploma.

Na zijn afstuderen vervulde hij van juli 1970 tot januari 1972 zijn militaire dienstplicht. Gedurende deze tijd was hij gedetacheerd bij de Inspectie Geneeskundige Dienst Koninklijke Landmacht te 's-Gravenhage.

In januari 1972 trad hij in aktieve dienst van het Koninklijke/Shell Laboratorium te Amsterdam. Gedurende ruim een jaar werd hier in de groep van Prof. Dr. W.M.H. Sachtler onderzoek verricht op het gebied van de katalyse.

Sinds 1 mei 1973 is hij als wetenschappelijk medewerker werkzaam bij de vakgroep chemische technologie van de Technische Hogeschool Eindhoven. Hier werd in de groep van Prof. Drs. H.S. van der Baan het onderzoek verricht beschreven in dit proefschrift.

Dankwoord

Dit proefschrift is tot stand gekomen door de samenwerking en inzet van vele medewerkers en studenten van de Technische Hogeschool Eindhoven. Met name geldt dit de vakgroep chemische technologie. Aan alle leden hiervan mijn hartelijke dank. Gaarne wil ik een aantal personen met name noemen.

In het bijzonder gaat mijn dank uit naar de heer W.J.G. van Lith, waarmee ik drie jaar zeer nauw heb samengewerkt en die in deze periode met grote toewijding en kennis van zaken heeft meegewerkt aan dit onderzoek. Wanneer de W.U.B. mijn aanwezigheid elders noodzakelijk maakte, kon ik steeds op zijn steun rekenen. Onze samenwerking zal ik niet licht vergeten.

Veel dank ben ik verschuldigd aan de afstudeerders H.J.A. Bleeker, J.J. van den Boom, A. Bosman, M.J.B.A. Lauwerijssen, J.F. Timmers en D.J.M. van der Vleugel en aan de HTS stagiaires Th.H.J. van Hoek en E. Olthuis. Zij allen hebben op enthousiaste wijze aan het onderzoek meegewerkt.

Voorts dank ik de afstudeerders A.J.W. Apers, F.H.M.M. Langen, J.A.M. Spierts, W.H.M. Tielen en J.N. van Wezel. Zij kozen als afstudeeronderzoek weliswaar de aselektieve oxidatie van koolwaterstoffen, doch stimuleerden door de vele discussies en prettige samenwerking indirect mede dit onderzoek.

De heren D. François en G.A. van der Put ben ik zeer erkentelijk voor de technische assistentie die zij bij de opbouw van de vele opstellingen hebben verleend.

Mijn dank gaat verder uit naar de heer R.J.M. van der Wey, die de tekeningen in dit proefschrift heeft verzorgd, de heer H.N.A.M. van der Meyden voor zijn medewerking en assistentie bij de uitvoering van dit proefschrift en mevrouw P.M. Th. Tilmans-Berger, die het vele typewerk heeft verricht.

De hulp verkregen van de vakgroep instrumentele analyse bij de identificatie van de reaktieprodukten en van de vakgroep electrochemie voor de stereoscan opnamen wordt zeer gewaardeerd.

Tenslotte dank ik Dr.Ir. D.C. Koningsberger voor de talrijke vruchtbare discussies over het in dit proefschrift beschreven onderwerp.

Stellingen

1. Bij de reduktie van vele als katalysator bekend staande oxydische systemen ontstaat een bij kamertemperatuur detecteerbaar breed ESR signaal ($\Delta H \sim 1500$ gauss), dat bij reoxydatie afneemt in intensiteit. Deze eigenschap en de verandering van het signaal met de temperatuur geven aanleiding het signaal toe te schrijven aan elektronen gelokaliseerd in vacatures in de bulk en/of aan het oppervlak. Het mogelijke belang van dit signaal voor de katalytische eigenschappen van deze oxyden is nog in onvoldoende mate onderkend.

2. Het gebruik van een thermobalans zonder analyse van de reaktieprodukten voor de bestudering van de kinetiek van de reduktie van oxydische systemen met organische substraten houdt het gevaar in dat het optreden van verschillende mechanismen niet wordt opgemerkt.

3. Bij het interpreteren van metingen verricht in zogenaamde "honeycomb" katalysatoren met hoge aktiviteit dient men rekening te houden met het optreden van radiale concentratiegradiënten in de afzonderlijke kanalen.
   W.H.M. Tielen, Afstudeerverslag Vakgroep Chemische Technologie, Technische Hogeschool Eindhoven (1976).

4. In het dehydrogeneringsmechanisme dat gehanteerd wordt voor de oxydatie van koolhydraten met platina katalysatoren komt de rol van aan het katalysator oppervlak geadsorbeerde zuurstof ten onrechte niet tot uiting.
   H. Wieland, Ber., 45, 2606 (1912);
   K. Heyns, en H. Paulsen, Adv. Carb. Chem., 17, 169 (1962).

5. Het belang van de drukafhankelijkheid van retentiegrootheden voor de identificatie van verbindingen met gas-vloeistof chromatografie heeft men zich tot nu toe onvoldoende gerealiseerd.
   J.A. Rijks, Proefschrift, Technische Hogeschool Eindhoven (1973).

6. Vanuit experimenteel standpunt is een bol de meest geschikte geometrie voor de bepaling van de concentratieafhankelijkheid van de diffusiecoëfficiënt van water in vloeibare voedingsmiddelen met behulp van (de)sorptie experimenten. Theoretisch wordt echter bij (de)sorptie in een vlakke laag een relatief groter concentratietraject beschreven.

   W.J.A.H. Schoeber, Proefschrift, Technische Hogeschool Eindhoven (1976).

7. De methode die Gustafson voorstelt voor het berekenen van de katalysator deactivering tijdens het katalytisch kraken van petroleumprodukten is aan bedenkingen onderhevig.

   W.R. Gustafson, Ind. Eng. Chem. Proc. Des. Develop., 11, 507 (1972).

8. De methode die door Kitatani et.al. is beschreven om te komen tot selektieve endoalkylering van cyclopropaanverbindingen is zeer waarschijnlijk niet toepasbaar op cyclopropanen, bereid door carbeenadditie aan trigesubstitueerde olefinen.

   K. Kitatani, T. Hiyama en H. Nozaki, J. Am. Chem. Soc., 97, 949 (1975);
   H.J.J. Loozen, Proefschrift, Technische Hogeschool Eindhoven (1976).

9. De relatief geringe hoeveelheid research die aan de toepassingsmogelijkheden van koolhydraten wordt besteed staat in schril contrast met hun overvloedig voorkomen en de potentieel gunstige eigenschappen van hun derivaten.

10. Met de potentiële bijdrage van de katalyse aan de verbetering van de energiehuishouding wordt nog in onvoldoende mate rekening gehouden.

11. Zij, die menen de stedebouwkundige waarde van een historische binnenstad te dienen door de thans bestaande bebouwing zo goed mogelijk, liefst in de oorspronkelijke staat, te conserveren, realiseren zich wellicht te weinig dat het historisch karakter van zo'n binnenstad, als een versteende doorkijk in de tijd, mede gediend is door toevoeging van duidelijk eigentijdse bebouwing, mits van voldoende stedebouwkundig en architektonisch niveau.

12. Een accountantsverklaring aangaande de jaarrekening van een onderneming zou voor het maatschappelijk verkeer aanzienlijk in waarde toenemen, indien de accountant zich hierin niet alleen zou uitspreken omtrent het eventueel niet nakomen van de bepalingen van Titel 6 (de Jaarrekening) van Boek 2 van het Burgelijk Wetboek, maar ook omtrent het eventueel niet nakomen van wettelijke regelingen op sociaal of economisch terrein, zoals de Wet op de Ondernemingsraden, Prijzenbeschikkingen en Loonmaatregelen.

13. Gelet op dat deel van het interieur van de kathedrale basiliek van St. Jan te 's-Hertogenbosch waarvan de herstelwerkzaamheden thans reeds beëindigd zijn, moet worden gevreesd dat het gehele interieur van deze kathedraal onherstelbaar "gerestaureerd" zal worden.

14. Dat in Nederland jan en alleman het tot lid van het kabinet kan brengen wordt uit onze democratische tradities als zeer gunstig beschouwd; dat in de praktijk echter ook werkelijk jan en alleman het zover brengt dient vraagtekens op te roepen.

15. Politieke "duidelijkheid" leidt tot onbestuurbaarheid van het land.

Eindhoven, 6 mei 1977. M.A.M. Boersma.